Draft Version 7/26/2010 8:14 AM
NUREG/CR – XXXX
SAND2008P – XXXX

State-of-the-Art Reactor Consequence Analysis (SOARCA) Project Best Modeling Practices Volume II

Manuscript Completed: XXXX
Date Published: XXXX

Prepared by:
Randall O. Gauntt, Mark T. Leonard, Kyle Ross, Kenneth C. Wagner

Sandia National Laboratories
Albuquerque, New Mexico 87185
Operated for the U.S. Department of Energy

NRC Leads:
NRC Project Manager: Terry Brock

U.S. Nuclear Regulatory Commission
Division of Systems Analysis
Washington, DC 20555-0001
NRC Job Code: XXXXX

Do we need to add herein all the stuff that suggested be taken out of the Summary document? eg The international program discussion

Z
25

Sandia is a multi-program laboratory operated by Sandia Corporation, a Lockheed Martin Company, for the United States Department of Energy's National Nuclear Security Administration under contract DE-AC04-94AL85000.

ABSTRACT

The modeling approached used in the State-of-the-Art Reactor Consequence Analysis project to characterize the release of radionuclides to the environment accompanying a postulated severe (core damage) accident is based on plant-specific applications of the MELCOR computer code. MELCOR is a state-of-the-art computational model developed by Sandia National Laboratories for the U.S. Nuclear Regulatory Commission. Due to large uncertainties in many aspects of severe accident behavior, MELCOR provides the code user a wide spectrum of options for modeling uncertain physical phenomena and characterizing plant response to beyond design basis accident conditions. Choices made by the code user to select among these options or, when necessary, develop new or enhanced modeling features are, therefore, an important aspect of the overall modeling approach.

This document describes the specific manner in which MELCOR modeling capabilities were used to represent important, but uncertain, aspects of severe accident behavior. This description includes choices made among alternate modeling options offered through code input, changes to selected input parameters from those offered as 'default' values, and in some cases user-generated 'models' to represent features of plant response to a severe accident that are not directly available in MELCOR. Collectively these features represent current "best practice" guidance for using MELCOR to calculate severe accident behavior in operating nuclear power plants.

Paperwork Reduction Act Statement

The information collections contained in this NUREG are covered by the requirements of 10 CFR Part 50, which were approved by the Office of Management and Budget (OMB), approval number 3150-0011.

This Page Intentionally Left Blank

TABLE OF CONTENTS

APPENDIXES

FIGURES

TABLES

This Page Intentionally Left Blank

ACRONYMS

AECL	Atomic Energy of Canada Limited
B&W	Babcock and Wilcox
BWR	Boiling Water Reactor
CCFL	Counter-Current Flow Limitation
CE	Combustion Engineering
CFD	Computational Fluid Dynamics
CRD	Control Rod Drives
DOE	Department of Energy
ECCS	Emergency Core Cooling System
EPRI	Electric Power Research Institute
IPE	Individual Plant Examination
IPEEE	Individual Plant Examination for External Events
LHF	Lower Head Failure
MCCI	Molten Core Concrete Interaction
NRC	Nuclear Regulatory Commission
NSSS	Nuclear Steam Supply System
ORNL	Oak Ridge National Laboratory
PWR	Pressurized Water Reactor
RAMCAP	Risk Analysis and Management for Critical Asset Protection
RCS	Reactor Coolant System
RPV	Reactor Pressure Vessel
SG	Steam Generator
SNL	Sandia National Laboratories
SOARCA	State-of-the-Art Reactor Consequence Analysis
SPAR	Standardized Plant Analysis Risk

This Page Intentionally Left Blank

1. INTRODUCTION

The evaluation of accident phenomena and the offsite consequences of severe reactor accidents has been the subject of considerable research by the NRC over the last several decades. As a consequence of this research focus, analyses of severe accidents at nuclear power reactors is more detailed, integrated and realistic than at any time in the past. A desire to leverage this capability to address excessively conservative aspects of previous reactor accident analysis efforts was a major motivating factor in the genesis of the State-of-the-Art Reactor Consequence Analysis (SOARCA) project. By applying modern analysis tools and techniques, the SOARCA project seeks to provide a body of knowledge that will support an informed public understanding of the likely outcomes of severe nuclear reactor accidents.

The primary objective of the SOARCA project is to provide a best estimate evaluation of the likely consequences of important severe accident events at reactor sites in the U.S. civilian nuclear power reactor fleet. To accomplish this objective the SOARCA project will utilize state-of-the-art computational analysis tools, which incorporate knowledge gained from the past 25 years of research. These tools require a large amount of input data by the code user to describe the physical configuration of the plant and to describe user preferences among alternate modeling options for uncertain severe accident phenomena. Further, the code also accepts certain types of user input that adds new modeling features to a MELCOR calculation. For example, 'control function' input can be included to define the response of specific plant components or systems to changes in thermodynamic or other environmental conditions that might occur during a particular calculation. The entire body of code input reflects the informed judgment of the code user on how a MELCOR model should be configured to generate a realistic estimate of plant response to a severe accident. Collectively, this information represents the "best practice" modeling approach for using MELCOR in performing severe accident progression and radionuclide source term calculations.

This report documents the best practice approach for performing MELCOR calculations for the SOARCA project. Section 2 describes the overall technical approach used in the current analysis and compares it to the technical approach used in the analyses documented in NUREG/CR-2239 (i.e., the Sandia Siting Study.) Section 3 describes the specific modeling practices used to develop and exercise the MELCOR models of PWR and BWR plants examined in this study. Section 4 offers a brief summary of the technical rationale for neglecting particular severe accident phenomena that were assumed to occur in past severe accident analyses.

This Page Intentionally Left Blank

2. TECHNICAL APPROACH

The technical approach used to calculate radionuclide release to the environment (i.e., the "source term") accompanying credible, but very low-frequency accident scenarios relies on the applications of the MELCOR computer code [1], which was specifically designed to calculate reactor and containment system response to postulated severe accidents. The technical approach to evaluating the consequences arising from the release of radioactive material to the environment involves a separate computer code (i.e., MACCS), which is described in a separate report [2]. Key differences in the approach used in the SOARCA Program from those used in past nuclear reactor radiological consequence calculations are described in Section 2.2.

2.1 Analytical Models

The technical approach that was adopted to define the quantitative characteristics of radiological release to the environment was to calculate temporal changes in reactor and containment conditions using MELCOR version 1.8.6. MELCOR is a large, integrated computer code developed at Sandia National Laboratories under the direction of the U.S. Nuclear Regulatory Commission and the joint sponsorship of international members of the Cooperative Severe Accident Research Program (CSARP). The code is "integrated" in the sense that it combines analytical models for a wide-spectrum of physical processes (previously evaluated as separate disciplines) into a single, numerically-coupled simulation. Among the technical disciplines addressed by MELCOR are:

- thermal-hydraulic response of the reactor coolant system (RCS) and containment to the postulated accident scenario,
- fuel (core) heat-up and physical degradation due to melting and loss of mechanical strength,
- fission product release from fuel, and
- transport of fission products (in vapor or aerosol form) away from the core, through the RCS and containment, to the environment.

Critical to quantitative evaluation of these disciplines are mathematical models for complex physical processes, such as: changes in the physical state (morphology) of core materials, generation and combustion of hydrogen as a byproduct of the oxidation of metallic components in the core, the erosion of concrete in regions of the containment under the reactor pressure vessel due to chemical decomposition by molten core debris, and mechanical failure of major structural barriers to fission product release (such as the reactor pressure vessel and containment). A detailed accounting and description of these models is not provided here. Instead, the reader is referred to the MELCOR Reference Manual [1] for this information. The information contained in this document is designed as a companion to the MELCOR code manuals, and provides a brief description of the way in which MELCOR models were used to represent aspects of nuclear power plant behavior during a severe accident that are (a) difficult to predict with high confidence due to uncertainties in their governing phenomena and (b) whose outcome is important to calculated results. Major uncertainties in MELCOR models for accident progression were addressed in two ways. First, the accident progression analysts developed a list of uncertain phenomena that can have a significant effect on the progression of the accident. Alternate ways of addressing each

phenomenon were considered and a 'best estimate' approach was developed by applying appropriate and available modeling tools in MELCOR. Calculations performed using the best estimate approach are referred to in this document as the 'base case' analysis, and the manner in which MELCOR models and input parameters were configured to represent uncertain and important events and processes is described in Section 3.1.

The proposed approach for addressing some accident phenomena required changes to the capabilities or of the MELCOR computer code, or enhancements to options for user input for certain models. These changes and enhancements are described in Section 3.2.

An independent expert panel was assembled to review the proposed base case approach. The review was conducted during a public meeting sponsored by the NRC on August 21-22, 2006 in Albuquerque, New Mexico [3]. Comments and recommendations made by the panel were evaluated by the SOARCA project team, and refinements or adjustments to the proposed base case were made to incorporate their views.

2.2 Important Differences in Approach from Prior Work

Radiological source terms to the environment used in NUREG/CR-2239 (i.e., the 'Sandia Siting Study') were developed from early research on severe accident behavior that followed the publication of WASH-1400 in 1975 and the accident at TMI-2 in 1979. This research was initiated to develop predictive methods for calculating fission product release and transport during a wide spectrum of postulated accident sequences involving substantial damage to fuel in the reactor core. Results of this work were documented in NUREG-0772 [4], which was published in 1981.

The analysis methods used to generate the 'Siting Source Terms' (SSTs) used in NUREG/CR-2239 involved the manual integration of calculations from several computer codes, as illustrated in Figure 1. Each code examined a particular portion of the overall analysis, such as RCS thermal-hydraulic response, core heat up and 'meltdown' (MARCH), fission product transport and deposition in the RCS (TRAP-MELT) and fission product retention in the containment before release to the environment (CORRAL, NAUA, etc.)[1]. The central element of this calculation scheme was the TRAP computer code, which used estimates of fluid velocities and RCS surface temperatures calculated by MARCH, combined with formulas for vapor and aerosol deposition rates, to characterize the extent to which fission products 'plate out' on RCS surfaces before being carried to the containment. Similar information regarding flow rates and temperatures in the containment were used to estimate deposition on containment surfaces[2].

Several major simplifications were involved in the NUREG-0772 calculations that have been eliminated in the current approach. Among the most important of these are:

- The source term analysis tools illustrated in Figure 1 represents a linear progression of calculations, in which results of one calculation become 'input' to a subsequent calculation. As a result, physical dependencies between processes modeled in

[1] A description of these codes can be found in references cited in NUREG-0772.

[2] The code system used to perform the calculations documented in NUREG-0772 developed later into the 'Source Term Code Package' (STCP), which was the predecessor of MELCOR as the NRC's principal tool for severe accident analysis.

different codes can only be represented in one direction. Feedback mechanisms are not directly accounted for. For example, decay heating of surfaces in the RCS or containment due to deposited radionuclides was not accounted for in the MARCH calculation of RCS thermal-hydraulic response. As a result, long-term revaporization of fission products from surfaces was not addressed as a late release mechanism.

In contrast, models for the processes governing severe accident progression and radionuclide release/transport are arranged into an integrated set of computational modules in MELCOR, which are solved in a single computational framework. Interdependencies among diverse phenomena are captured directly in the numerical solution.

- The release of fission products from fuel was not integrally-linked to the calculation of time-dependent changes in fuel temperatures by the MARCH code. Results of the MARCH calculations were used to inform the analysts about the time at which fuel failure would be expected to begin for a particular accident sequence, but fission product release rate was not explicitly (numerically) coupled to the calculated fuel temperature history. Rather, an average (constant) release rate was defined as input to the TRAP-MELT calculations based on limited data from early experimental measurements. Distinct release rates were defined for iodine, cesium and (collectively) all other particulate matter.

  In contrast to this simplified approach, MELCOR calculates a time-dependent release rate of fission products from the core, based on a validated correlation of fission product release rate and the temperature history calculated at 50 distinct regions of fuel assemblies (five radial rings and ten axial levels).

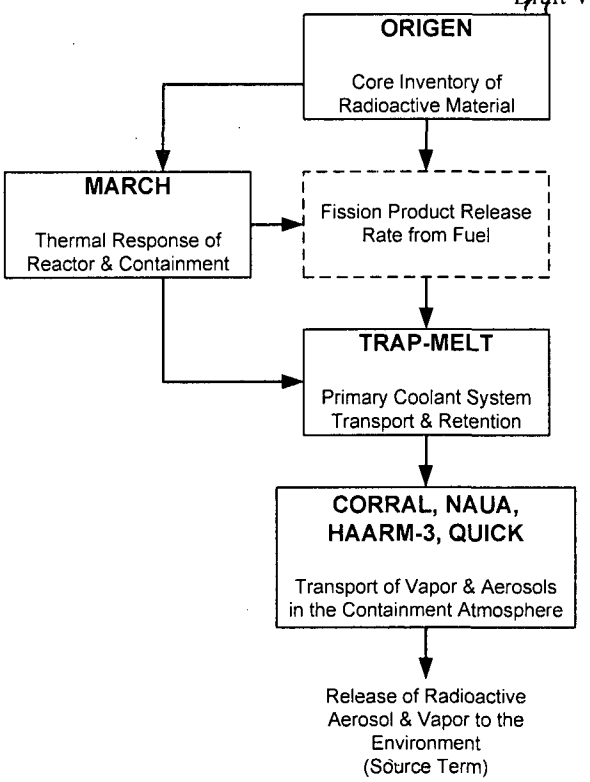

Figure 1 Computational Methods used to Derive Source Terms in NUREG-0772.

- A linear series of control volumes (each with internal surfaces) was used to represent fission product transport and deposition within the primary coolant system. Fission product retention in the containment was calculated by applying a variety of computational models to the entire containment free volume, which account for various aerosol and vapor deposition and attenuation mechanisms. An illustration of a typical nodalization scheme used for the TRAP-MELT calculation of RCS retention is shown in Figure 2.

  In contrast, the spatial nodalization of the reactor pressure vessel, primary coolant system and containment in the MELCOR models developed for PWRs and BWRs recognizes much more geometric detail. For example, the entire PWR RCS was represented by four spatial regions in the NUREG-0772 calculations. The MELCOR model of the same 3-loop Westinghouse PWR used in the current analysis uses 25 control volumes for the core region alone; over 100 control volumes are used to represent the entire RCS. This dramatic increase in detail provides much greater resolution of the driving forces governing fission product transport and deposition. In particular, local fluid velocities and temperatures, structural surface temperatures and associated temperature gradients are all calculated in greater detail than was available at the time of the analyses supporting NUREG/CR-2239.

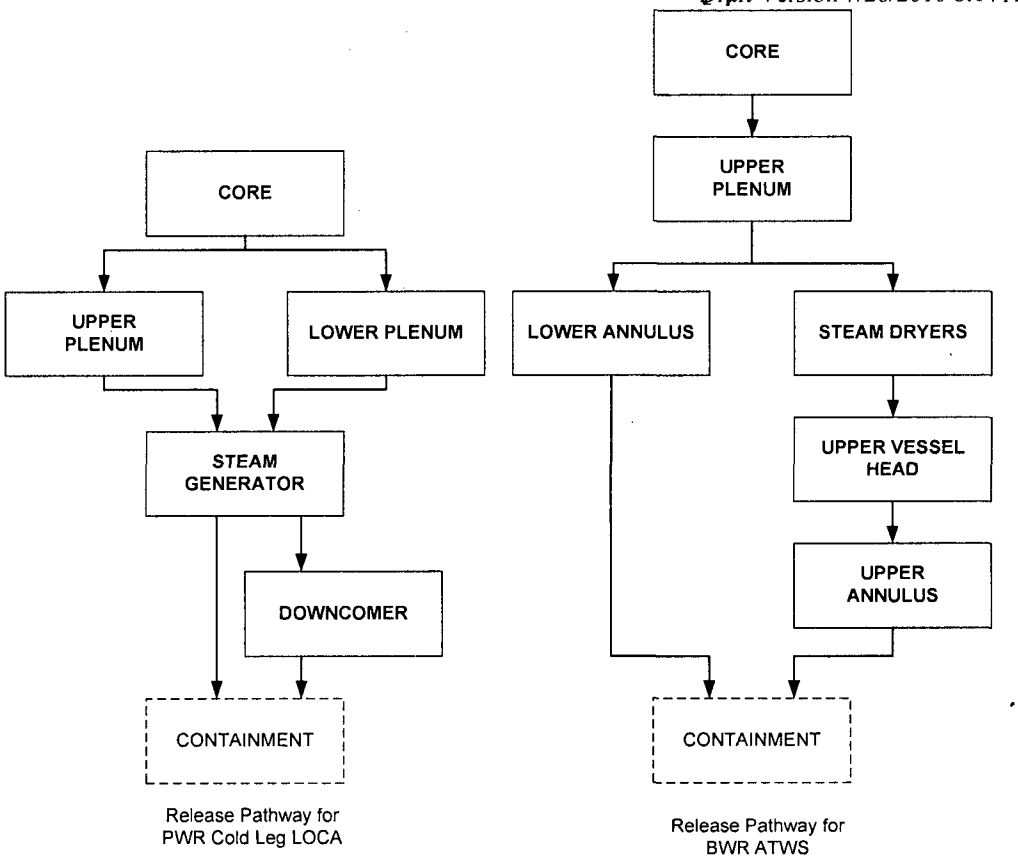

Figure 2 Typical Spatial Nodalization of RCS in the NUREG-0772 Methodology.

This Page Intentionally Left Blank

3. MELCOR BEST-PRACTICE FOR SEVERE ACCIDENT ANALYSIS

This chapter describes modeling practices applied to severe accident progression calculations performed with MELCOR. This description is not comprehensive. That is, the standard approach to modeling all phenomena governing fuel damage, fission product release and other aspects of plant response to postulated severe accident is not provided here. Rather, a small sub-set of the large body of important phenomena is addressed. The basic criteria used to determine which phenomena to include in this discussion were that the phenomenon or event (a) was an important contributor to the progression of the accident and (b) was addressed in the calculations by user-generated models or input data that are different from, or augment, default input parameters available in MELCOR.

It should also be noted that although many of the practices described in this section are expressed in terms of their implementation in the MELCOR models developed for the SOARCA project, they involve phenomenological considerations and uncertainties that have broader applicability.

Best-practice modeling features described this chapter fall into several different categories. One very broad category is severe accident modeling features that are controlled or influenced by user input. Modeling practices within this category can take several forms depending on the specific type of user input used to influence or define a MELCOR model. One form within this broad category involves changes to values of input parameters ~~that~~ from those set within the code as default values. These parameters span a wide spectrum from coefficients of heat transfer correlations to numerical convergence criteria. A second form is input that selects a particular model among many options that are offered in MELCOR. An example of this form of user-influenced modeling practice is the correlation used to calculate the release rate of fission products from over-heated fuel. MELCOR offers several types of correlations, and the user must select one. A third form of user influence on a MELCOR calculation is an analytical expression or implementation logic developed by the user (typically via control functions) to represent an aspect of severe accident progression that is not directly represented as a 'model' within MELCOR. An example of this type of modeling practice is a user-specified correlation or condition that determines if, and when, a particular component would fail to function. Failure of a safety/relief valve to reclose due to repeated cycles, or enhanced leakage through an over-heated reactor coolant pump seal would fall into this category.

Each of these forms of models that are influenced by user input to MELCOR is discussed in Section 3.1. Changes to default MELCOR input parameters are also tabulated in Appendix A. A listing of user selections of modeling options and other user-generated models or calculation control logic is given in Appendix B.

It should be noted that implementation of these modeling practices in a plant-specific MELCOR model depends on the details of that model and is not described in this report. Important modeling details, including significant deviations from best practice, are provided in the documentation associated with the plant-specific MELCOR models developed for use in the SOARCA project.

A second broad category of changes to MELCOR modeling practices involve changes to MELCOR coding (Fortran) to accommodate advanced modeling needs for the SOARCA

project. In some cases, these changes codified modeling practices that had been implemented through user input in many past NRC applications of MELCOR. Incorporating the user-generated input directly into the code simplified user input and enhanced the fidelity of the modeling practice among MELCOR models for various nuclear power plants. Enhancements to the MELCOR code that were implemented as part of the SOARCA project are described in Section 3.2.

3.1 MELCOR User-Specified Best Modeling Practices

Several of the modeling practices that are defined or controlled by user input are applied in calculations of severe accident progression for a PWR or BWR. Others are specific to one design or the other. Generic modeling practices (i.e., those applied to both designs) are described in Section 3.1.1. PWR- and BWR-specific modeling practices are then described in Sections 3.1.2 and 3.1.3, respectively.

3.1.1 Generic Light-water Reactor Best Practices

Modeling practices discussed in this section are applied to both MELCOR models of PWRs and BWRs. The specific manner in which they are implemented can vary slightly between the two, but the physical processes that are represented in these models are consistent between the two designs.

3.1.1.1 Changes to Default Input Parameters

At the start of the SOARCA projects, several MELCOR code development activities were identified to enhance the code. Some non-default values had been regularly used in MELCOR analysis at Sandia National Laboratories. The incorporation of these items as code defaults ensured consistent application of these recommended defaults. The new defaults are summarized Appendix A (also see Section 3.2).

3.1.1.2 Changes or Enhancements to Standard MELCOR Modeling Options

Fuel degradation and relocation treatment

An additional model has been added to characterize the structural integrity of the fuel rods under highly degraded conditions. As the fuel temperature increases, an oxide shell forms on the outer surface of the fuel cladding. Since the oxide shell has a higher melting temperature than the unoxidized Zircaloy inside of the fuel rod, the Zircaloy on the interior of the cladding will become molten once the temperature rises above the melting temperature (see Figure 3). Based on observations from Phebus tests, MELCOR includes a molten Zircaloy breakout model as the oxidized Zircaloy losses structural integrity. Subsequently, MELCOR did not have a thermal-mechanical model for failure of the oxidized Zircaloy shell holding the fuel rods. Due to the loss of unoxidized Zircaloy following the breakout phenomena, it was observed that the fuel rods could remain standing for long periods of time at very high temperatures. The only calculated failure mechanisms included (a) failure due to melting the oxidized shell or (b) failure of the supporting structure. The new model acknowledges a thermal-mechanical weakening of the oxide shell as a function of temperature. As the temperature rises above Zircaloy melting temperature (i.e., represented as 2098 K in MELCOR) towards 2500 K, a thermal lifetime function linearly accrues increasing damage from 10 hours to 1 hour until a predicted local thermo-mechanical failure, respectively (see Table 1). This enhancement (a) eliminates a single threshold temperature for failure of the

oxide shell, (b) recognizes an increased likelihood for thermal-mechanical failure of the brittle oxide shell at high temperatures, and (c) is functionally similar to a model in the MAAP code. Preliminary sensitivity studies have shown that this model does not have a significant impact of the resultant source term magnitude and timing but ~~provides~~ does provide more consistent core collapse timing. consistent with what?

Table 1 Time versus Temperature Relationship for Intact Fuel Rod Collapse

Temperature	Time to Failure
2000 K	Infinite
2090 K	10 days
2100 K	10 hr
2500 K	1 hr
2600 K	5 min
2700 K	30 sec

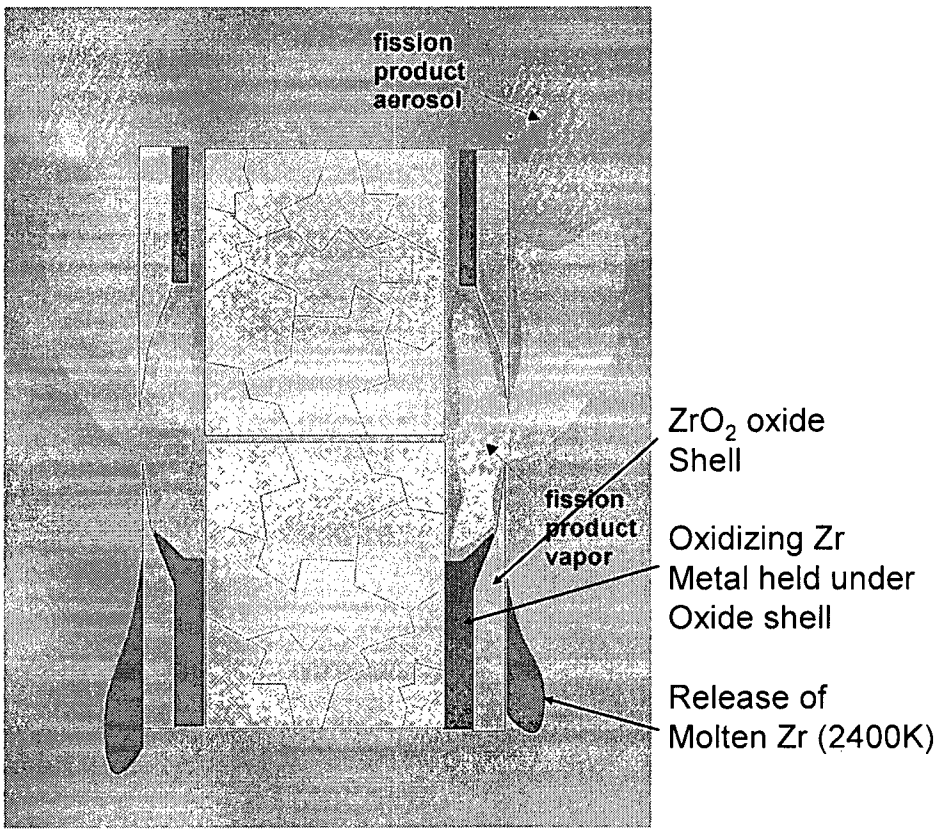

Figure 3 MELCOR Depiction of the Fuel Rod Degradation.

Lower plenum debris/coolant heat transfer

Direct interaction between over-heated (possibly molten) core debris and a pool of water can occur at two key junctures in the chronology of a severe accident in an LWR. The first major juncture is when core debris relocates from a position above the lower core support structures; the second juncture is when the reactor vessel lower head fails and core debris relocates onto the floor of the containment. The thermo-mechanical interactions between core debris and water during these periods of debris relocation can be either benign or extremely energetic, depending on several factors:

- the thermodynamic state of the debris (temperature and morphology),
- composition of the debris (unoxidized metals, ferric oxides, ceramics, etc.)
- debris relocation geometry (coherent pour, massive slump, cascade of particulate, etc.)
- depth and temperature of water pool (saturated or subcooled), and
- initial pressure of the confining vessel.

Proper accounting for the interaction between fuel and coolant at these two junctures can have a significant effect on the prediction of severe accident chronology, challenges to containment integrity and the resulting source terms. For example, relocation of core debris into the lower head without significant interaction with residual water below the lower core support structure can result in rapid heating and early failure of lower head structures. Conversely, significant interaction between core debris and water can significantly delay the time of vessel breach, produce large quantities of steam (leading to enhanced oxidation of metallic components) and potentially result in a coolable debris bed in the lower head.

Ex-vessel interactions between core debris and water on the containment floor can be equally important to severe accident progression. The possibility of avoiding fission product release from fuel debris during corium-concrete interactions by quenching core debris upon release from the reactor vessel is a significant enough reason for properly characterizing ex-vessel debris-coolant interactions.

Most studies of debris-coolant interactions have viewed the phenomenon as a precursor to steam explosion. However, most experiments involving molten debris-coolant interactions do not result in a steam explosion. These less energetic events are of equal (perhaps greater) value to the analysis of severe accident progression as they provide valuable information on debris quenching and long-term coolability. Published literature describing these studies was reviewed to determine the depth of water required to sufficiently fragment and cool molten core debris. This depth of water could then be applied to typical in-vessel or ex-vessel situations in which the coolability of relocating debris needs to be evaluated in MELCOR. Data from five different test series and a total of 29 different experiments were examined. Key measurements from these tests are listed in Table 2.

Analysis of hydrodynamic breakup behavior in these tests resulted in estimates of the vertical distance a molten jet must travel in a pool of water to fully quench the molten debris. This distance (referred to as the molten jet breakup length) was estimated to be between 20 and 50 jet diameters for melts without unoxidized metals, and between 10 and 20 diameters for melts with unoxided melts. Test results indicate that molten jet breakup occurs at both the leading edge and along the trailing column. Steam production at the leading edge leads to jet

breakup. Steam moving through the pool alongside the molten jet also contributes to jet breakup. When unoxidized metals are present, steam oxidizes metals at the jet surface releasing additional energy to the steam/water mixture and enhancing breakup along the trailing jet column.

If these figures are applied to full-scale reactor conditions, and one can postulate a representative diameter of the jet of molten core debris that would emerge from the reactor vessel lower head after failure, the minimum depth of water required to quench the debris can be estimated. For example, if one assumes the characteristic diameter of the molten jet is roughly the diameter of a single 'unit cell' of a reactor fuel assembly (i.e., approx. 10 cm), fragmentation and quenching of the molten material would be achieved in 2 to 5 m of water (for oxidic melts) and 1 to 2 m of water for metallic melts. This distance is well within the range of water depth in the lower plenum of a typical BWR at the time lower core support plate failure first occurs, initiating large-scale in-vessel debris relocation. Therefore, a best-estimate characterization of debris behavior operates under the assumption of efficient debris provided a sufficiently deep pool of water remains in the lower plenum.

→ cooling? quenching? heat transfer?

MELCOR parameters for the 'falling debris quench' model were, therefore, changed to effect efficient heat transfer. In particular, the debris hydraulic diameter was defined correspond to average end-state conditions observed in the FARO tests and the average 'fall velocity' was set to a value that caused the temperature of falling debris to decrease by an amount that ensured debris temperatures in the lower head were below the film boiling limit. In addition, the one-dimensional counter-current flow limitation (CCFL) limitation was removed from the overlying debris heat transfer model to represent water penetration into the debris bed, perhaps through 2- or 3-dimensional circulation flow patterns. This modeling approach resulted in debris cooling if there was a pool of water in the lower plenum and delayed heat up of the vessel lower head until the overlying water had evaporated.

Table 2 Summary of Data from Molten Debris-Coolant Interactions Experiments

	Melt				Pool				Pool/Melt Ratios		Other Initial Conditions			FCI		Debris		
Experiment	Composition (w/o)	Mass (kg)	Superheat (K)	Jet Diameter (cm)	Mass (kg)	Surface Area (cm^2)	Depth (m)	Subcooling (K)	Mass --	Cross-Sectional Area --	Initial Pressure (MPa)	Melt free fall in gas (m)	Free volume (m^3)	Trigger	Event	Oxidation (%)	MMD (mm)	Energy Release (MW/kg)
FARO L-06	80% UO2 20% ZrO2	18		10	120	1735	0.87	Saturated	7	22	5	1.66	0.464	No	B	na	4.5	
FARO L-08#	80% UO2 20% ZrO2	44		10	255	3959	1	Saturated	6	50	5	1.53	0.875	No	B	na	3.8	0.8
FARO L-11	76.7% UO2 19.2% ZrO2 4.1% Zr	151		10		3959	2	Saturated		50	5	1.09	1.28	No	B	100	3.5	
FARO L-14#	80% UO2 20% ZrO2	125	200	10		3959	2.05	Saturated		50	5	1.04	1.26	No	B	na	4.8	0.8
FARO L-19	80% UO2 20% ZrO2	157	200	10		3959	1.1	Saturated		50	5	1.99	1.635	No	B	na	3.7	
FARO L-20	80% UO2 20% ZrO2	96	300	10		3959	1.97	Saturated		50	2	1.12	1.291	No	B	na	4.4	
FARO L-24	80% UO2 20% ZrO2	176	150	10		3959	2.02	Saturated		50	0.5	1.07	1.266	No	E	na		
FARO L-29	80% UO2 20% ZrO2	39		5	492	3959	1.48	97	13	202	0.21	0.74	3.54	No	B	na		
FARO L-31	80% UO2 20% ZrO2	92	117	5	481	3959	1.54	104	5	202	0.22	0.77	3.53	No	B	na	3.2	
KROTOS-30	Al2O3	1.40	248	3	7.5	71	1.08	80	5	10	0.1	0.46		No	SE	na		
KROTOS-32	80% UO2 20% ZrO2	2.61	190	3	7.1	71	1.08	22	3	10	0.1	0.46		No	B	na	2.5	0.87
KROTOS-33	80% UO2 20% ZrO2	2.80	190	3	7.7	71	1.08	75	3	10	0.1	0.46		No	B	na	2	0.97
KROTOS-35	80% UO2 20% ZrO2	1.42	150	3	7.7	71	1.08	10	5	10	0.1	0.46		Yes	E	na		
KROTOS-36	80% UO2 20% ZrO2	2.80	152	3	7.7	71	1.08	79	3	10	0.1	0.46		Yes	B	na		
KROTOS-37	80% UO2 20% ZrO2	2.92	145	3	34.5	314	1.105	79	12	44	0.1	0.44		Yes	B	na	1.4	
KROTOS-38	Al2O3	1.52	340	3	34.5	314	1.105	79	23	44	0.1	0.44		Yes	SE	na		

Table 2 (continued)

TROI-1	ZrO2	5.00	400	3.7	283	4225	0.67	5	57	393	0.1	3.5	8.032	No	SE	na		
TROI-2	ZrO2	5.50	400	5.2	283	4225	0.67	8	51	199	0.1	3.5	8.032	No	B	na		
TROI-3	ZrO2	4.88	400	6	283	4225	0.67	50	58	149	0.1	3.5	8.032	No	B	na		
TROI-4	ZrO2	4.20	400	2.8	283	4225	0.67	81	67	686	0.1	3.5	8.032	No	SE	na		
TROI-5	ZrO2	2.90	400	3.8	283	4225	0.67	36	98	373	0.1	3.5	8.032	No	SE	na		
CWTI-9	60% UO2 16% ZrO2 24% SS	4.00	160	2.54			0.36	6			0.1	0.2		No	B	67%	0.78	
CWTI-10	60% UO2 16% ZrO2 24% SS	4.00	160	2.54			0.36	75			0.1	0.2		No	B	10%		
FITS-0D*	Thermite	17.8	375	5	182.9	3721	0.51	0	10	190	0.085	1.79	5.6	No	E	24%	4.6	
FITS-2D*	Thermite	19.0	375	5	95.3	1444	0.66	169	5	74	1.1	2.7	5.6	No	B	20%		
FITS-2DR*	Thermite	18.7	375	5	95.3	1444	0.66	158	5	74	1.1	2.7	5.6	No	B	25%		
FITS-3D*	Thermite	18.9	375	5	86.6	5776	0.15	37	5	294	0.7	1.6	5.6	No	B	82%		
FITS-5D*	Thermite	19.2	375	5	383	5776	0.66	83	20	294	0.083	1.6	5.6	No	SE	20%	0.5	
FITS-8D*	Thermite	19.5	375	5	21.3	1444	0.15	0	1	74	0.083	2.7	5.6	No	E	26%	3.4	

* FITS melt superheat value estimated based on alumina melting point, melt jet diameter is arbitrary
\# FARO melt energy released is provided in MJ/kg

B - Benign
E - Eruption
SE - Steam Explosion

Fission product release, speciation, and volatility[3]

Insights developed over the past 5 years into recent experimental programs has updated the recommended MELCOR specifications for modeling the release of fission products from reactor fuel under severe accident conditions. The new models have been incorporated as new defaults in the MELCOR code (see Section 3.2). Separate specifications are provided for use in spent fuel pool release conditions owing to differences in the reduction/oxidation potential in air oxidizing conditions. Some review of the motivation for the new modeling approach follows with an assessment of the new model against fission product release experiments.

Past versions of MELCOR primarily used the CORSOR-M release model for calculating fission product release as described in the MELCOR Reference manuals and in a Battelle report by Ramamurthi and Kuhlman titled "Refinement of CORSOR – An Empirical In-Vessel Fission Product Release Model [32]." Also described in these references are the CORSOR and the Booth diffusion release model, implemented in MELCOR as the CORSOR-Booth optional release model. The CORSOR and CORSOR-M models are classified as *fractional release rate* models, differing only slightly in mathematical form, which specify the fractional release rate of the fission product inventory remaining unreleased up to that time. These are empirical models that are based largely on the small-scale HI and VI experiments performed at ORNL.

The Booth diffusion model is by comparison a physics-based model, albeit oversimplified, that describes the transport of fission products within fuel grains to the grain surface as a diffusion process. In the MELCOR implementation of the Booth diffusion treatment, an additional gas-phase transport process is imposed in moving fission products from the grain surfaces to the atmosphere. Elements such as molybdenum that are modeled in MELCOR as having very low vapor pressures are ultimately released at a low rate regardless of the rate of diffusion within the grain. Once released from the fuel, fission product class combinations can be defined, such as CsI, in order to represent fission product chemistry and speciation. In the present code architecture, multiple combination assignments such as CsI and Cs_2MoO_4 were not foreseen and must be approximated. Once assigned to the chemical class on release, generally no additional chemistry is allowed, an exception being CsI chemisoprtion with subsequent revaporization of iodine, leaving the permanently chemisorbed Cs attached to a deposition surface.

Critical assessments of these models and their performance have been limited, partly owing to lack of additional quality data from which to render a judgment. One assessment performed by ORNL with MELCOR 1.8.2 surveyed the performance of the MELCOR default models when applied to the VI series of tests [33]. The report observed that while total releases could often be adequately predicted that the time-release signature was often not very good. Recommendations were provided for code modeling improvements, including provision to vary release based on the H_2/H_2O environment. Recently however, additional experimental data is increasingly available from international testing programs, in particular the French VERCORS program and the Phebus

[3] The recent modifications to Version 1.8.6 (Version YR) for the SOARCA program implemented the new ORNL-Booth fission product release model as the new default model (see Section 3.2). In Version 1.8.6, the new defaults are invoked with the Version "2.0" keyword. All subsequent 2.X code versions will automatically use the new ORNL-Booth model as the default fission product release model.

integral experiments, and recent user assessment of current MELCOR release models in the prediction of these tests has illuminated some deficiencies that are partly remedied in the recommendations of this report. The Phebus experiments in particular reveal shortcomings of the empirical CORSOR and CORSOR-M models with respect to release rates during the initial fuel heatup, and have been found to significantly overestimate early release rates even though total integral releases might compare reasonably well. Additionally, the integral Phebus tests provide release data under conditions that are significantly less coherent (and more prototypic by the way) in terms of temperature and oxidation/reduction conditions than in the small scale tests (HI, VI and VERCORS) where the fuel sample is small, temperatures are uniform and oxidation/reduction conditions controlled and constant. The Phebus experiments, we contend, provide conditions for release that are more representative of conditions expected in the full-scale reactor accident case, and are used as the principal reference for judging the performance of the MELCOR release models.

MELCOR Release Models

The various release rate models in MELCOR are briefly summarized as follows. The original CORSOR model correlates the *fractional* release rate coefficient in exponential form,

$$k = A\ \exp(BT) \qquad for\ T \geq T_i \qquad \text{Eq. 1}$$

where k is the release rate (fraction per minute), A and B are empirical coefficients based on experimental data, and T is the core cell component temperature in degrees Kelvin. Different values for A and B are specified for three separate temperature ranges. The lower temperature limit T_i for each temperature range and the A and B values for that range are defined for each class in sensitivity coefficient array 7101. If the cell temperature is below the lowest temperature limit specified, no release is calculated.

CORSOR-M

The CORSOR-M model correlates the same release data used for the CORSOR model using an Arrhenius form,

$$k = k_o \exp(-Q/RT) \qquad \text{Eq. 2}$$

The values of k_o, Q, and T are in units of min^{-1}, kcal/mole, and K, respectively. The value of R is 1.987 x 10-3 in (kcal/mole)K^{-1}. The values of k_o and Q for each class are implemented in sensitivity coefficient array 7102.

CORSOR-Booth

The CORSOR-Booth model considers mass transport limitations to radionuclide releases and uses the Booth model for diffusion with empirical diffusion coefficients for cesium releases. Release fractions for other classes are calculated relative to that for cesium. The effective diffusion coefficient for cesium in the fuel matrix is given by

$$D = D_o \exp(-Q/RT) \qquad \text{Eq. 3}$$

where R is the universal gas constant, T is the temperature, Q is an activation energy, and the pre-exponential factor D_0 is a function of the fuel burn-up. The cesium release fraction at time t is calculated from an approximate solution of the diffusion equation for fuel grains of spherical geometry [34],

$$f = 6\sqrt{\frac{D't}{\pi}} - 3\,D't \qquad \text{for } D't < 1/\pi^2 \qquad \text{Eq. 4}$$

$$f = 1 - \frac{6}{\pi^2}\exp(-\pi^2\,D't) \qquad \text{for } D't > 1/\pi^2 \qquad \text{Eq. 5}$$

where

$D't$ = Dt/a^2 (dimensionless), and

a = equivalent sphere radius for the fuel grain.

The release rate of Cs during a time interval t to t+ Δ t from the fuel grain is calculated as

$$\text{Release rate}_{Cs} = \frac{\left[f\left(\sum D'\Delta t\right)_{t+\Delta t} - f\left(\sum D'\Delta t\right)_t\right]V\rho}{F\Delta t} \qquad \text{Eq. 6}$$

where ρ is the molar density in the fuel, V is the fuel volume, F is the fraction of the Cs inventory remaining in the fuel grain, and the summations are done over the timesteps up to time $(t + \Delta t)$ and t, respectively.

The release rate formulation in the CORSOR-Booth model is also limited by mass transfer through the gas-phase. The gas-phase mass transport release rate from the fuel rod for species k, $\dot{m}_k$, is calculated using an analogy from heat transfer as

$$\dot{m}_k = \left[\frac{A_{fuel}\,Nu\,D_{k,gas}}{D_{fuel}\,RT}\right]\cdot\left(P_{k,eq} - 0\right) \qquad \text{Eq. 7}$$

where

D_{fuel} = diameter of fuel pellet

A_{fuel} = fuel rod flow contact area

$D_{k,gas}$ = diffusivity of class k in the gas mixture

Nu = Nusselt number

$P_{k,eq}$ = equilibrium vapor pressure of class k at temperature T.

In the mass transfer term the driving potential is the difference in pressure at the surface of the grain and the pressure in the free stream atmosphere, here assumed to be approximately zero.

The effective release rate for Cs given by Equation 6 is a combination of the rates given by diffusion and by gas-phase mass transport. Therefore, the contribution from diffusion only is taken as

$$DIFF_{Cs} = \left[\frac{1}{\text{Release rate}_{Cs}} - \frac{1}{\dot{m}_{Cs}} \right]^{-1} \quad \text{Eq. 8}$$

The diffusion release rate for species other than cesium is given by multiplying the cesium release rate by an appropriate scaling factor S_k for each RN class k:

$$DIFF_k = DIFF_{Cs} S_k \quad \text{Eq. 9}$$

The combined mass transport and diffusion release rate $\dot{m}_{tot,k}$ for class k is then

$$\dot{m}_{tot,k} = \frac{1}{DIFF_k^{-1} + \dot{m}_k^{-1}} \quad \text{Eq. 10}$$

Inspection of equations 10 together with equation 7 reveals that the release predicted by the MELCOR models can be mass transfer limited by low vapor pressures even if the diffusive transport is large.

Known Limitations of MELCOR Release Models

The fission product release models implemented in previous versions of MELCOR (i.e., before Version 1.8.6 (RO) and the code modifications cited in Section 3.2) are quite simplified and are more than 10 years dated as indicated in the principal reference for the MELCOR models. The implemented models base the release of all radionuclide chemical classes on the release predicted for Cs, which in the Booth model is appropriately considered a diffusion process. Scaling factors are used to estimate release of other species based on the data fit to experimentally observed Cs release in spite of the fact that it is recognized that likely not all fission product classes diffuse at the same rate out of the fuel grains, nor are all principal release mechanisms well represented as a diffusion process. Consideration of speciation in MELCOR release models is crude and for the most part fixed at the time of release to represent the predominating speciation. The vapor pressures of the MELCOR release classes are defined to represent the presumed fission product speciation.

A better treatment would be to allow the vapor pressure to be adjusted to account for local speciation affected by oxidizing or reducing conditions and to then ~~source~~ these species into appropriate chemical classes. Such modifications are probably needed for Ba, Mo, UO_2 and Ru. Provision does exist to consider the extent of cladding oxidation to attempt to simulate retention Te or Ba, but data are needed to use this provision effectively. Separate diffusion coefficients for each of the volatile classes would probably be appropriate, and a UO_2 oxidation model is needed to account for the effect of stochiometry on diffusion and to predict fuel volatilization. UO_2 volatilization may be responsible for release of UO_3 as well as other non-volatile species owing to physical stripping of the fuel matrix containing the fission products. A number of more recently evolved release models consider the effect of fuel stochiometry on the diffusion coefficient as well as the oxidizing/reducing potential of the environment [35][36][37][38]. The VICTORIA code considers a large number of potential fission product species in a

thermodynamic equilibrium approach; some simplifications to this potentially numerically burdensome approach may be needed [39].

In the more recent models, often, with respect to release behavior, fission products are classified into three main groups, volatile (i.e., Xe, Cs, I, Te), semi-volatile (i.e., Ru, Ba, La, Ce), and non-volatile (i.e., UO_2 and actinides – Ce and La might belong here also). Volatile fission products are released based on the Booth diffusion model where the diffusion coefficient includes effects of UO_2 hyper-stochiometry. The hyper-stochiometry in turn is determined by a fuel oxidation model. Release of semi-volatile fission products are strongly affected by vapor pressure which in turn is affected strongly by speciation determined by the oxidizing/reducing conditions resulting from air/steam/hydrogen/Zr-metal in the release location. Non-volatile release may be dominated by UO_2 volatilization by formation of UO_3, producing fuel matrix degradation and fuel vaporization. The French Elsa code follows this approach, using models similar to those reported by Lewis et al.[35][36].

A more detailed (and flexible) release modeling was needed. The importance of accounting for speciation and the ensuing effect on specie volatility (vapor pressure) is clear. In the best practices approach, as described in the following section, the dominant speciation at the time of release is specified and used globally throughout the core region. A more elegant model would allow variation of release speciation as conditions in the core change locally and temporally with respect to steam and hydrogen concentrations. In the case of air exposure, such as in spent fuel pool accidents, different assumptions about speciation, especially concerning Ru release, are needed.

Assessment of MELCOR Default Release Models

~~Whereas~~ while the HI-VI ORNL tests provided the original basis for development of the MELCOR fission product release models, the Phebus FPT-1 integral experiment is used as the principal basis for evaluation of release modeling options. In previous assessment exercises, in particular the ISP-46 (International Standard Problem 46 [41]), while the MELCOR default CORSOR-M release model was found to predict reasonable total release fractions for many fission products, the empirical model was observed by many MELCOR ISP participants to over predict the initial release rates. Similar rapid early release is also observed for the CORSOR option. The Booth diffusion treatment for release was thought to be a potentially superior release model since it has some basis in a physical transport process, however, investigation of the MELCOR CORSOR-Booth option using the default Booth release parameters was found to produce inferior results, with total release of Cs and other fission products being significantly under predicted in test FPT-1. In view of this, review of the literature revealed numerous more recent other parameter-fits to the Booth solution.

Modifications to MELCOR Booth Release Modeling

A number of these alternative models are reported in an ORNL report that recommends updated values for the previously discussed models [11]. Shown in Figure 4 are release fractions predicted at a constant temperature of 2000 K by the various release models discussed in the ORNL report. From this it can be seen that releases predicted by fractional release rate model, CORSOR-M produces the largest release rate of all of the models. This trend is consistent with

observations from analyses considering measured releases from FPT-1. Similarly, the CORSOR-Booth diffusion model produces the lowest release rate of all of the models. This too is consistent with MELCOR analyses of FPT-1 using these modeling parameters. Judging that a best fit might lie somewhere in between these extremes, the ORNL-Booth parameters were subsequently investigated in MELCOR analyses of FPT-1, wherein significantly improved release signatures were obtained. The ORNL-Booth parameters were recommended over the CORSOR-Booth parameters in the 1995 ORNL report. The ORNL-Booth model is specified by the parameters in Table 3. Figure 4 shows other comparisons between the ORNL-Booth and CORSOR-M release behaviors. The fractional release rate (%/min) for the two models obtained by differentiating the release fractions in Figure 5 are shown in Figure 6.

Table 3 CORSOR-Booth, ORNL-Booth and Modified ORNL-Booth Parameters

	CORSOR-Booth	**ORNL-Booth**	**Adjusted ORNL-Booth**
Diffusion coeff. D_o	2.5×10^{-7} m^2/sec	1×10^{-6} m^2/sec	1×10^{-6} m^2/sec
Activation Energy Q	3.814×10^{5} joule/mole	3.814×10^{5} joule/mole	3.814×10^{5} joule/mole
Grain radius, a	6 μm	6 μm	6 μm
Class Scale Factors	---	---	---
Class 1 (Xe)	1	1	1
Class 2 (Cs)	1	1	1
Class 3 (Ba)	3.3×10^{-3}	4×10^{-4}	4×10^{-4}
Class 4 (I)	1	0.64	0.64
Class 5 (Te)	1	0.64	0.64
Class 6 (Ru)	1×10^{-4}	4×10^{-4}	0.0025
Class 7 (Mo)	0.001	0.0625	0.2
Class 8 (Ce)	3.34×10^{-5}	4×10^{-8}	4×10^{-8}
Class 9 (La)	1×10^{-4}	4×10^{-8}	4×10^{-8}
Class 10 (U)	1×10^{-4}	3.6×10^{-7}	3.2×10^{-4}
Class 11 (Cd)	0.05	0.25	0.25
Class 12 (Sn)	0.05	0.16	0.16

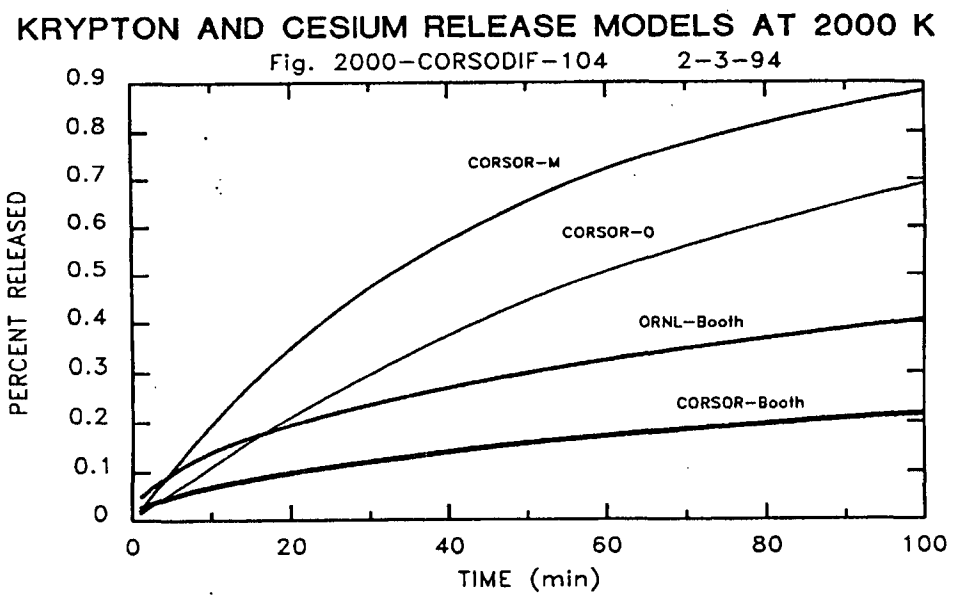

Figure 4 Release Fractions for Different Release Models – release temperature=2000 K.

[*Note CORSOR-M produces largest release whereas CORSOR-Booth produces the smallest release.*]

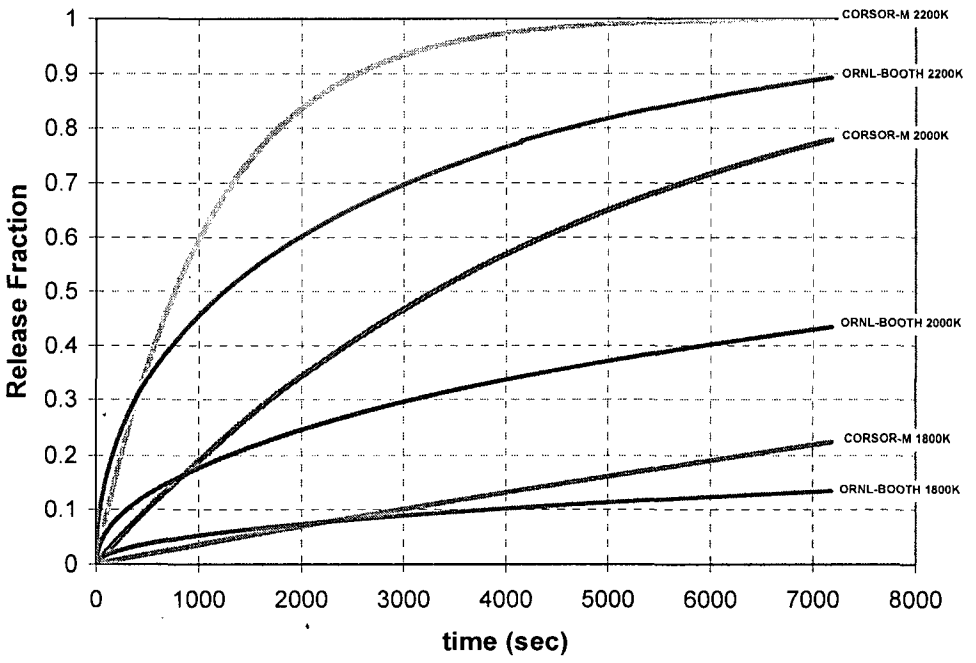

Figure 5 Release Fractions at Constant Temperature for ORNL-Booth versus CORSOR-M

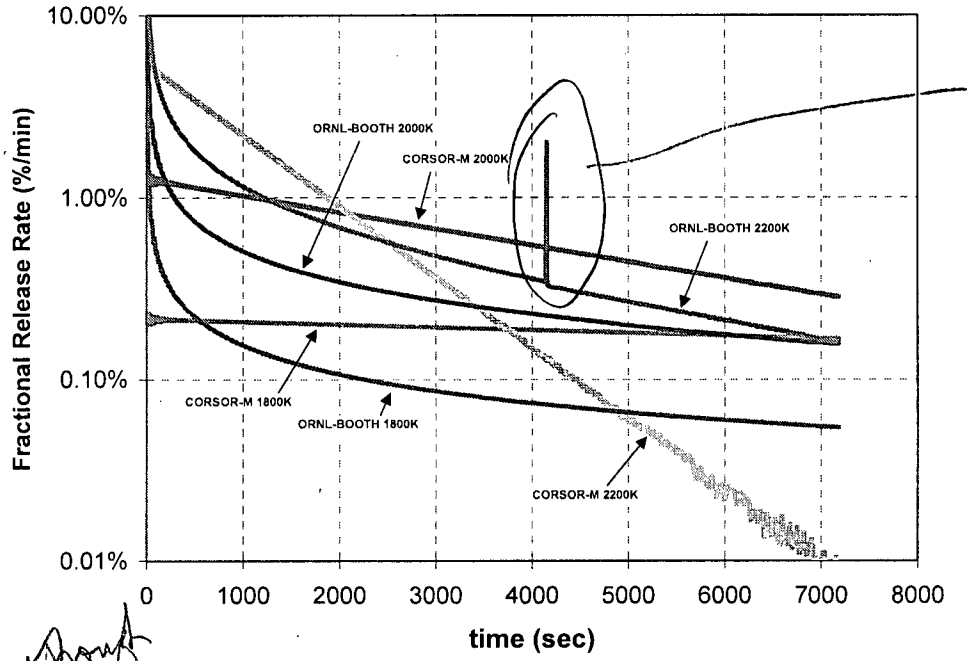

Figure 6 Fractional Release Rate (%/min) – the time derivative of release fraction.

While significant improvements in release behavior were obtained for the analysis of the FPT-1 test with the as-reported ORNL-Booth parameters, some additional modification to the MELCOR release model was pursued. Evidence from the Phebus experiments increasingly indicates that the dominant chemical form of released Cs is that of Cs_2MoO_4. This is based on deposition patterns in the Phebus experiment where Cs is judged to be in aerosol form at 700°C, explaining deposits in the hot upper plenum of the Phebus test section, and deposition patterns in the cooler steam generator tubes. In recognition of this, the vapor pressure of both Cs and Mo classes were defined to be that of Cs_2MoO_4. While having little effect on the net release of Cs, this change had a significant effect on the release of Mo. In MELCOR, by default the Mo vapor pressure is so exceedingly low that the net release is limited by the vapor transport term, as expressed in Eq. 7 and Eq. 8. Vapor pressures for selected fission product species are shown in Figure 7. Defining the Mo vapor pressure to be that of Cs_2MoO_4 produced significantly improved predicted Mo release rate with respect to observed FPT-1 releases, as will be seen in the following section.

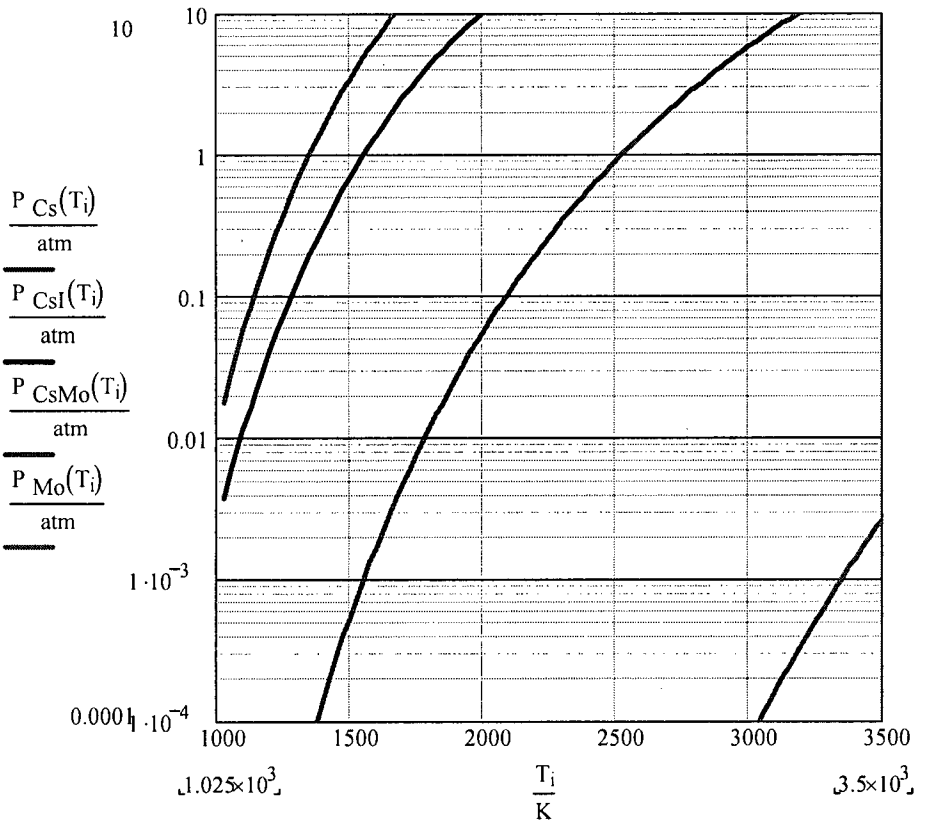

Figure 7 Vapor Pressure of Selected Species.

Assessment of Modified ORNL-Booth Model Against Phebus FPT-1

The Phebus program provides probably the best source of prototypic data on fission product release from irradiated fuel, benefiting from many lessons learned from earlier similar experimental efforts and from advances in testing technology, instrumentation, etc. A schematic of the Phebus test facility is shown in Figure 8. A previously irradiated fuel bundle of about a meter in length is situated in the irradiation cavity in the Phebus test reactor and caused to undergo severe damage from nuclear heating and oxidation by injected steam. Fission products released from the test bundle flow through a heated section representing the reactor coolant system, through a simulated steam generator tube where strong deposition can occur, and into a simulated containment where fission product fallout occurs.

PHEBUS facility

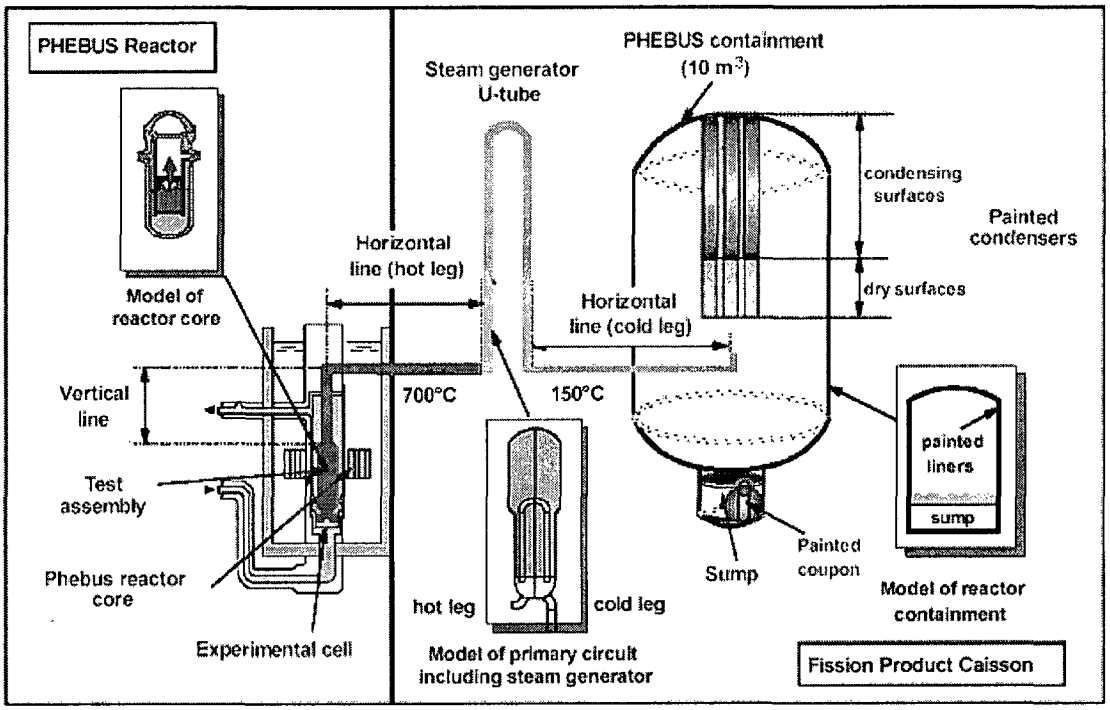

Figure 8 Schematic of the Phebus Test Facility Showing Test Fuel Bundle, Heated Lines, Steam Generator Tube and Simulated Containment.

Shown in Figure 9 is the nuclear heating history that was used in test FPT-1 to heat the bundle to simulate severe accident decay heating conditions. The chemical heating produced by steam-Zr oxidation is also shown in the figure. The temperature response of the test fuel is shown in Figure 10 where the temperature transient resulting from the additional oxidation heating is clearly evident. During this time, fission products are also released where oxidation conditions vary from oxidizing to reducing, depending on elevation in the test bundle. Figure 11 shows the end state of the test bundle following conclusion of the experiment.

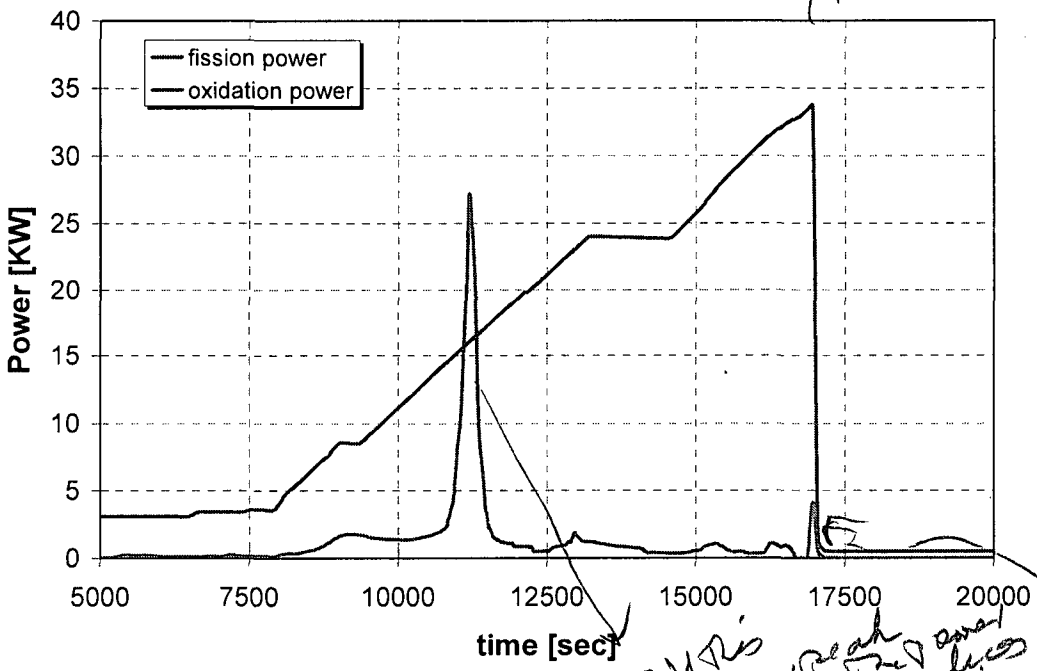

Figure 9 FPT-1 Nuclear and Chemical Heating History.

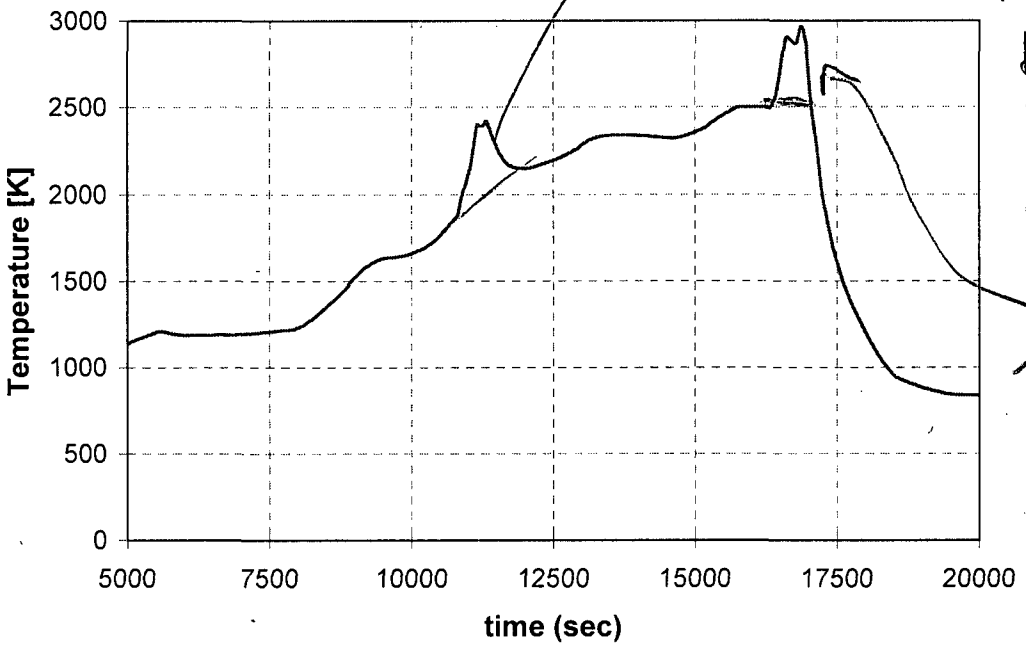

Figure 10 FPT-1 Maximum Bundle Temperature History.

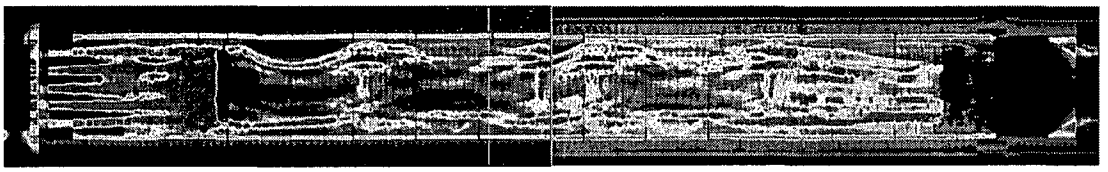

Figure 11 Emission Gamma Tomography of the End-State Condition of Test FPT-1.

The following figures (Figure 12 through Figure 23) show the results of using the modified ORNL-Booth model for fission product release in the FPT-1 analysis. In most cases significant improvement is realized in both the early release time signature as well as for total predicted released. Where available, Phebus data is presented. The release for the Barium class for the ORNL-Booth model is low relative to the data, whereas the release predicted using the CORSOR-M model is high. Improvement to this observed release proved illusive and it is believed that some adjustments to the vapor pressure for Ba to account for some not yet understood Barium speciation could produce some improvement. Adjustments to both vapor pressure and scaling factors were rationalized for Mo release based on Phebus program findings, producing good agreement with experiment. The Ru vapor pressure was increased by a factor of 10 arbitrarily to account for some greater volatility attributed to formation of oxides under moderately oxidizing conditions, and the Booth scaling factor was adjusted to gain agreement with experimental observations. The Booth scaling factor for UO_2 was increased significantly in order to gain agreement with test observations. This also is rationalized as due to effects of fuel oxidation and greater volatility of fuel oxides. Ce and La release parameters were not adjusted owing to lack of experimental basis, however, one could reason that their releases ought to roughly follow UO_2 release if fuel matrix stripping follows from fuel volatilization. The following section presents comparisons of the modified ORNL-Booth model against ORNL VI tests and more recent VERCORS test data.

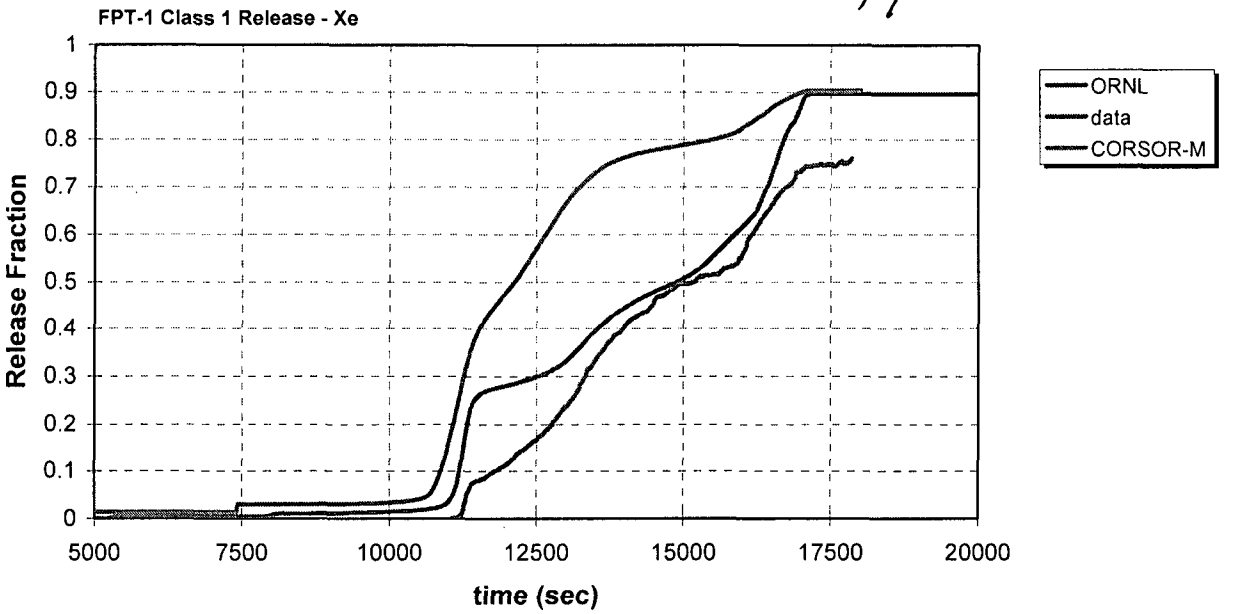

Figure 12 Comparison of ORNL-Booth versus CORSOR-M for Xe Release (Class 1).

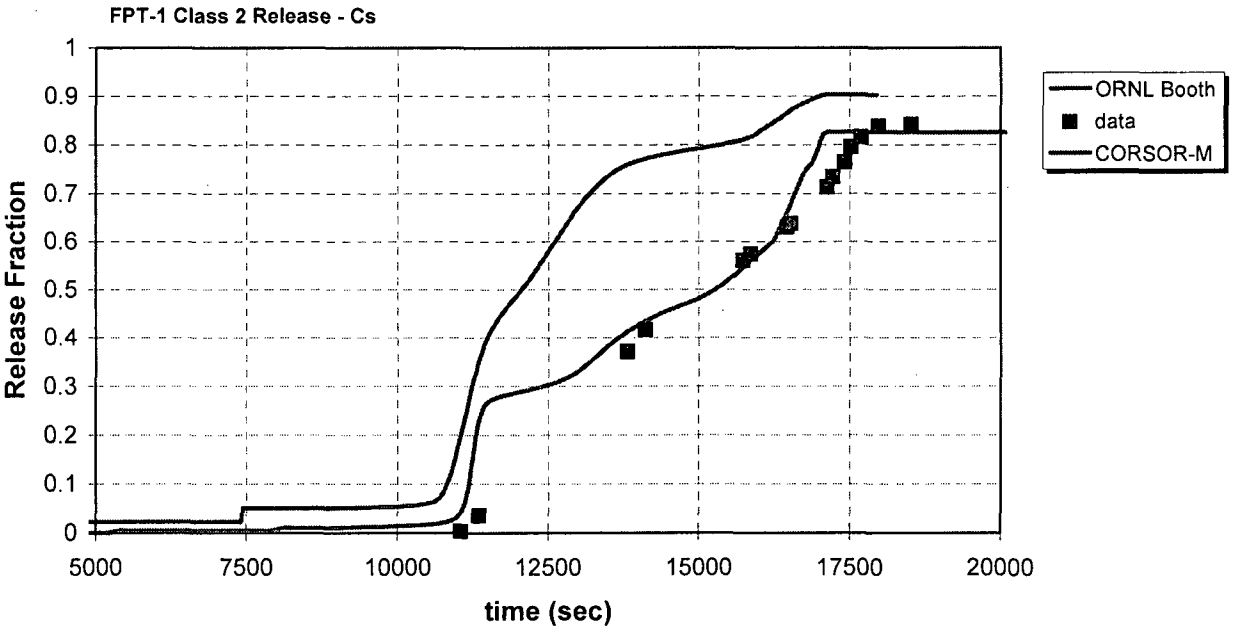

Figure 13 Comparison of ORNL-Booth versus CORSOR-M for Cs Release (Class 2).

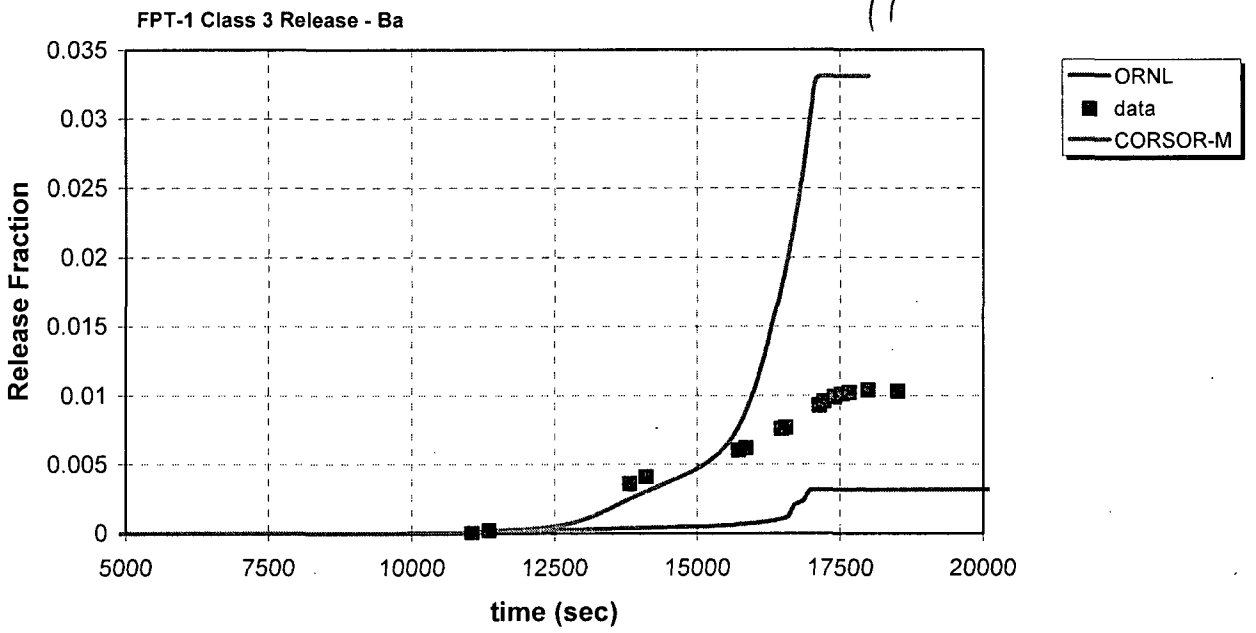

Figure 14 Comparison of ORNL-Booth versus CORSOR-M for Ba Release (Class 3).

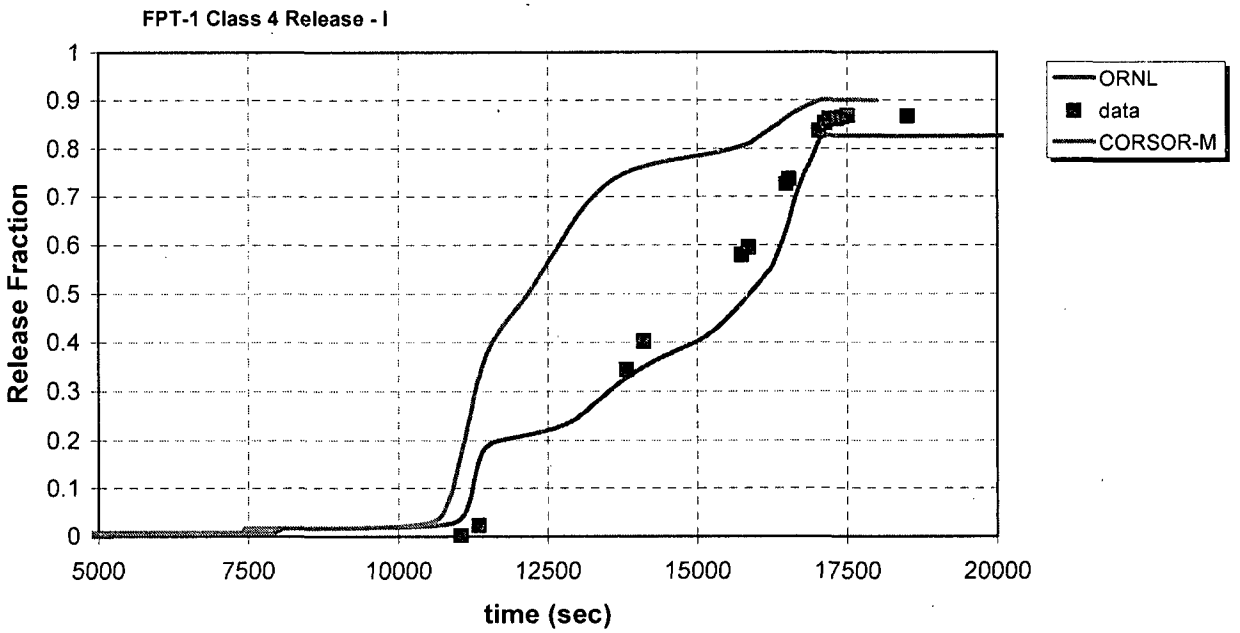

Figure 15 Comparison of ORNL-Booth versus CORSOR-M for I Release (Class 4).

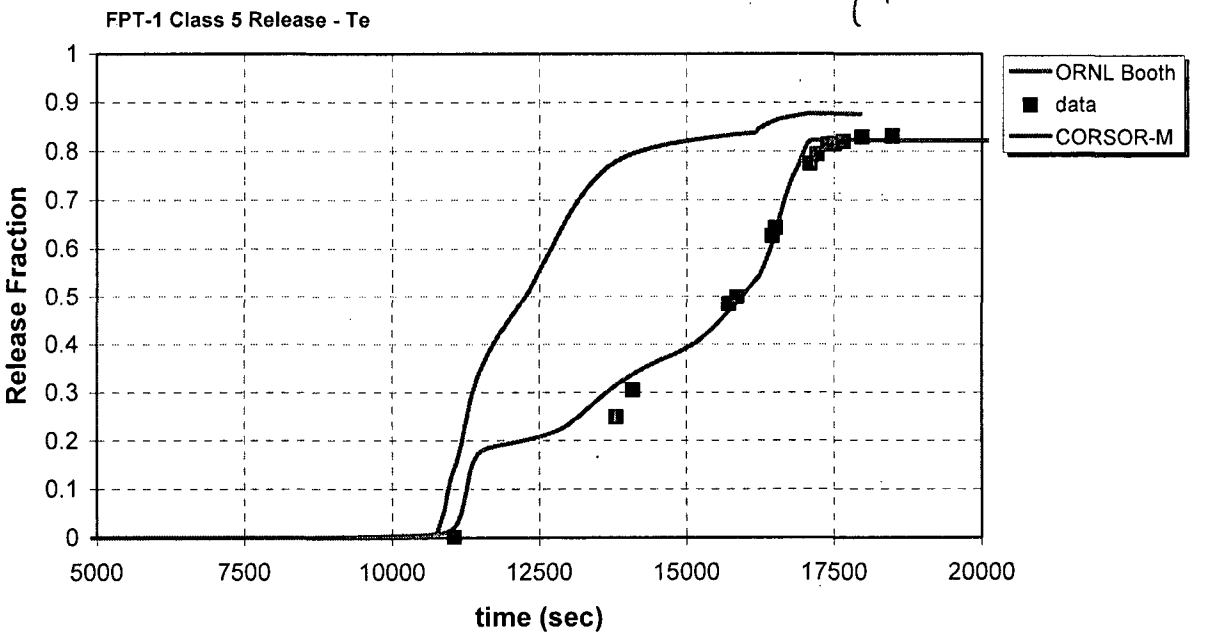

Figure 16 Comparison of ORNL-Booth versus CORSOR-M for Te Release (Class 5).

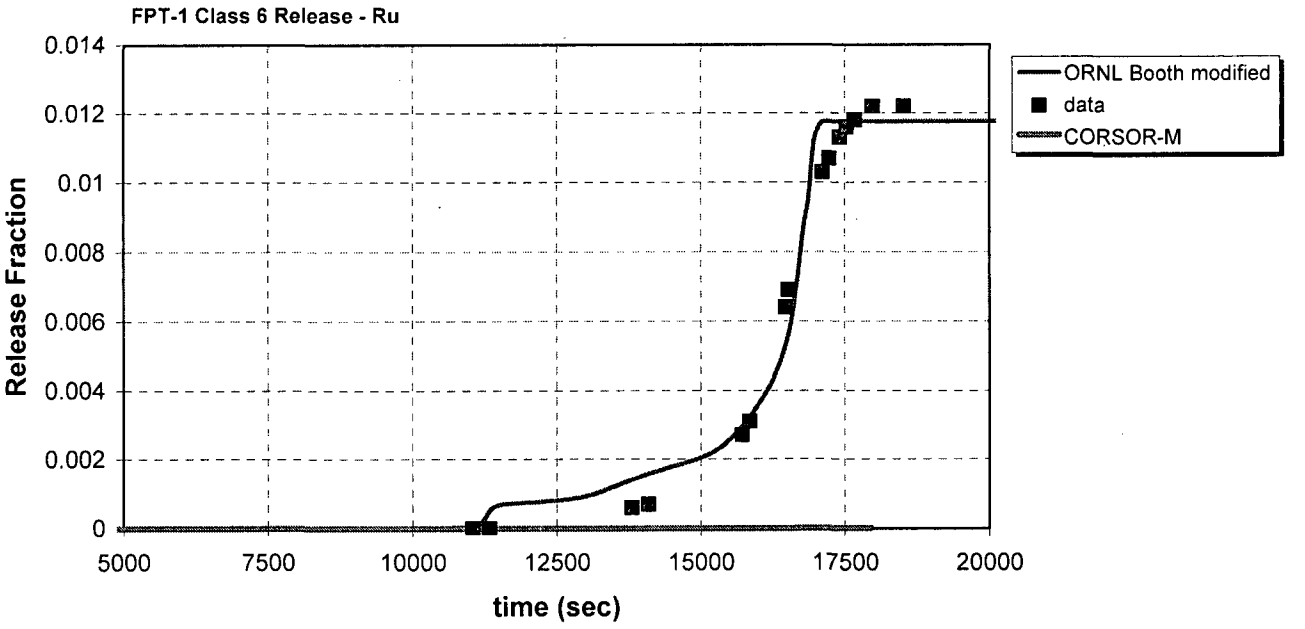

Figure 17 Comparison of ORNL-Booth versus CORSOR-M for Ru Release (Class 6).

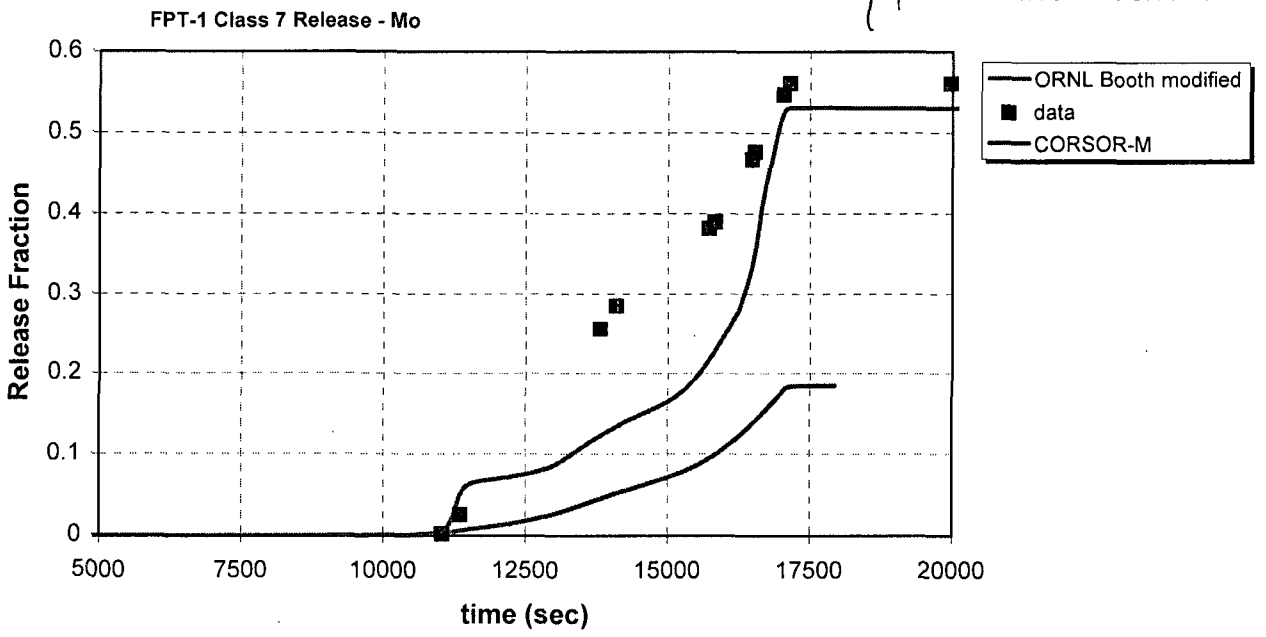

Figure 18 **Comparison of ORNL-Booth versus CORSOR-M for Mo Release (Class 7).**

[Note: The Mo vapor pressure was set to correspond to Cs_2MoO_4.]

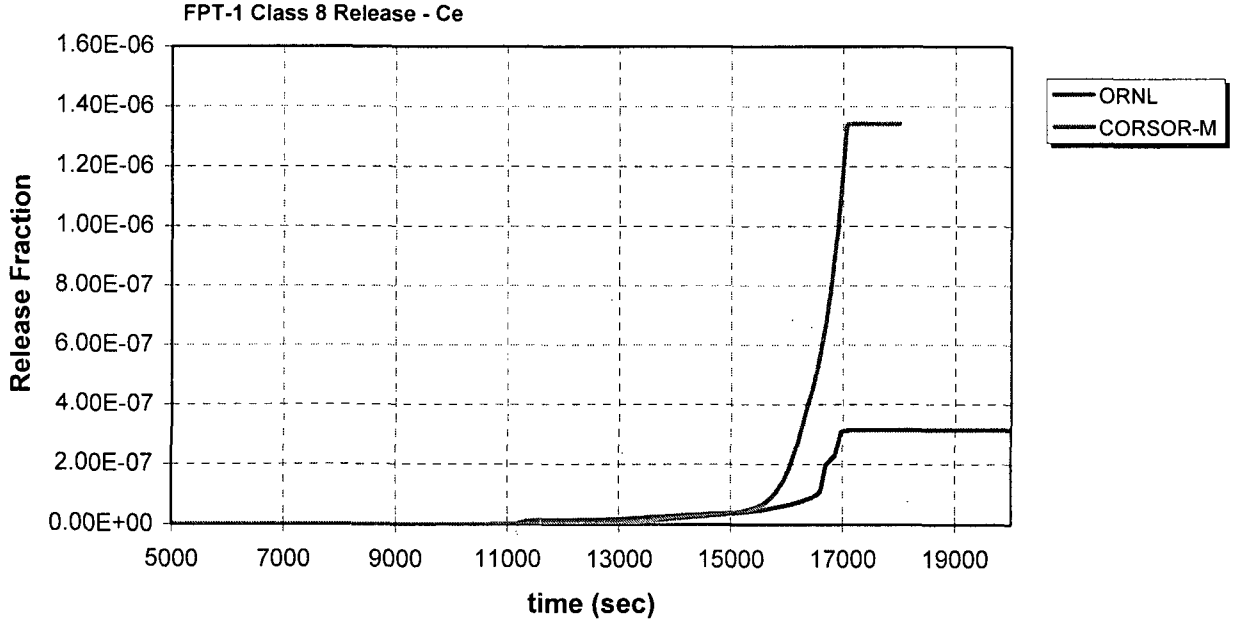

Figure 19 **Comparison of ORNL-Booth versus CORSOR-M for Ce Release (Class 8).**

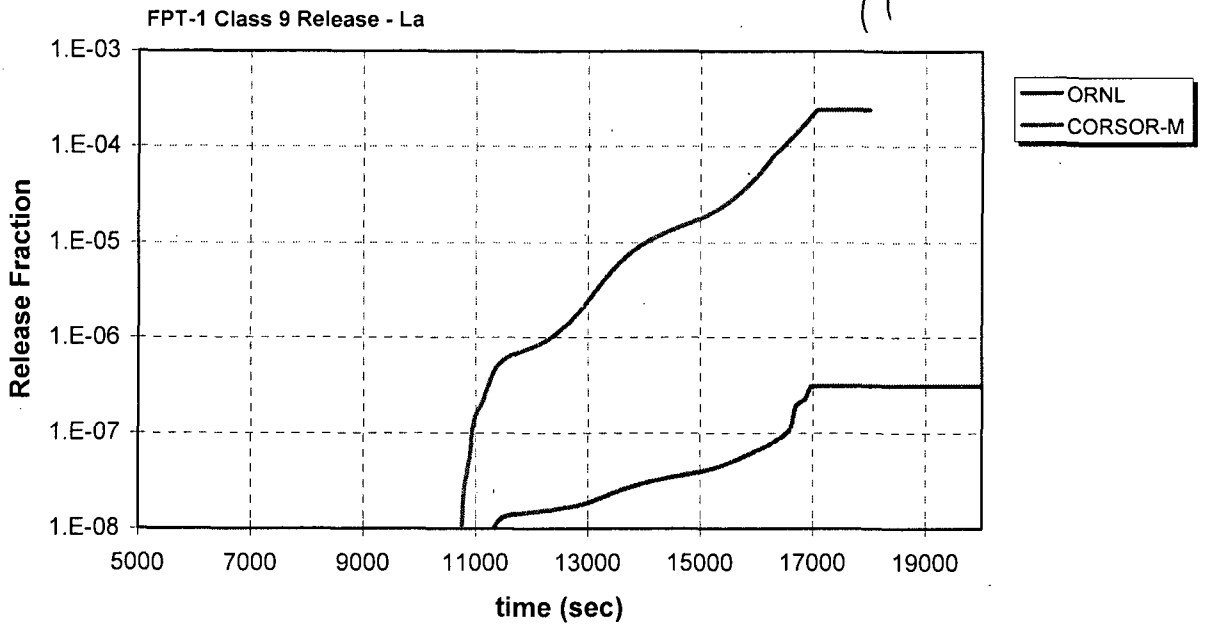

Figure 20 Comparison of ORNL-Booth versus CORSOR-M for La Release (Class 9).

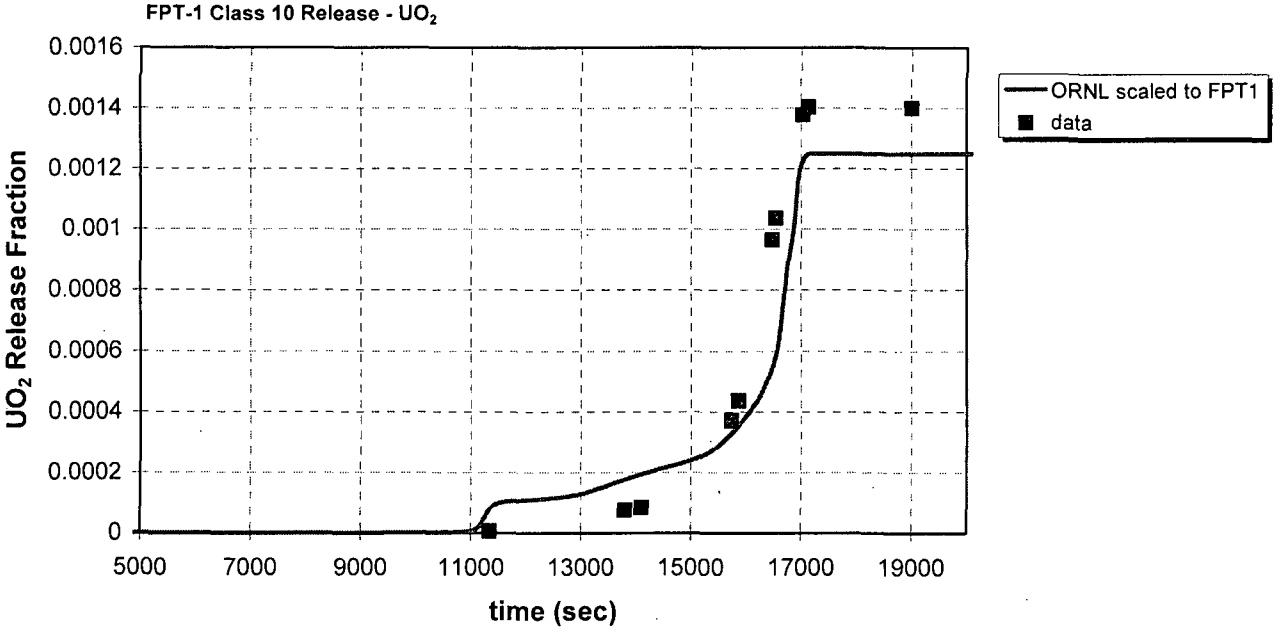

Figure 21 Comparison of ORNL-Booth versus CORSOR-M for UO_2 Release (Class 10).

[Note: The UO_2 scaling factor was adjusted to match observed releases. La and Ce releases are not expected to be greater than UO_2 release, but may be less owing to lower volatility.]

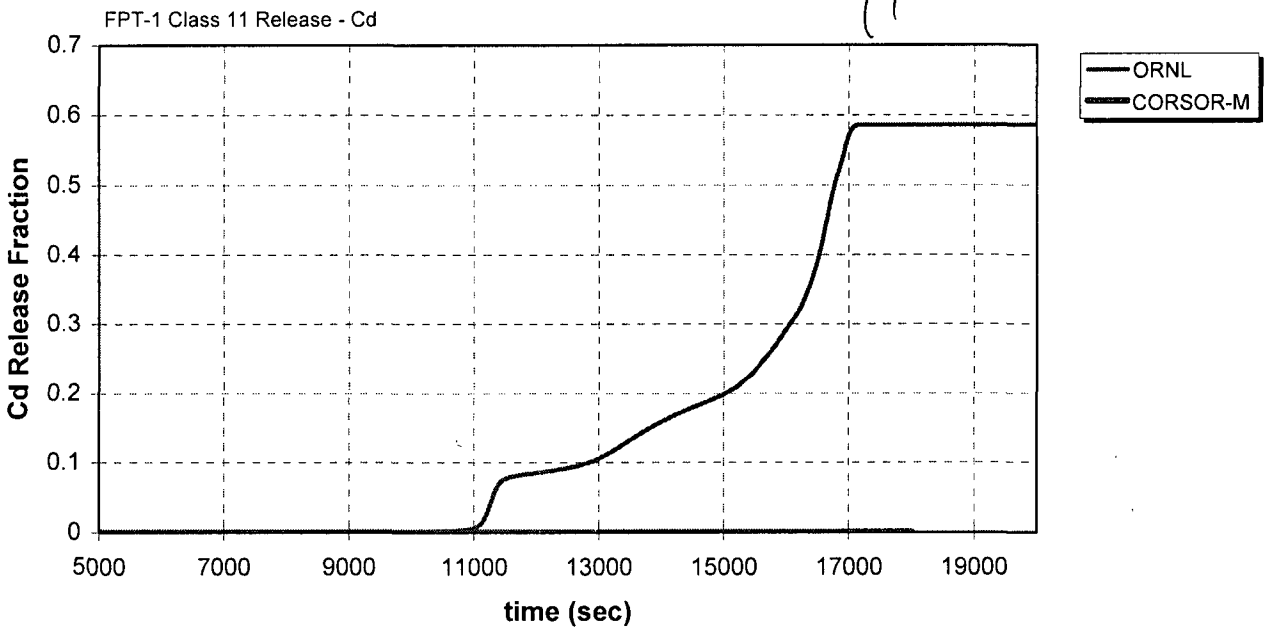

Figure 22 Comparison of ORNL-Booth versus CORSOR-M for Cd Release (Class 11).

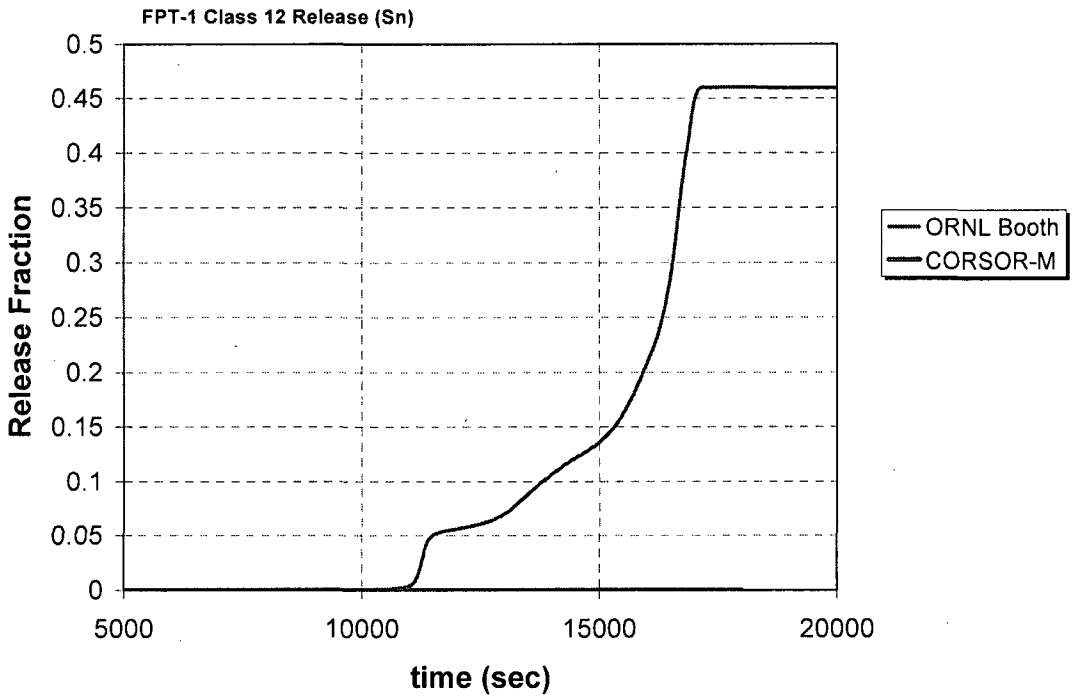

Figure 23 Comparison of ORNL-Booth versus CORSOR-M for Sn Release (Class 12).

Comparison to ORNL VI Tests and VERCOR Tests [43]

After optimizing the ORNL-Booth fission product release parameters for the FPT-1 experiment, is was of interest to compare the modified model to the original ORNL test data upon which the CORSOR-M models was developed. The following section explores the application of the modified ORNL-Booth release modeling to selected ORNL-VI test results and the VERCORS test data. The comparisons are made mainly to the Cs release observed in these experiments since all other releases are simply scaled to the Cs release in the Booth implementation in MELCOR, and these data were readily available. In the case of VERCORS 4, more data on release of other fission products were readily available and comparisons to these releases included. The MELCOR models were obtained form a recent IBRAE MELCOR Validation exercise [40] investigating the MELCOR default release models. The experimental data are taken from reference [40]. These analyses were performed using a MELCOR model of these simple experiments. The present analyses make use of the modified ORNL-coefficients and compare results with the MELCOR default CORSOR-M release model. A schematic of the VERCORS testing facility is shown in Figure 24, the general layout is similar in the ORNL VI tests. The tests examined are summarized in Table 4. The tests involved both oxidizing and reducing conditions.

G. Ducros et al. / Nuclear Engineering and Design 208 (2001) 191–203

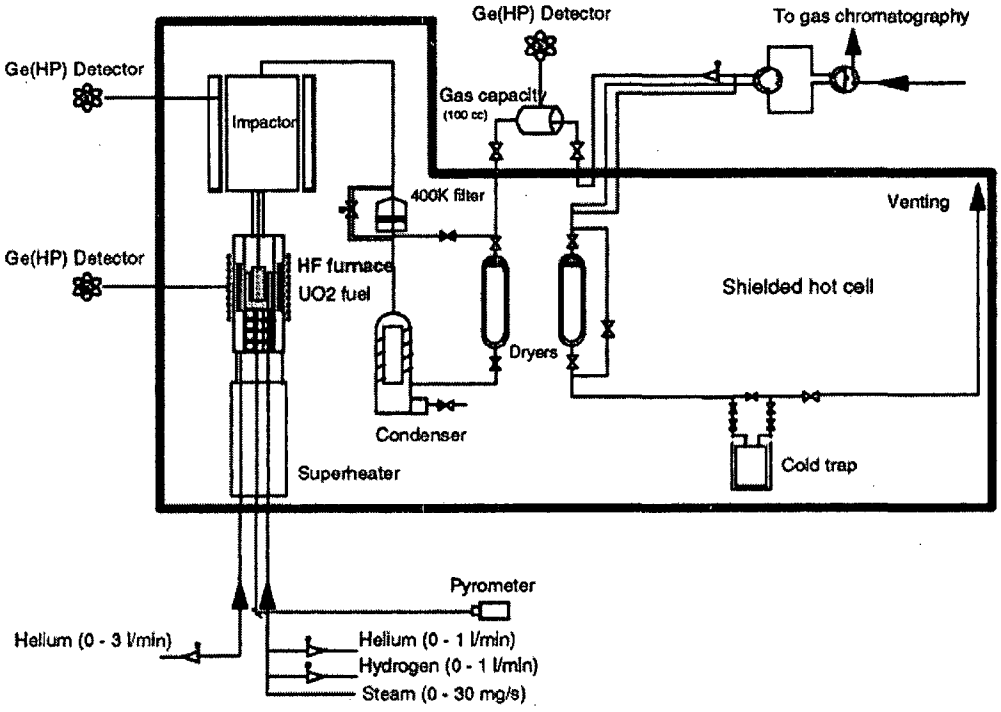

Figure 24 Schematic of VERCORS Test Facility for Measuring Fission Product Release from Small Fuel Samples.

Table 4 Test Conditions for Selected ORNL VI Tests and VERCORS Tests

Test	Hydrogen	Steam	Max Temperature
ORNL VI-2	0	1.8 liter/min	2300 K
ORNL VI-3	0	1.6 liter/min	2700 K
ORNL VI-5	0.4 liter/min	0	2740 K
VERCORS 2	0.027 gm/min	1.5 gm/min	2150 K
VERCORS 4	0.012 gm/min	1.5 – 0 gm/min	2573K

In almost all cases, the modified ORNL-Booth model produces improved signatures, as shown in Figure 25 through Figure 27 for the VI tests and in Figure 28 through Figure 34 for the VERCORS tests.

In Test VI-2 run under steam conditions, the peak temperature attained was ~2300 K. Both models over-predicted the Cs release for this test, with the modified ORNL-Booth treatment performing slightly better (Figure 25). Test VI-3 was similar to VI-2 except that higher temperatures were attained. In this test, both models were closer to the data, and again the modified ORNL-Booth model performing somewhat better (Figure 26). From these two tests, it would seem that release rate in the 2300 K range is still slightly over-predicted for oxidizing conditions. Test VI-5 conducted under reducing conditions was well predicted by both models, as shown in Figure 27. Table 5 through Table 7 provides total releases predicted by CORSOR-M and ORNL-Booth compared with totals reported for the ORNL VI tests 2, 3 and 5.

Both VERCORS 2 and 5 were run in mixed conditions with both steam and hydrogen. In VERCORS 5, the steam flow was reduced to zero (reducing conditions) for the high temperature plateau. Test VERCORS 2, like ORNL-VI2 was performed at a lower temperature and produced a comparatively lower Cs release (Figure 28). The modified ORNL-Booth model captured this lower release where the CORSOR-M model did not. Test VERCORS 4 was performed under completely reducing conditions during the release phase. In this case CORSOR-M under-predicted release, whereas the modified ORNL-Booth model reasonable well captured the release behavior.

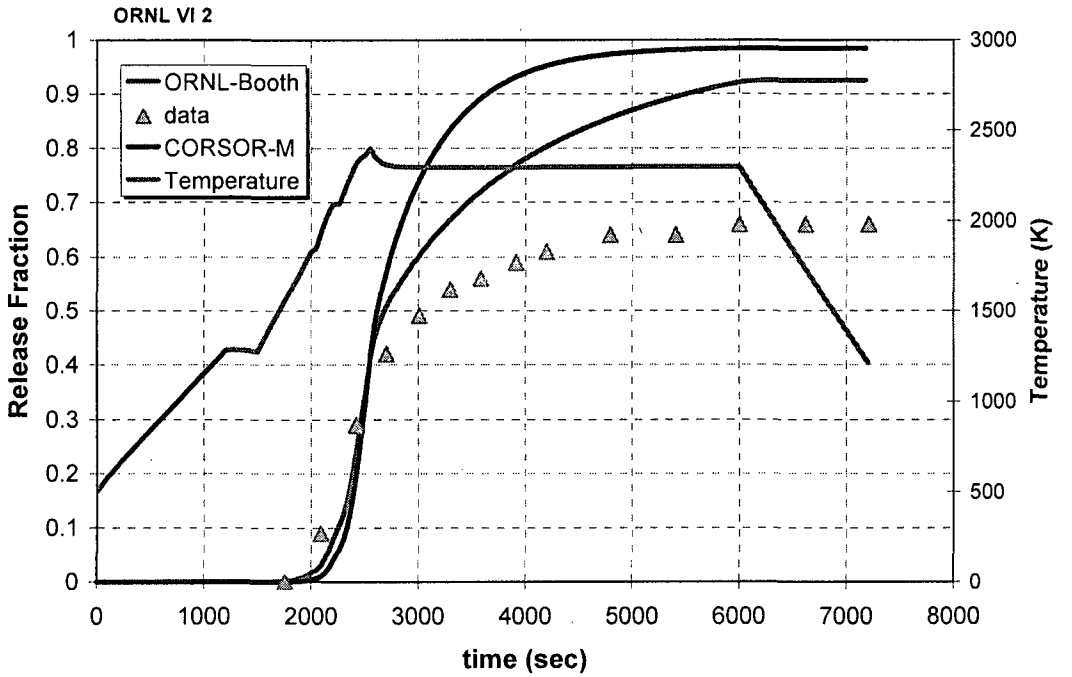

Figure 25 **Comparison of Cs Release for Modified ORNL-Booth with CORSOR-M for VI-2 Run under Steam Oxidizing Conditions.**

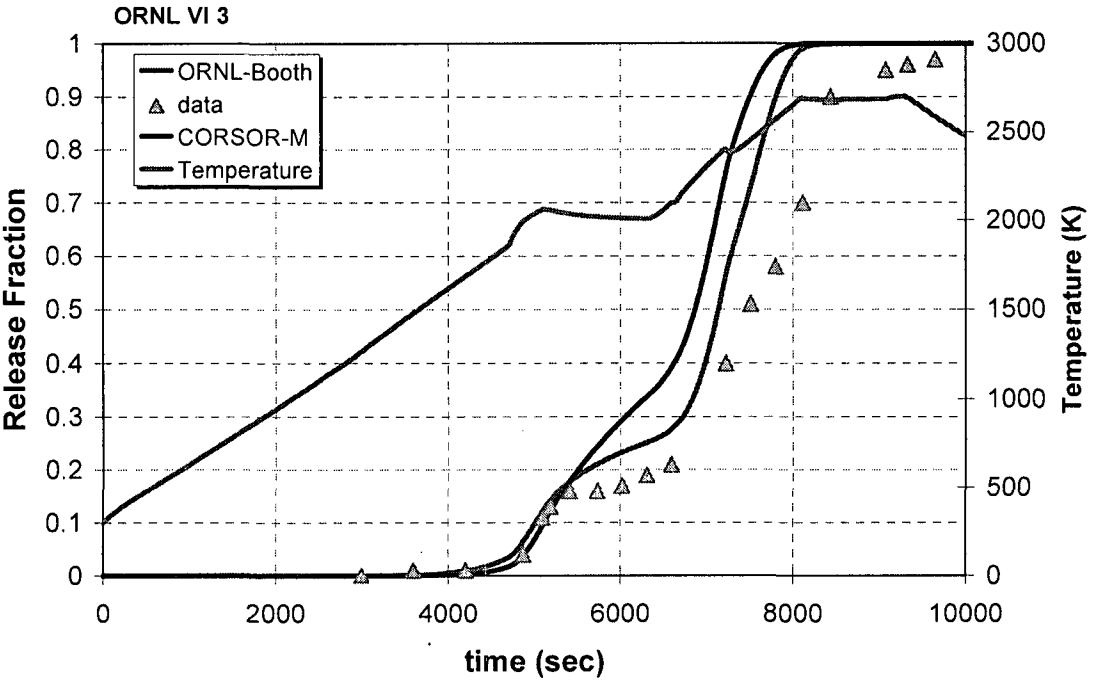

Figure 26 **Comparison of Cs Release for Modified ORNL-Booth with CORSOR-M for VI-3 Performed under Steam Oxidizing Conditions.**

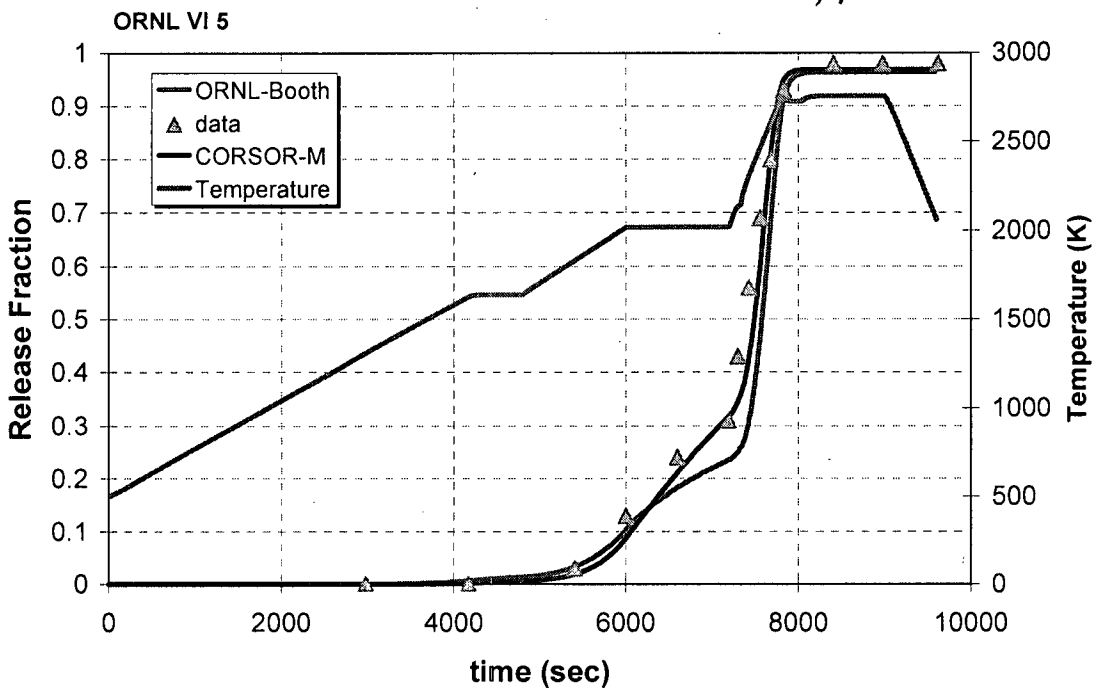

Figure 27 **Comparison of Cs Release for Modified ORNL-Booth with CORSOR-M for VI-5 Performed under Steam Reducing Conditions.**

Table 5 **Total Release from ORNL VI-2**

	Experiment	CORSOR-M	ORNL-Booth
Kr	*	0.98	0.92
Cs	0.67	0.98	0.92
Ba	0.18	0.003	0.002
Sr		0.003	0.002
I	0.4	0.98	0.81
Te		0.97	0.81
Ru		1×10^{-7}	0.006
Mo	0.86	0.06	0.42
Ce		1×10^{-8}	1.1×10^{-7}
Eu		1×10^{-5}	1.1×10^{-7}
U	0.003	1×10^{-5}	0.001
Sb	0.68	0.04	0.93

Table 6 Total Release from ORNL VI-3

	Experiment	CORSOR-M	ORNL-Booth
Kr	1	1	1
Cs	1	1	1
Ba	0.3	0.04	0.004
Sr	0.03	0.04	0.004
I	0.8	1	1
Te	0.99	1	0.99
Ru	0.05	10^{-5}	0.03
Mo	0.77	0.15	0.88
Ce	0	2×10^{-6}	4×10^{-7}
Eu	0	0.0005	4×10^{-7}
U	0	0.0005	0.003
Sb	0.99	0.2	0.93

Table 7 Total Release from ORNL VI-5

	Experiment	CORSOR-M	ORNL-Booth
Kr	1	0.97	0.96
Cs	1	0.97	0.96
Ba	0.76	0.04	0.005
Sr	0.34	0.04	0.005
I	0.7	0.97	0.96
Te	0.82	0.95	0.96
Ru	0	10^{-5}	0.03
Mo	0.02	0.11	0.85
Ce	0.02	3×10^{-6}	4×10^{-7}
Eu	0.57	0.0008	4×10^{-7}
U	0	0.0008	0.003
Sb	0.18	0.19	0.89

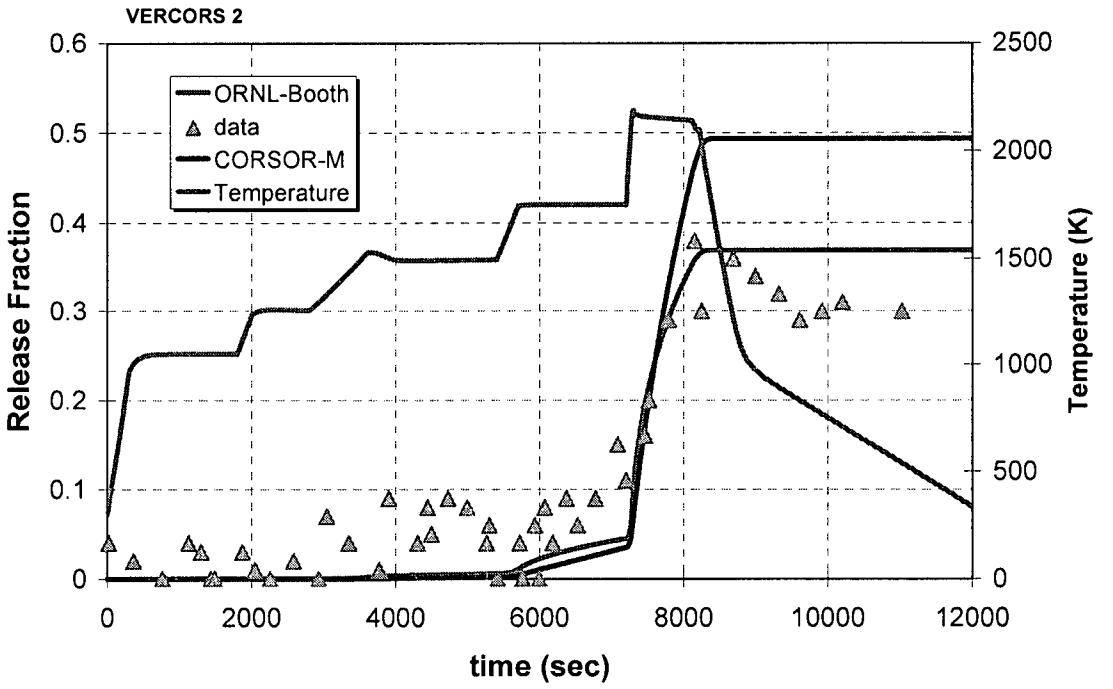

Figure 28 Comparison of Cs Release for Modified ORNL-Booth with CORSOR-M for VERCORS-2.

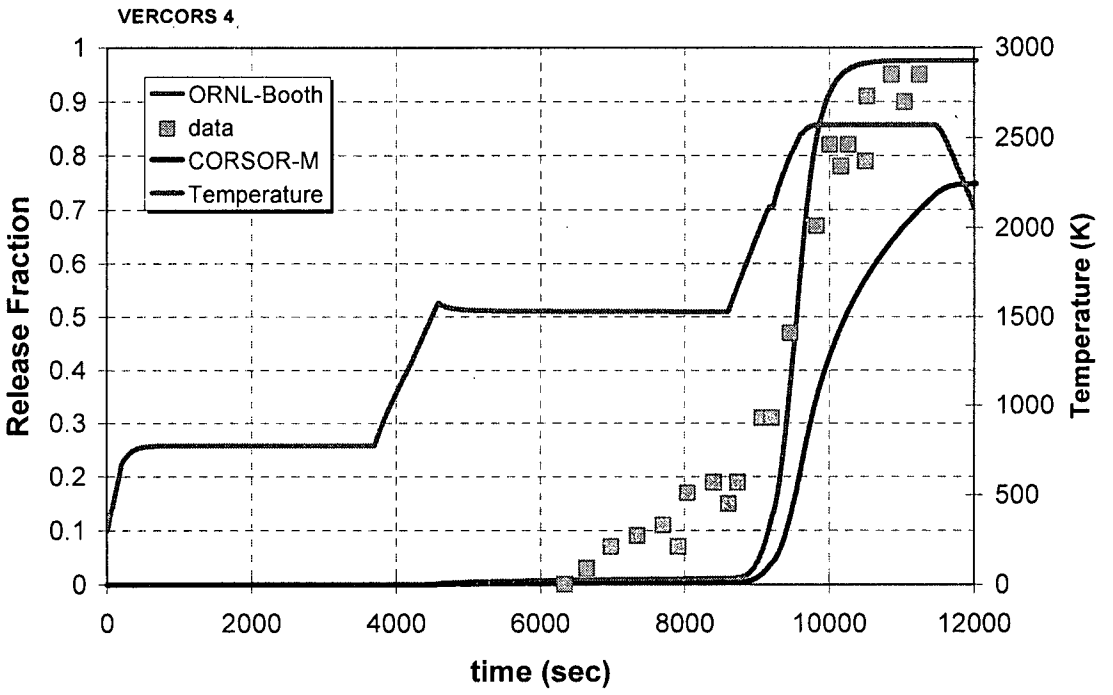

Figure 29 Comparison of Cs Release for Modified ORNL-Booth with CORSOR-M for VERCORS-4.

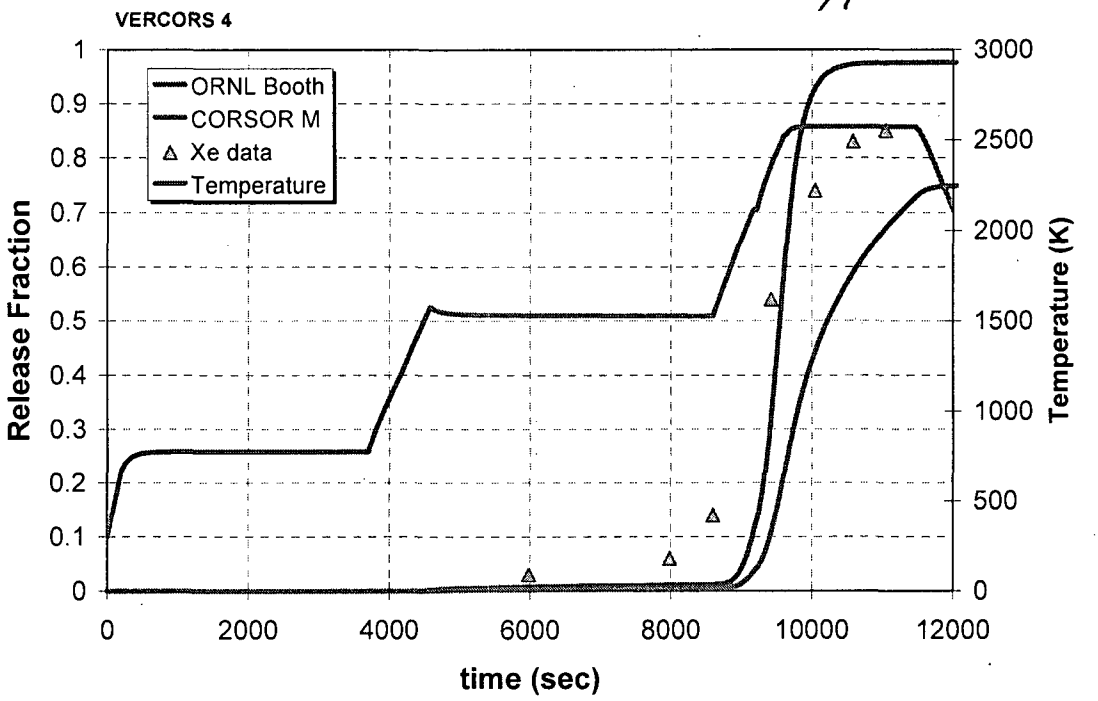

Figure 30 **Comparison of Xe Release for Modified ORNL-Booth with CORSOR-M for VERCORS-4.**

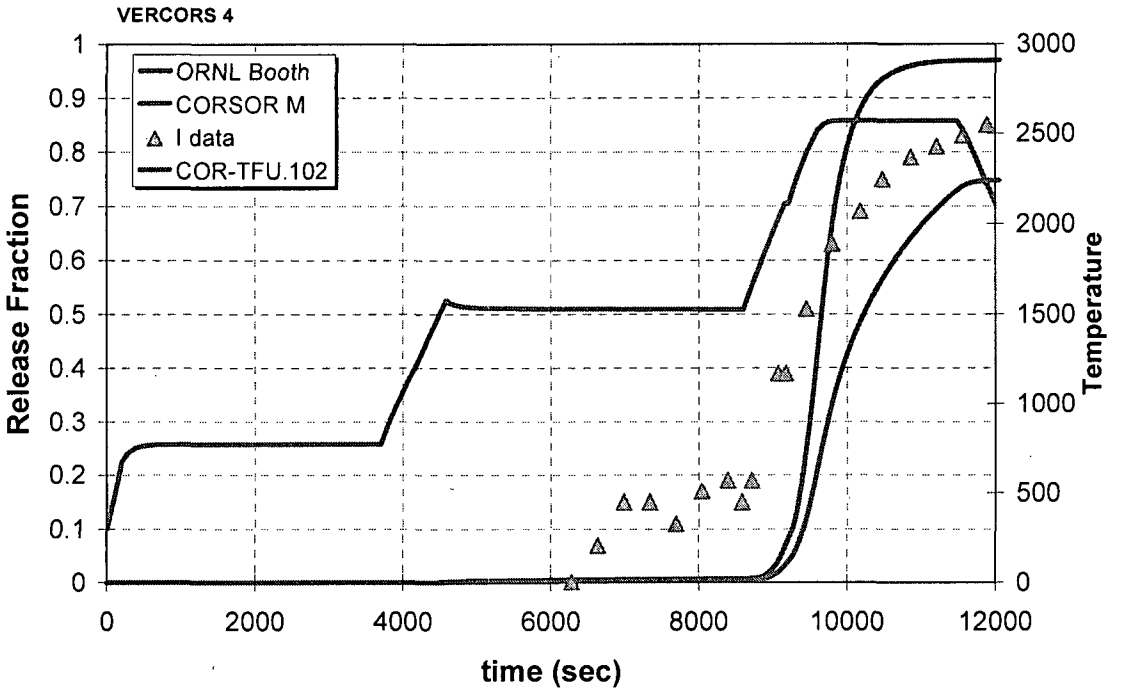

Figure 31 **Comparison of Iodine Release for Modified ORNL-Booth with CORSOR-M for VERCORS-4.**

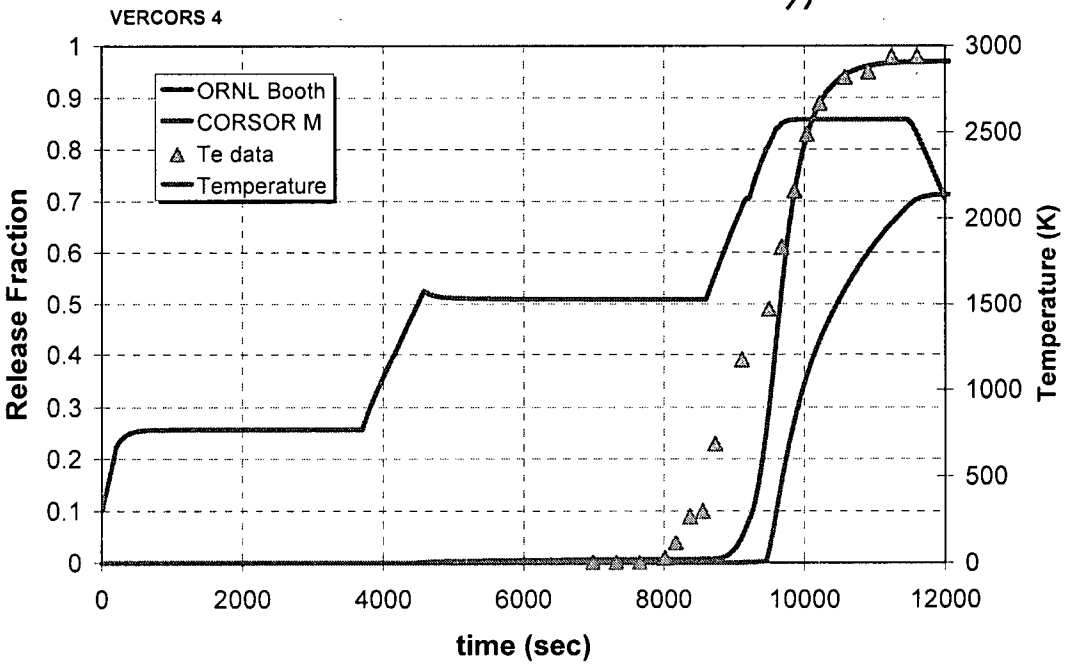

Figure 32 Comparison of Te Release for Modified ORNL-Booth with CORSOR-M for VERCORS-4.

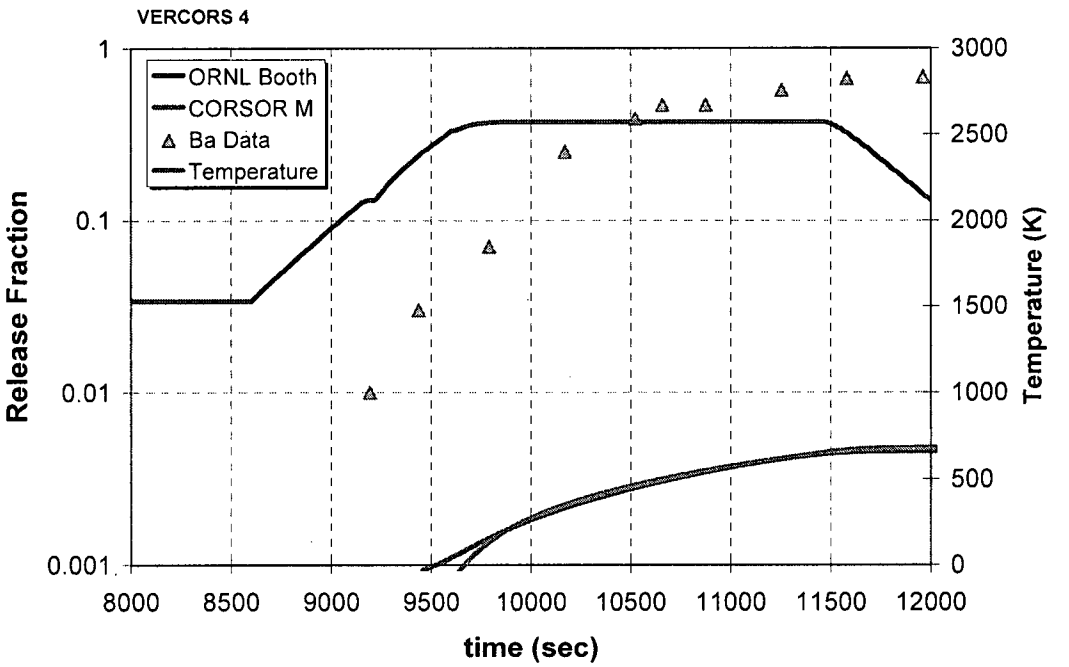

Figure 33 Comparison of Ba Release for Modified ORNL-Booth with CORSOR-M for VERCORS-4.

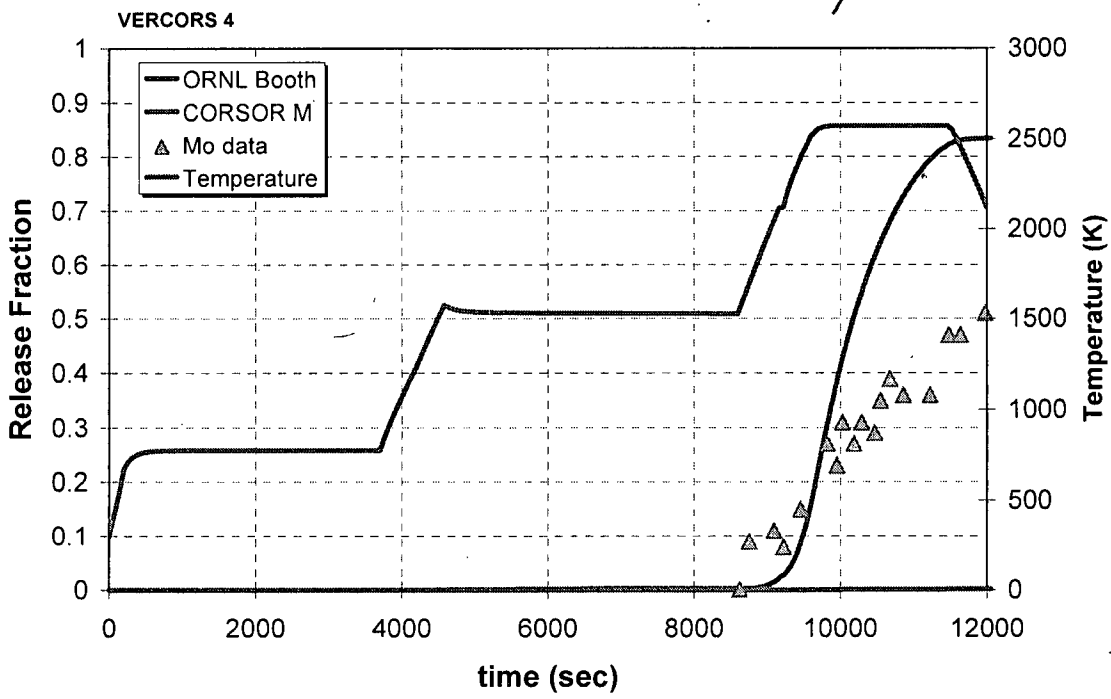

Figure 34 Comparison of Mo Release for Modified ORNL-Booth with CORSOR-M for VERCORS-4.

On balance, the use of the modified ORNL-Booth model produces significantly improved predictions for both the in-pile Phebus FPT-1 test as well as for the original small scale ORNL VI and French VERCORS tests upon which the original CORSOR and Booth models were developed. Barium behavior however remains somewhat problematic in that the small-scale tests generally predict release greater Ba than is ever observed in the in-piles tests. We believe this is due to the fact that in the small-scale tests, the cladding is generally completely oxidized, whereas considerably less coherent conditions are encountered in the in-pile integral tests. It is conjectured that the Ba speciation in the small-scale tests is more volatile than that produced in the in-pile tests where unoxidized Zr is plentiful.

Evaluation of Fission Product Deposition Modeling

Deposition in FPT-1 Circuit (RCS Deposition)

The modified ORNL-Booth release models have been shown to produce favorable release signatures when examining the Phebus FPT-1 test and produce good comparisons with the ORNL VI and French VERCORS tests. The modifications to the vapor pressures for Cs and Mo, which produced favorable release behavior in FPT-1, will have an effect on the subsequent deposition of these species in the RCS piping. The effect is illustrated in the following two figures showing deposition patterns in the Phebus FPT-1 test circuit and model containment.

Figure 35 shows the predicted deposition distribution in the FPT-1 experiment when the default CORSOR-M release model was used. While the total Cs release compares reasonably well with the measured value, and the total Cs transported to the containment is about right, the distribution of Cs deposits in the heated test section above the fuel (upper plenum) and in the steam generator tube do not compare all that well with the experiment. Deposits in the steam generator are over-predicted and deposits in the heated plenum above the fueled region are under-predicted. In fact, deposits of Cs in the plenum were never greater than 0.1% and were predicted to be completely revaporized before the end of the test. Under-predicting deposition in the hot plenum region is a big factor in the over-predicting of the steam generator tube deposits.

Figure 36 shows the Cs distribution predicted for FPT-1 when the modified ORNL-Booth model is used. The lower vapor pressure of the presumed Cs_2MoO_4 results in Cs predicted to be in aerosol form in the hot upper plenum region and as a result, Cs deposited in the upper plenum remains for the duration of the test. This together with a slightly lower total Cs release results in half as much predicted to be deposited in the steam generator tubes, considerably closer to the observed tube deposition. The amount reaching the containment remains about the same, which from a "release to the environment" point of view, one can observe that either model retains about the right amount of fission product within the simulated RCS. The changes in Cs deposition within the RCS could of course alter the decay heat distributions throughout the RCS, which in turn could affect revolatilization of other more volatile deposited species, such as CsI, which is transported in addition to the presumed dominant Cs_2MoO_4.

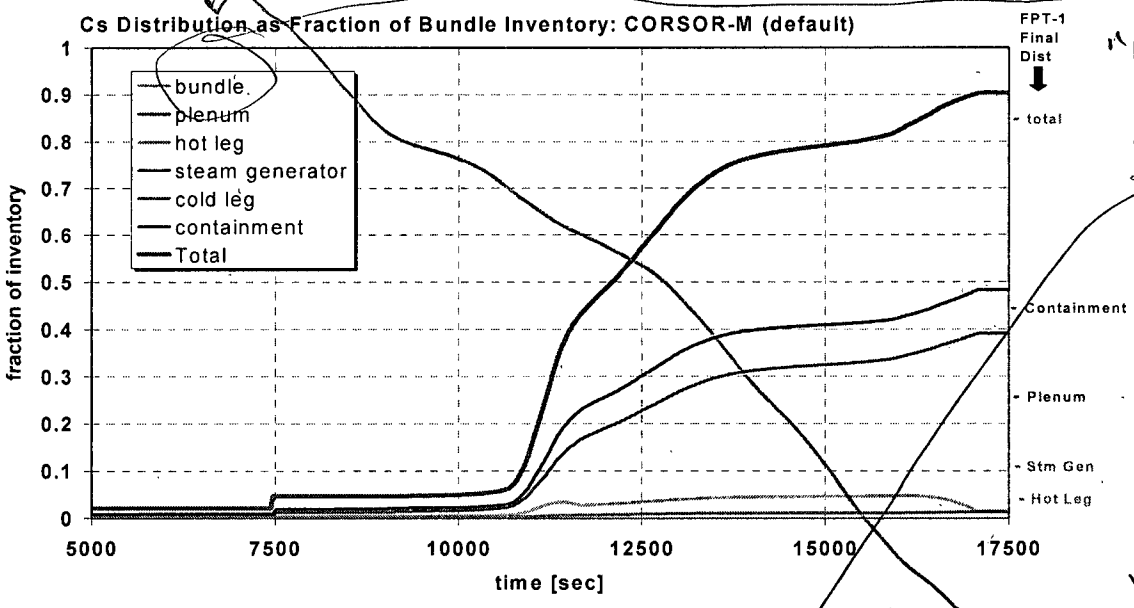

Figure 35 MELCOR-predicted Fission Product Deposition in FPT-1 Circuit Using Default CORSOR-M Release Modeling.

[Note: Predicted plenum deposits for this case were less than 0.1%, not visible on this scale, and were subsequently revaporized.]

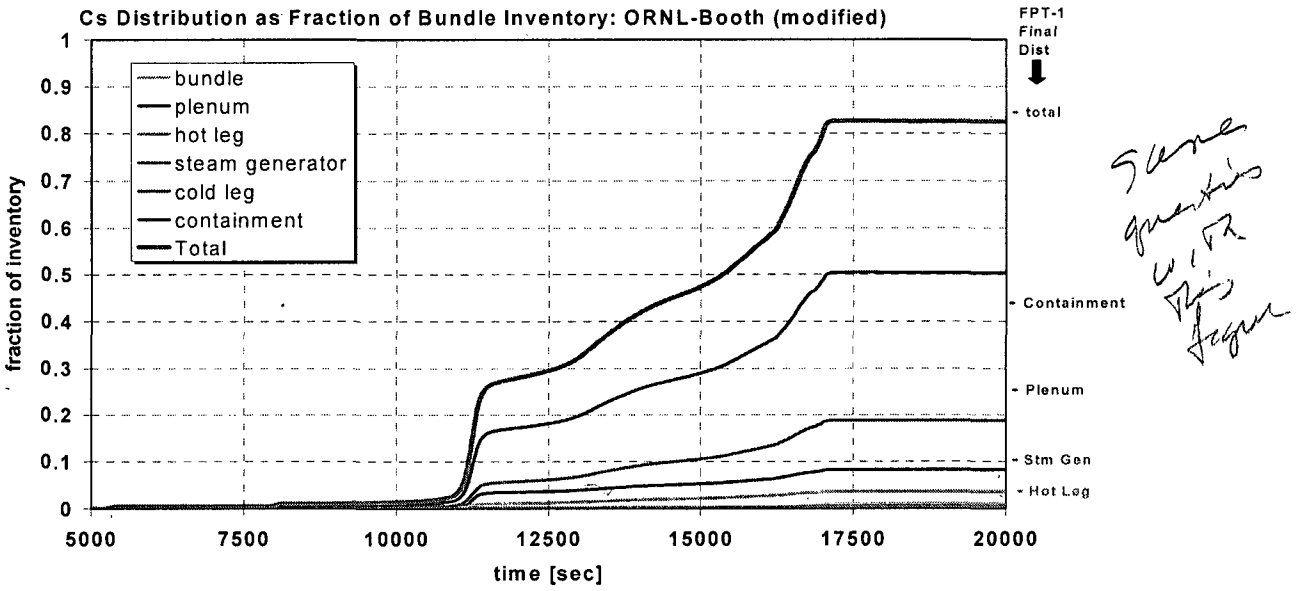

Figure 36 MELCOR-predicted Fission Product Deposition in FPT-1 Circuit Using Default ORNL-Booth Release Modeling.

Deposition within the Phebus Containment

For completeness, the deposition behavior calculated for the FPT-1 containment model is shown in the following figures. Shown is the total airborne aerosol mass predicted using the sources resulting from the ORNL-Booth release modeling. The suspended mass is normalized to the peak value in order to make comparison to the measured data, this normalization made necessary because of differences between the magnitude of mass predicted to be transported to the containment, and the measured value. MELCOR predicted only about half of the suspended total mass that was measured. The discrepancy is due to not activating the Ag release model for the Ag/In/Cd control rods and the Re in the experiment thermocouples.

The overall depletion signature prior to the peak airborne value compares quite well. After reaching the maximum value however, the MELCOR predicted suspended mass depletes less rapidly than was actually observed. This is apparently due to MELCOR under-predicting the particle size as shown in Figure 38, and consequently under-predicting the gravitational settling component of containment deposition. Certainly the under-prediction of the suspended mass by a factor of two also resulted in lower aerosol number concentration, perhaps significantly so if the mass is missing from the smaller particle size range, and this may in turn have resulted in slower particle agglomeration rate and therefore smaller agglomerated particle sizes. If so, this could explain the lower aerosol depletion rate by gravitational settling.

Diffusiophoresis is the other dominant form of aerosol deposition in the FPT-1 containment, and may also be under-predicted, however test data do not provide resolution in this respect. Under-prediction of the containment depletion rate errs on the conservative side since more

fission products remain suspended in this analysis that might be available for release to the environment. This report will be updated when a new analysis is completed including MELCOR's Ag release model.

New Speciation Modeling[4]

Based on the chemical analysis of the deposition and transport of fission products through the simulated reactor coolant circuit to the containment in the Phebus facility tests, the cesium was found to have combined with molybdenum as cesium molybdate. This was unexpected because molybdenum has a low vapor pressure and was not expected to be released in large quantities. However, the molybdenum combined with the cesium and formed cesium molybdate. The resultant vapor pressure of cesium molybdate is much higher than molybdenum (see Figure 7). Consequently, the chemical speciation of the cesium was changed from cesium hydroxide and cesium iodide to cesium molybdate and cesium iodide. In both cases, all the iodine was assumed to be bound with cesium. In addition, the remaining cesium is now modeled as bonding with molybdenum based on the Phebus results. A small portion of cesium that forms cesium hydroxide is modeled for the initial gap release (also see Appendix B for details).

In summary, the best practices speciation manually reconfigures (i.e., through user input specifications) the cesium, iodine, and molybdenum radionuclide and decay heat classes as follows,

- Class 2 - Characteristic released compound is CsOH with the default inventory representative of the cesium in the fuel gap except what is already included in Class 16.
- Class 4 – Characteristic released compound is I_2 with the default inventory completely transferred to Class 16.
- Class 7 – Characteristic released compound is Mo with the default inventory reduced by the amount allocated to Class 17.
- Class 16 - Characteristic released compound is CsI with the default inventory representing all of Class 4 and the sufficient Cesium from Class 2 to form CsI.
- Class 17 – Characteristic released compound is Cs_2MoO_4 with the remainder of the Class 2 cesium not in the gap (already included in Class 2) or already combined with Class 16. Sufficient molybdenum is included from Class 7 to Class 17 to form Cs_2MoO_4. The released vapor pressure and compound mass is consistent with Cs_2MoO_4.

The gap inventory is specified as follows [47],

- Class 1 – 5% of the noble gases
- Class 2 – Required amount of cesium not in gap of Class 16 to yield a 5% total cesium gap inventory

[4] Whereas the recent modifications to Version 1.8.6 (Version YR) for the SOARCA program implemented the new ORNL-Booth fission product release model as the new default model (see Section 3.2), the associated reconfiguration of the radionuclide masses must be done through user input specification as summarized in this section.

- Class 3 – 1% of the barium inventory
- Class 4 – No Class 4 iodine in gap
- Class 5 – 5% of the tellurium inventory
- Class 7 – No mass in the gap
- Class 16 – 5% of the Class 16 inventory to yield 5% of the total iodine inventory in the gap
- Class 17 – No mass in the gap (all Cs gap mass is located in Classes 2 and 16)

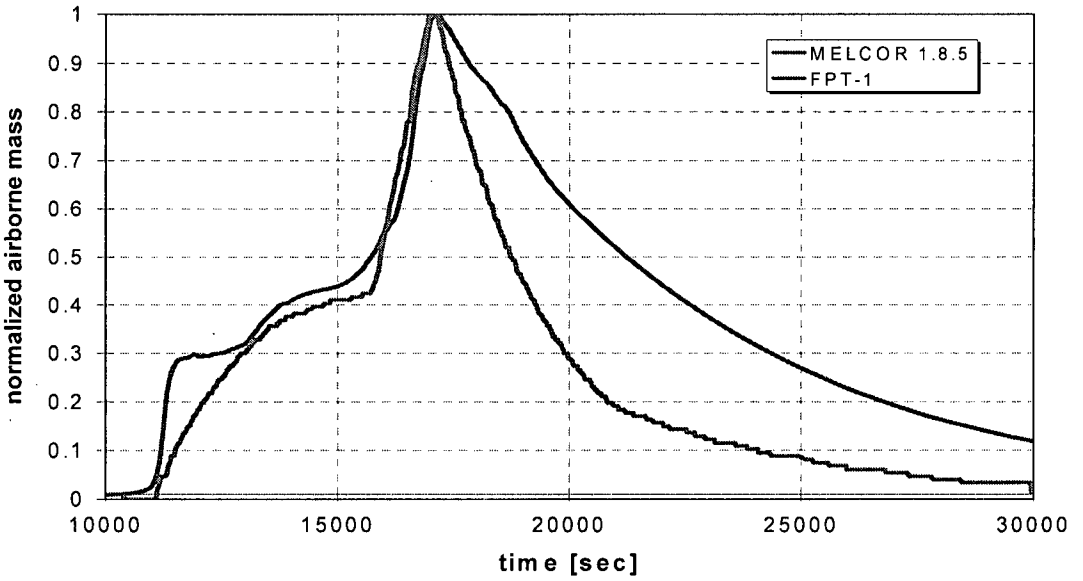

Figure 37 Normalized Aerosol Depletion Rate of Airborne Aerosol in FPT-1 Containment.

[Note: The under-prediction of gravitational settling may be the reason for too-low predicted depletion rate.]

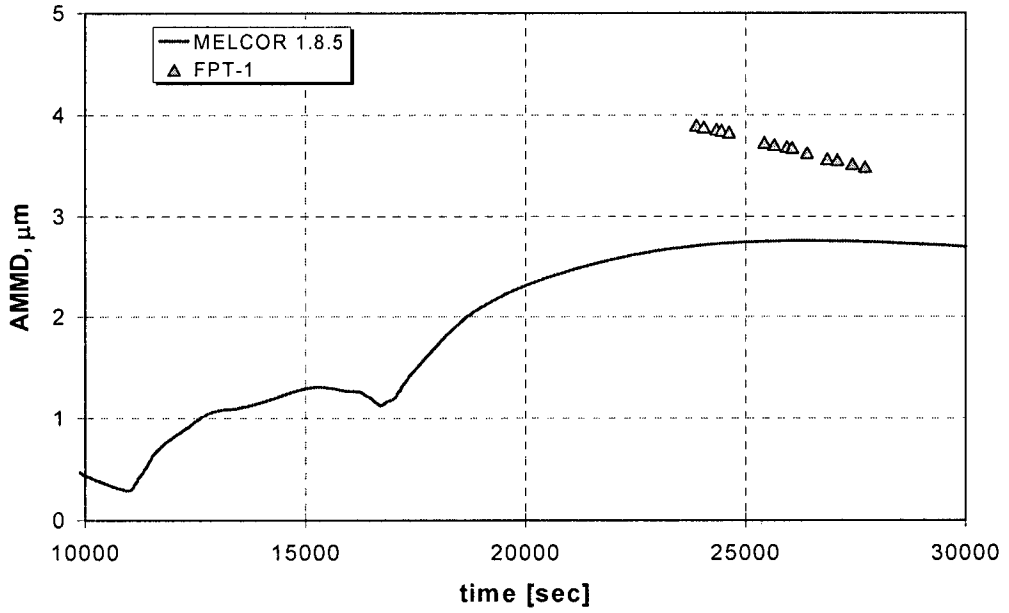

Figure 38 Predicted and Measured Aerodynamic Mass Mean Aerosol Diameter in FPT-1 Containment.

[Note: Under-prediction of the agglomeration rate from too-low airborne total mass may be responsible for the under-prediction of the mean particle size.]

Vessel lower head failure and debris ejection

The base case approach for modeling lower head failure (LHF) of the vessel and debris ejection includes some special non-default modeling options in MELCOR. A schematic of MELCOR's lower head heat transfer model is shown in Figure 39. The solid debris convects to the lower head wall. Solid debris in the lower plenum is assumed to be wettable by lower plenum water, if present. Earlier versions of MELCOR included a one-dimensional model for the CCFL on water access to the debris. The one-dimensional CCFL greatly restricted the debris heat transfer and was highly susceptible to the lower plenum core cell nodalization (see core plate failure discussion). The new heat transfer model recognizes the potential for multi-dimensional flow patterns in the lower plenum without a one-dimensional CCFL restriction. Hence, the film and nucleate boiling debris bed-to-water heat transfer correlations are applicable for debris submerged under water.

Any molten debris will convect to the lower head using the molten debris bed heat transfer correlations. A separate lower temperature metallic molten pool (MP1) can exist as well as a higher melting temperature mixed oxide molten pool (MP2). There is two-dimensional radial and azimuthal conduction through the vessel wall. On the outer surface of the vessel, there is heat transfer to the flooded cavity using inverted cylindrical nucleate boiling correlations.

The other key modeling options include the method for modeling LHF and assumptions regarding the resultant discharge of debris. Penetration failure is not modeled as a mechanism for vessel failure. Rather, only gross creep rupture of the lower head is modeled. In the SNL LHF tests [20], gross creep rupture of the lower head was measured to be the most likely mechanism for vessel failure. In addition, past observations using MELCOR's penetration model suggest that it lacks sufficient spatial resolution to adequately model the multi-dimensional heat transfer effects (i.e., it is a relatively simple lumped capacitance model). The lower head creep rupture model uses the code's default settings. A Larson-Miller parameter is calculated using a one-dimensional temperature profile through the lower head. A cumulative strain is calculated using a lifetime rule and failure occurs with an 18% strain. Upon vessel failure, molten and solid debris are assumed to discharge simultaneously.

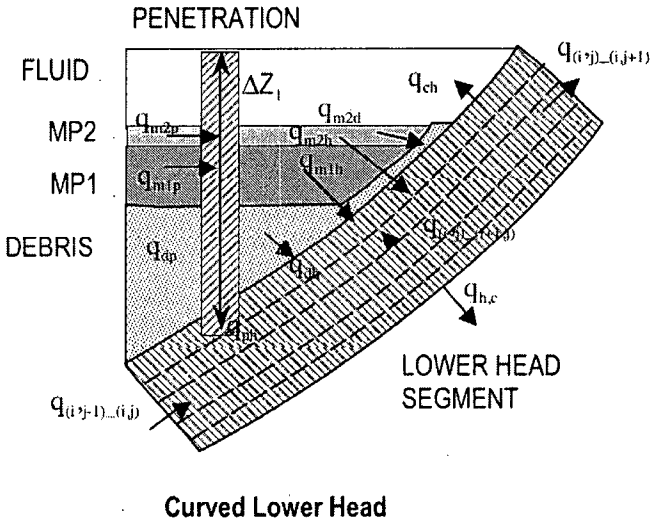

Figure 39 MELCOR Lower Head Nodalization.

Ex-vessel phenomena - CCI and hydrogen combustion

Following vessel failure, core-concrete interactions (CCI) will take place in the reactor cavity of the containment. If there is a pool of water in the reactor cavity, then there is simultaneous debris heat transfer to the overlying pool of water and into the concrete. If there is inadequate heat transfer to cool the debris, the debris will ablate the concrete and release combustible gases. However, if the debris is cooled below the concrete ablation temperature, then there is no combustible gas production and, therefore, no accompanying pressure loading and combustion potential. The simplified one-dimensional geometric configuration of the debris underestimates heat fluxes observed in the MACE experiments [21]. In particular, the MACE tests showed cracking and multi-dimensional effects that greatly enhanced the amount of cooling when water was present. To modify MELCOR CCI model to replicate the heat fluxes observed the MACE tests, the debris conductivity (i.e., a method to reflect cracks and multi-dimensional effects) and surface heat flux were enhanced. As shown in Figure 40, an enhanced conductivity of 10*K to

100*K matched the range of the MACE data (1-5 MW/m^2). A lower bound of a 10x conductivity multiplier was used on the ex-vessel debris-to-water heat transfer model. The modeling changes enhanced the maximum debris-water heat transfer and increased ex-vessel debris cooling while water was present. The concrete ablation rate was unchanged without water.

The default MELCOR ex-vessel combustion model was used. Special attention was made to include horizontal and vertical propagation of burns and the time delay for the flame front to span the width of the control volume. MELCOR does not include models for detonation, which are expected to be highly unlikely. Hence, all burns are subsonic deflagrations with appropriate models for steam dilution, hydrogen and oxygen concentrations, and propagation to adjacent locations. Finally, in cases without an obvious ignition source, sensitivity calculations will be performed that delays combustion until there is an ignition source in the containment (e.g., debris ejection at vessel failure).

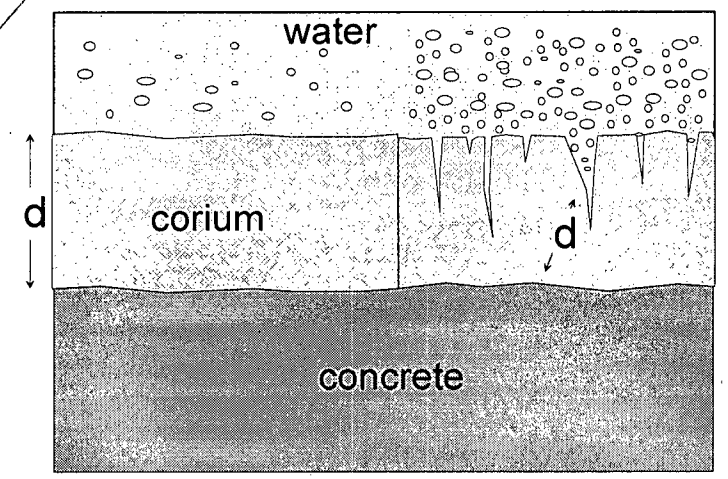

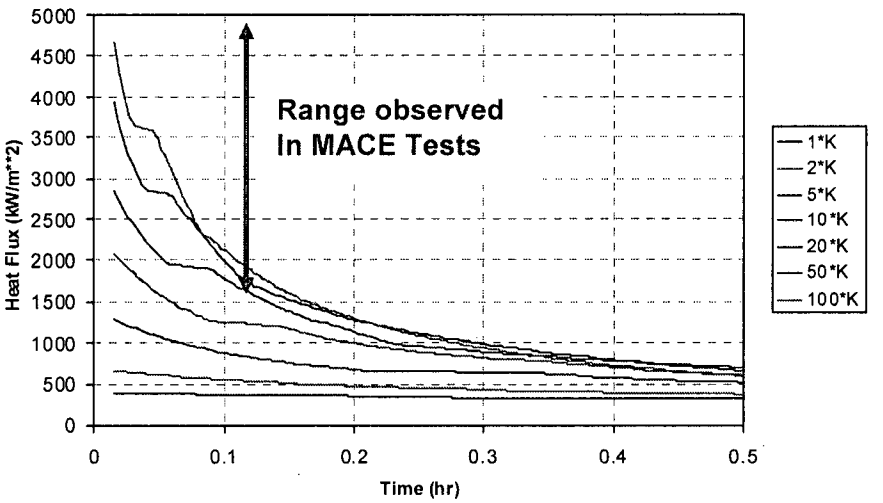

Figure 40 Heat Transfer from an Overlying Water Pool to an Ex-vessel Debris Bed.

3.1.1.3 User-generated Models

Safety relief valve cycling and failure

Safety and relief valves are installed in all nuclear power plants to provide over-protection and can be manually actuated if requisite support systems are available (e.g., electric power, control air, etc.), or open automatically if internal pressure exceeds pre-defined set points. Examples of such valves include:

- Pressurizer power-operated relief valve (PORV) and safety valves (SVs) [PWR],
- Steam generator PORVs and SVs [PWR], and
- Main steam line safety/relief valves (S/RVs) [BWR].

MELCOR models of PWR and BWR systems provide a detailed accounting of these valves, including the actuation conditions, support system dependencies and failure characteristics. Failure, in this context, means failure to reclose after successfully opening to relief pressure.

Two modes of failure are represented in the MELCOR models. The first failure mode represents stochastic failure of the valves to reclose when pressure reduces below the closure set point. Mechanisms for failure (to reclose) are identical to those incorporated in the random event captured in the Probabilistic Risk Assessment (PRA) for most nuclear power plants. The second failure mode represents the possibility that moving internal components of a typical safety or relief valve (e.g., valve stem) would expand due to internal heating during the late phase of core damage, eliminating clearances needed to fully close the valve. The method used to represent each failure mode is described below:

Stochastic failure

Mean failure-to-open and failure-to-reclose probabilities for the specific type(s) of valve(s) installed at a particular plant were obtained from plant data (if available) or from generic failure data documented in NUREG/CR-6928. In all cases examined thus far, the probability for failure to reclose was much greater than a failure to open; therefore failure to open is currently ignored in the MELCOR simulations.

In the MELCOR models a particular valve is assumed to seize in the open position if the total number of cycles exceeds the value corresponding to a maximum tolerable failure probability. In PWR simulations, the maximum cumulative failure probability is 50%; in BWR calculations, the value is 90%[5]. In the PWR model for Surry, this probability corresponds to 247 cycles for the pressurizer PORV and 256 cycles the SVs. The corresponding values for the steam generator PORV and SVs were 119 and 256 cycles, respectively. Failure of the BWR S/RVs occurs when the number of cycles exceeds 208.

[5] Different cumulative failure probabilities (i.e., confidence in failure-to-reclose) were not selected based on physical arguments. Rather, for consistency, it was judged that the total (maximum) number of cycles should be approximately the same in both models, thus requiring slightly different values for the failure probability.

Seizure after opening with high gas temperatures

Periodic cycling of a safety or relief valve with very high internal gas temperatures will cause the valve body and internal components to slowly increase in temperature. At some temperature, thermal expansion (or perhaps evening yielding of small internal components) will prevent the valve stem from moving and re-seating. No data or models are available that clearly identify the temperature at which seizure would occur. However, stainless steel looses its strength at temperatures above approximately 1000 K. Therefore, it was judged that moving components within the valve would deform under persistent internal exposure to temperatures above this value. In the absence of definitive failure data, it is assumed that the valve will fail if the vented gas exceeds 1000 K for more than 10 cycles.

3.1.2 Pressurized Water Reactor Best Practices

Pump seal leakage and blowout

Based on insights from the Surry IPE, which used the Rhodes probabilistic model for seal leakage, a simple model has been incorporated into MELCOR. The key attributes of the model are implemented as follows. Upon a loss of seal cooling in a station blackout sequence, the seals will leak at 21-gpm. In an unmitigated station blackout scenario, the fluid exiting the loop seal will approach saturation conditions at approximately 2 hours and the seal leakage flow will increase to 182 gpm per reactor coolant pump. The seal leakage values are based on normal operating conditions. The flow rate will change appreciably as a function of pressure, subcooling, and steam quality.

Loop seal clearing and effects on progression

NRC has a separate research program examining thermally-induced steam generator tube failure. Detailed SCDAP/RELAP5 calculations are being performed to investigate the timing and sensitivity of high temperature natural circulation tube failure versus failures of other components in the RCS during severe accident natural circulation conditions. The clearing of the loop seal was identified as key event that could increase the likelihood of tube failure under certain circumstances. Furthermore, NUREG-1570 previously assessed the potential for tube failure in high-pressure station blackout conditions.

MELCOR includes basic thermal-hydraulic models for loop seal clearing and the prediction of thermal failure of steam generator tubes. However, the thermal gradients and flow behavior is extremely complex in the RCS during natural circulation conditions. The base case response utilizes the MELCOR models for natural circulation (i.e., discussed further below), loop seal clearing, and thermally-induced RCS component failures. Sensitivity calculations were also performed that assume steam generator tube failure before hot leg nozzle failure (i.e., the first creep rupture location calculated in the Surry SBO calculations).

RCS natural circulation treatment

Natural circulation is important in severe accident sequences because circulating steam from the core to upper reactor internals, the hot leg, and the SGs (1) transfers heat away from the core, (2) changes the core melt progression, and (3) changes in-vessel fission product distribution. More importantly, the resultant heating of the piping connected to the vessel could progress to a thermal stress (i.e., creep rupture) failure of the primary pressure boundary and a subsequent depressurization. As shown in Figure 41 [17], three natural circulation flow patterns can be expected during a severe accident; (1) in-vessel circulation, (2) countercurrent hot leg flow, and (3) loop natural circulation. For high pressure accidents that do not include pipe breaks on the RCS (e.g., a station blackout), whole loop, single-phase natural circulation flow (i.e., the left-hand side of Figure 41) is not expected during the core degradation phase of the accident. Consequently, the prediction of the first two natural circulation flow patterns is most critical for impacting severe accident progression. The first two natural circulation flow patterns have been studied (a) experimentally in the 1/7th-scale natural circulation test program by Westinghouse Corporation for the Electric Power Research Institute (EPRI) [22], [23], (b) computationally using the FLUENT computational fluid dynamics computer program [24], [25], and (c) analytically using SCDAP/RELAP5 [17]. Subsequently, MELCOR was used to model the 1/7th-scale natural circulation tests [26].

More recently, NRC has continued improving natural circulation modeling as part of the steam generator tube integrity program [27], [28]. The natural circulation modeling techniques used in MELCOR plant models were based on work performed as part of the code assessment of the 1/7th-scale tests [26], which closely followed the previous work performed by Bayless [18]. The natural MELCOR modeling approach in the Surry model has been recently updated to incorporate some of the modeling advances used by Fletcher using SCDAP/RELAP5 [27]. The key features of the MELCOR natural circulation models, which were adapted from the recent SCDAP/RELAP5 work, are the following:

- 5 radial rings in the vessel and upper plenum for natural circulation
    - Separate axial and radial flow paths throughout the core and upper plenum
    - Radial and axial blockage models in the core during degradation
- Explicit modeling of all internal vessel structures for heat transfer
    - Convective heat transfer
    - Gas-structure radiation in the upper plenum
    - Structure-to-structure thermal radiation within the core
    - Variable Zircaloy emissivity as function oxide layer thickness
    - Variable steel emissivities in the core as a function temperature

The hot leg is divided in half to represent the counter-current natural circulation flow. The flow rate is matched to a Froude Number correlation from the FLUENT computational fluid dynamics (CFD) analysis [27],

$$Q = C_D [\, g\,(\Delta\rho / \rho)\, D^5 \,]^{1/2}$$

where,

- Q is the volumetric flow rate in the hot leg,
- $C_D = 0.12$ (from FLUENT CFD calculations),
- g is the acceleration due to gravity,
- ρ is the average fluid density,
- $\Delta\rho$ is the density difference between the hot and cold fluid streams, and
- D is the pipe diameter

- Steam generator tube-to-hot leg flow ratio tuned results from the FLUENT CFD analysis [27]
  - Tube mass flowrate/hot leg mass flow rate (M-ratio) = 2
- Explicit modeling of all key heat transfer processes in the hot leg and the steam generator
  - Augmented convective heat transfer in hot leg based on FLUENT turbulence evaluations
  - Gas-to-structure radiative exchange in the hot leg and steam generator
  - Ambient heat loss through the piping and insulation
- Steam generator mixing fractions based on FLUENT CFD analysis [27]
  - Inlet plenum subdivided into 3 regions for hot, mixed, and cold regions
  - Flow ratio into hot tubes tuned to a 0.85/0.15 split
  - Flow ratio into cold leg piping tuned to a 0.85/0.15 split
  - Flow divided in the SG tubes in a 41% / 59% tube split[6]
- Individual modeling of relief valves
  - When the valves are lumped, it creates a very large flow that non-physically disrupts natural circulation flow patterns and the timing of the valve openings
- Creep rupture modeling
  - Hot leg nozzle carbon safe zone region
  - Hot leg piping
  - Surge line
  - Steam generator inlet tubes

The MELCOR hot leg and SG nodalization for Loop A is shown in Figure 42. Control volume reactor system codes like MELCOR or SCDAP/RELAP5 have limitations in modeling buoyancy plumes associated with natural circulation flow. Hence, the MELCOR system model analyses

[6] It was not practical to represent the 41%/59% hot/cold split of the SG tube regions in the MELCOR model due to the complications of a single model nodalization for all conditions. A 50%/50% tube split was used.

are performed by incorporating flow buoyancy or drag adjustments to the hot leg circulation rate to achieve the target value for hot leg discharge coefficient. The drag coefficient was formulated based on an experimental correlation for flow through horizontal ducts connecting two tanks containing fluids of different densities. The special natural circulation flow paths described above are shown in red in the figure. The natural circulation control logic identifies single potential single-phase natural circulation conditions and activates the special flow paths to achieve the conditions described above.

Finally, it should be noted that the recent work of Fletcher [27] for the NRC steam generator tube integrity program revealed a sensitivity of tube failures to the hot and cold tube split, the tubes receiving the peak plume temperatures, and the highly refined axial nodalization through the tube sheet and into the steam generator. These specific aspects of the modeling specifically addressed the potential for a thermally-induced steam generator tube rupture (TI-SGTR), which were not incorporated in the MELCOR models.[7] To evaluate this potential consequence while acknowledging the potential limitations in the MELCOR model and/or vulnerabilities or defects in the plant tubes, the SOARCA program will perform sequences where TI-SGTRs were specified to occur prior to other RCS natural circulation failures.

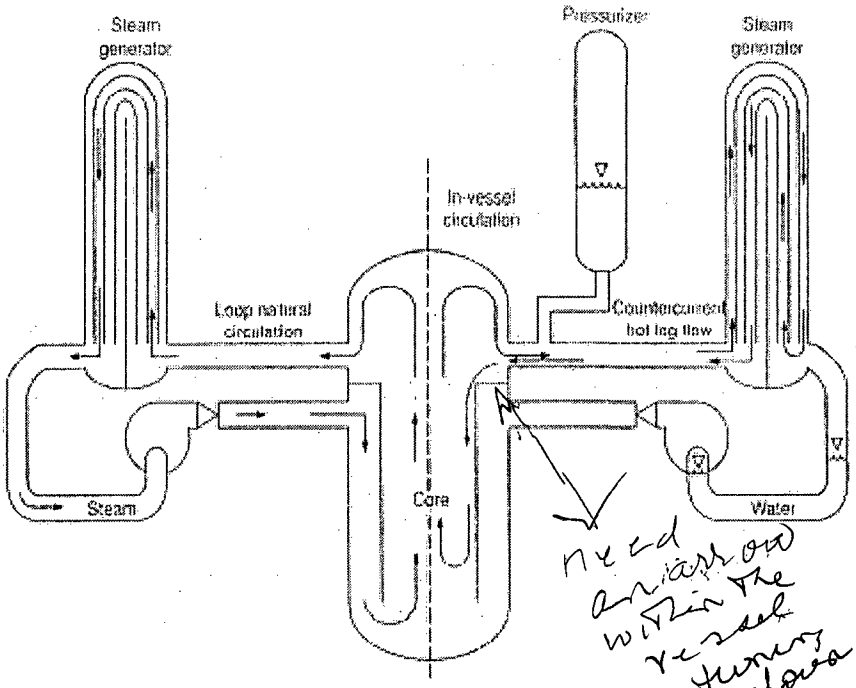

Figure 41 In-vessel, Full-loop, and Hot Leg Natural Circulation Flow Patterns in a PWR Severe Accident.

[7] Unlike SCDAP/RELAP5, MELCOR can not be renodalized at the start of the natural circulation phase with a more detailed model. Consequently, the MELCOR model must calculate the early two-phase thermal-hydraulic transient, the natural circulation phase, the post creep rupture blowdown, the accumulator reflood of the degraded core, and the final boil-off and core degradation to vessel failure. It was not practical to use a highly detailed steam generator nodalization for the scope of a MELCOR source term calculation.

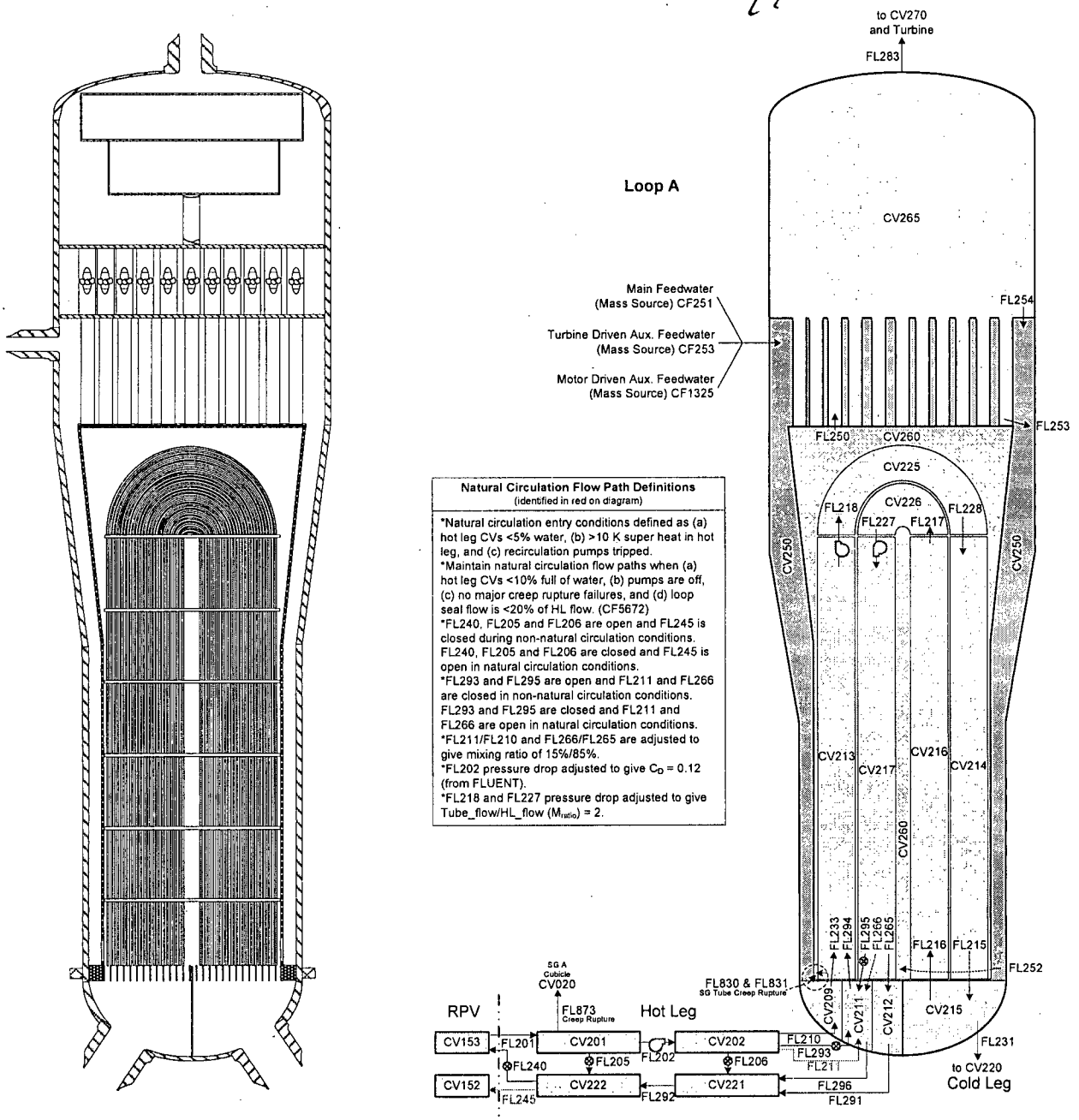

Figure 42 MELCOR Hot Leg and Steam Generator Nodalization including the Special Natural Circulation Flow Paths.

Core plate failure

The timing of core plate failure effects the relocation of the degraded core materials from the core region into the lower plenum. As discussed above, the hot relocated core materials will boil away the water in the lower plenum, which will lead to vessel LHF. The MELCOR representation of the Westinghouse core plate assembly includes a separate representation of the various supporting structures. At the lowest level is the bottom support casting. The bottom

support casting is part of the integrated core barrel structure. The ~~mass~~ weight of the core is transmitted from the core plate via support columns that span the gap to the core support forging. Within the gap is a flow mixer plate (see Figure 43).

The MELCOR lower-head support nodalization is shown in the left-hand side of Figure 44. The ~~weight of the~~ core material mass is transmitted through the columns to the bottom support casting. The local thermal-mechanical failure of the lower core plate, the flow mixer plate, and the lower support forging are calculated within MELCOR using Roark's engineering stress formulas. The failure is based on exceeding the yield stress at the local material temperature conditions. After the core plate fails, it is assumed that the debris falls past the columns but is temporarily supported by the flow mixer plate. However, since the flow mixer plate is relatively thin, the hot debris will quickly fail the plate (i.e., again according to the Roark stress formulas). The debris subsequently falls to the lower support forging, which is very thick but eventually fails. The sequential failure of the supporting structures is affected by vessel water level, which is also exposed to the sequentially relocating debris. Once the lower support forging fails, the debris falls onto the lower head.

Fully molten materials will relocate through the structures until it freezes on supporting structures or reaches the lower head. Due to the high melting temperature of U-Zr-O eutectic core debris material (i.e., assumed to melt at 2800 K), most of the fuel and cladding debris will be frozen during the core support structure failures. However, some unoxidized Zr or control material may have enough superheat to relocate through the structures onto the lower head.

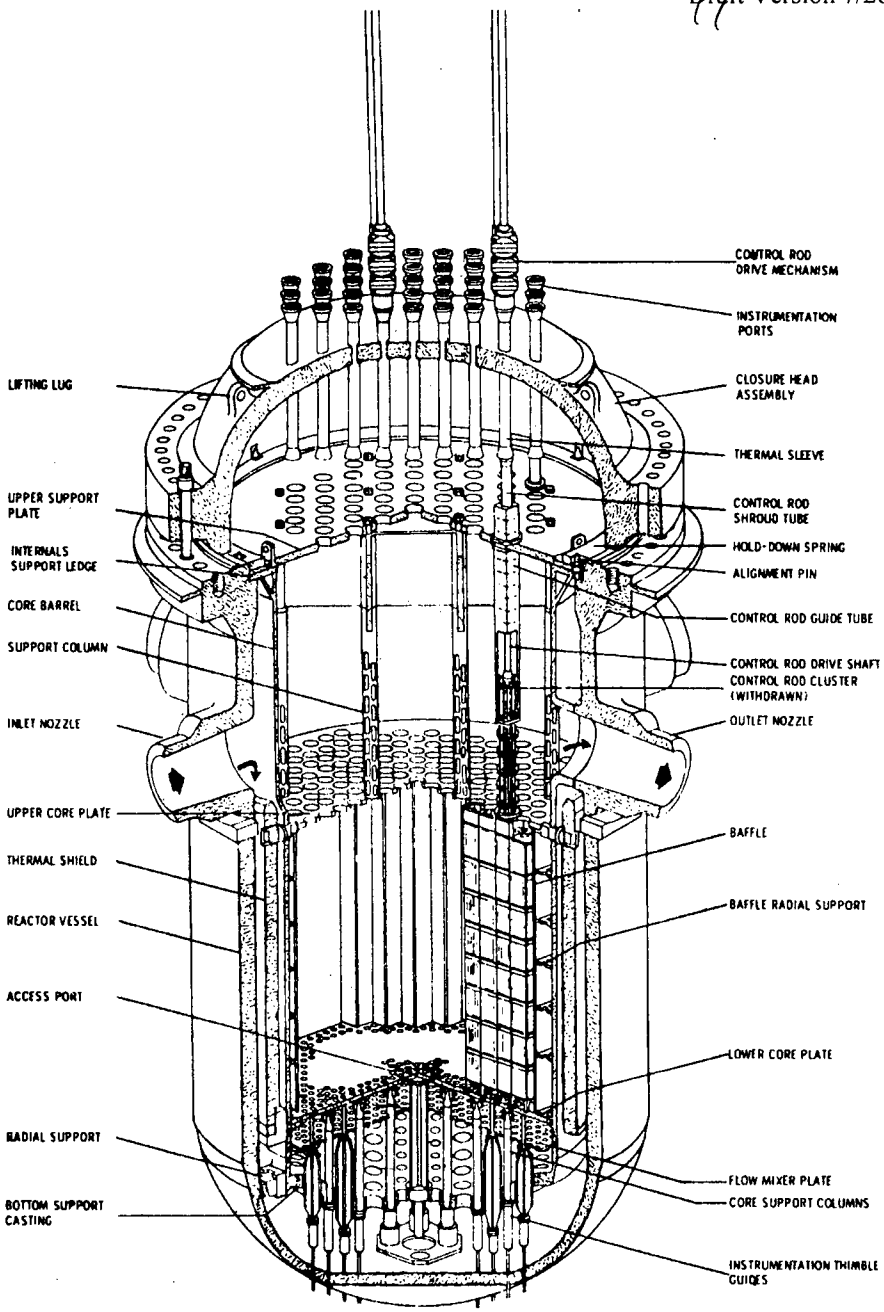

Figure 43 Westinghouse PWR Reactor Vessel Internals.

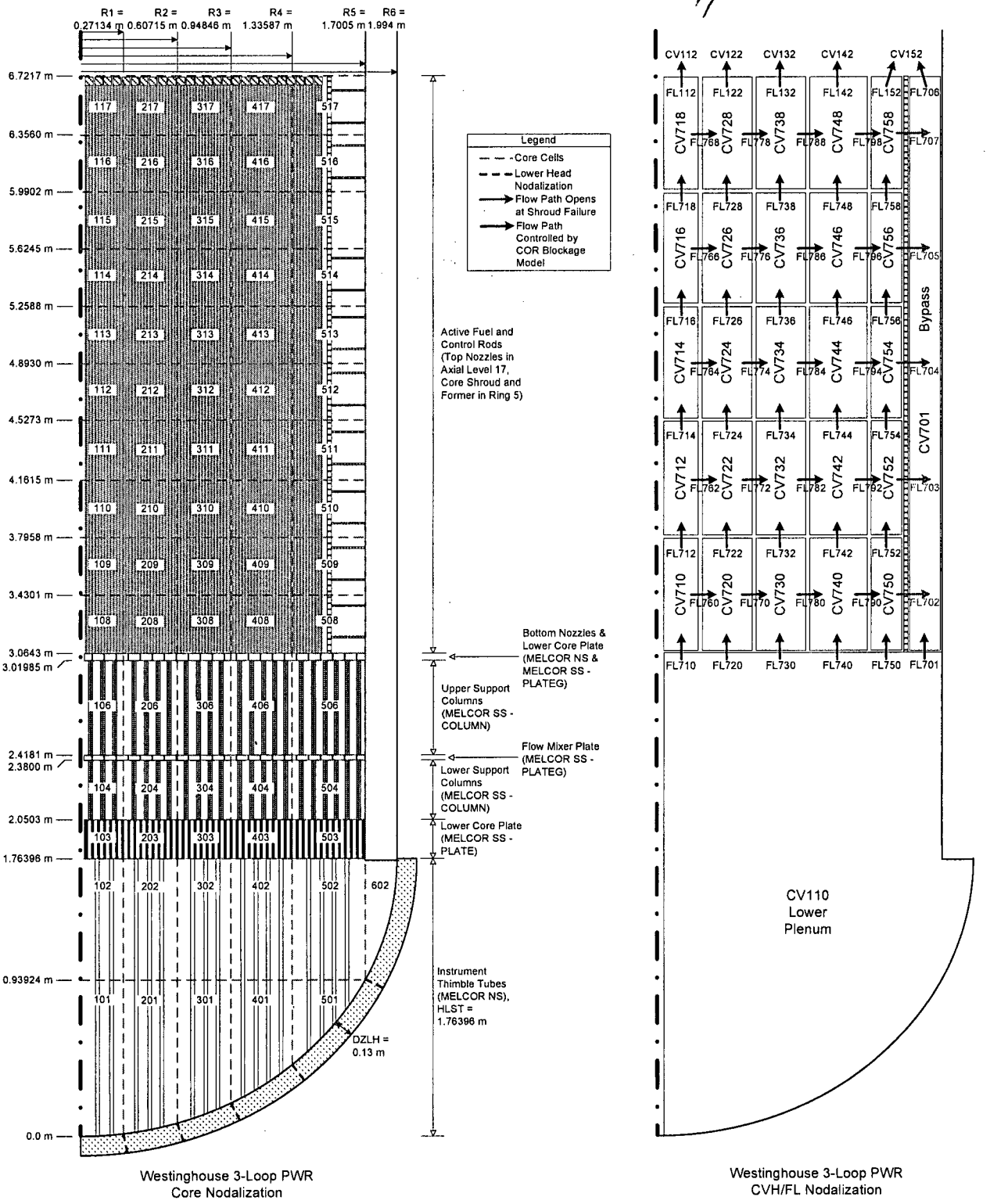

Figure 44 MELCOR Westinghouse Lower Vessel Nodalization.

3.1.3 Boiling Water Reactor Best Practices

Debris Spreading on the Drywell Floor of a BWR Mark I Containment

The floor of a Mark I containment is divided into three distinct regions for the purposes of modeling molten-core/concrete interactions, as illustrated in Figure 45. The first region (which receives core debris exiting the reactor vessel) corresponds to the reactor pedestal and sump floor areas (CAV 0). Debris that accumulates in the pedestal can flow out into the second region (through an open doorway in the pedestal wall), corresponding to a 90° sector of the annular portion of the drywell floor (CAV 1). If sufficient debris accumulates in this region, it can spread further into the third region, which represents the remaining portion of the drywell floor (CAV 2). Debris within each region is assumed to be fully-mixed, but has a distinct temperature and composition from neighboring regions.

Two features of debris relocation among the three regions are modeled. The first models debris overflow from one region to another. The second manages debris spreading across the effective radius of the regions outside the reactor pedestal (CAV 1 and 2). Control functions monitor debris elevation and temperature within each region, both of which must satisfy user-defined threshold values for debris to move from one region to its neighbor. More specifically, when debris in a cavity is at or above the liquidus temperature of concrete, all material that exceeds a predefined elevation above the floor/debris surface in the adjoining cavity is relocated (6 inches for CAV 0 to CAV 1, and 4 inches for CAV 1 to CAV 2). When debris in a cavity is at or below the solidus temperature of concrete, no flow is permitted. Between these two debris temperatures, restricted debris flow is permitted by increasing the required elevation difference in debris between the two cavities (more debris 'head' required to flow).

Debris entering CAV 1 and CAV 2 are not immediately permitted to cover the entire surface area of the cavity floor. The maximum allowable debris spreading radius is defined as a function of time. If the cavity debris temperature is at or above the liquidus, input within the seq-trip.gen file determines the shortest transit time (and therefore maximum transit velocity) of the debris front to the cavity wall (10 minutes for CAV 1 and 30 minutes for CAV 2.) When the debris temperature is at or below the concrete solidus, the debris front is assumed to be frozen. A linear interpolation is performed to determine the debris front velocity at temperatures between these two values[8].

Put the footnote reference here

The reactor operators what the concrete temp rather than debris temp - you don't know the reason why could then go the page.

How much difference would the debris liquidus solidus temps be? Is that difference important?

[8] The debris spreading model compares debris temperatures to the liquidus and solidus temperatures of concrete because MELCOR does not currently allow user access to the debris liquidus and solidus temperatures.

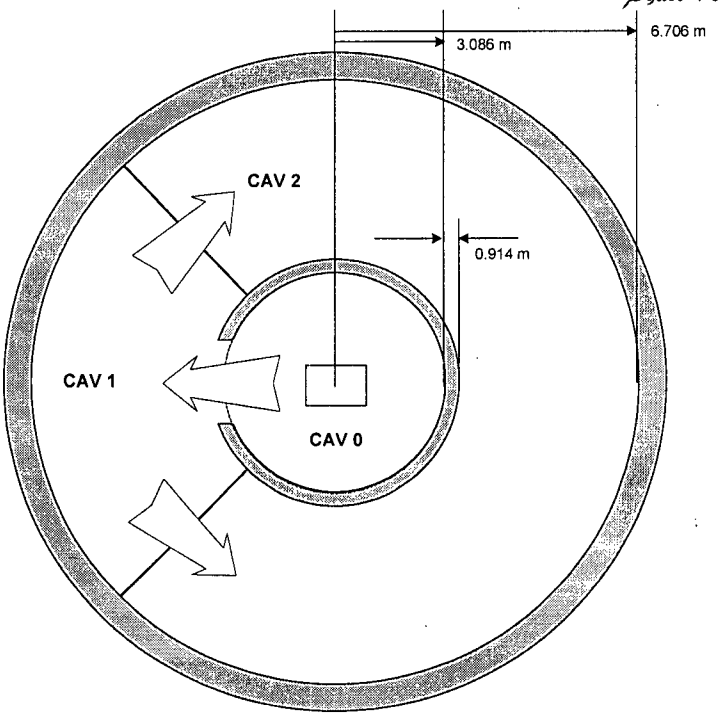

Figure 45 Discrete Regions of the Drywell Floor to Represent Debris Spreading.

Release of Structural Aerosols

Experimental measurements of aerosol release and transport during fuel assembly melting consistently show significant releases of non-radioactive species such as tin and (in PWR assembly experiments) Ag-In-Cd. The former is released primarily from fuel cladding (tin is an alloy constituent of Zircaloy); the latter is released from (PWR) control rods.

The default configuration of vapor and aerosol release models in the RN Package of MELCOR does not account for the release of these materials during core degradation. Rather, it focuses on the release and transport of fission products. An exception to this statement is the VANESA model for vapor and aerosol releases that occur during corium-concrete interactions, which accounts for significant releases of non-radioactive gases and aerosols from the decomposition of concrete. During the in-vessel phase of an accident, however, the CORSOR models are not normally configured to account for the release of non-radioactive species from core structures other than UO_2 (fuel).

Solution

Options are available in MELCOR 1.8.6 to extend the application of in-vessel radionuclide release models to "non-fuel" materials in the COR Package. These options do not represent a mechanistic treatment of diffusion and release of volatile constituents from core structures. Rather, they provide a simple framework for extending the CORSOR models for radionuclide release to examine the effects of the additional mass associated with aerosols generated during the oxidation and melting of cladding and control rod steel. This model was exercised in a

sample BWR calculation to determine how it might be used to include the effects of aerosol generation from core structures in future source term calculations.

The "non-fuel" aerosol release model works as follows:

1. The user assigns non-fuel materials recognized by the COR Package to an RN class. The list of materials included in this association are:
   - Unoxidized Zirconium,
   - Zirconium Oxide,
   - Unoxidized steel associated with control rods (blades),
   - Oxidized steel associated with control rods (blades), and
   - Control rod poison.

   The fraction of the total mass of each of these materials that is available as a potential aerosol source is also defined. In principle, this fraction should represent the mass fraction of volatile constituents in the material. This information is specified on input records for card RNCRCLxx.

2. The release rate associated with core structure materials is estimated using the active RN fission product release model (i.e., the user-selected version of CORSOR.) Scalar multipliers are applied to CORSOR to represent differences in the release rates associated with migration through a UO_2 matrix versus Zircaloy, steel, or other core structural materials. The CORSOR release rate multipliers are specified via sensitivity coefficient 7100. The temperature used to calculate the release rate of a particular material is tied to the corresponding structure temperature in the COR Package (i.e., zirconium to fuel cladding, and steel plus control poison to non-supporting structure.)

Modeling the evaporation and release of control poison in BWRs is not a concern because the vapor pressure of boron carbide is very high (sublimation occurs at temperatures above 2500°C). However, release of non-radioactive vapor and aerosols due to chemical reactions between B_4C and steam is modeled by the B_4C oxidation model in the COR Package. The mass of vapor species generated by these reactions is transferred to the CVH Package for transport; the mass of condensed aerosols (primarily B_2O_3) is transferred to the RN Package for transport.

Aerosol generation from the destruction of PWR control material requires special models beyond those described above (see next section.)

Model Limitations

A significant limitation of the non-fuel release modeling framework in MELCOR is that the mass of materials represented in the COR Package is not decremented to reflect the amount sourced to the RN Package. Further, there is no numerical limit to the amount of structural aerosol that can be generated for a given core material. Therefore, material fractions and CORSOR release rate multipliers must be defined carefully to prevent non-physical results. More on this problem is offered in the example calculation results below.

Very recent work at Sandia has augmented the non-fuel release option with a new model specifically designed for modeling Ag-In-Cd release from PWR control rods. This model is only available in the most recent (developmental) version of the code, and was not examined in the sample calculations described below. Work by J. Birchley of PSI on Phebus FPT-1 [9] suggests the non-fuel release option is not a satisfactory method of accounting for aerosol release from PWR control rods. As a result, test applications of the new Ag-In-Cd model are strongly recommended to determine how it can be used to account for absorber release in PWR applications.

so how did we do this in SOARCA since this document purports to be a SOARCA best practice.

Target Quantities of Structural Aerosols

No direct experimental information on release rates of core structural materials is available to aid in selecting appropriate multipliers for the non-fuel release option in MELCOR. However, post-test measurements of aerosol deposition during in-pile tests provide an integral picture of the quantity of material released during core degradation. In Phebus, for example, R. Gauntt related the following observations:

> The tin content in unoxidized Zircaloy is significantly reduced from its normal levels, but not completely depleted. In contrast, no tin is typically found in remnants of ZrO_2. The total quantity of tin measured on downstream surfaces represents roughly half of the total mass available.

Sources of data to quantify the release of volatile constituents of other core structure materials, such as stainless steel were not identified. Based solely on the physical properties of stainless steel alloying element, one might expect to see manganese (roughly 2 wt/%), but none is described in Phebus data reports. Therefore, no recommendations can be made at this time regarding the release of materials other than Sn from Zircaloy.

Sample Full-Scale BWR Calculations

The non-fuel release modeling option was tested using an early version of the MELCOR model for a BWR/4 reactor and a short-term station blackout (ST-SBO) sequence. This test version of the model is based on early Peach Bottom core designs, which were comprised of 8x8 or 9x9 fuel assemblies and associated channel boxes. The MELCOR model of these early core designs had approximately 74,000 kg of Zircaloy in the core[10]. Therefore, the total available mass of tin that could be released during a full core melt accident is approximately 1073 kg. The objective of these test calculations was to evaluate sensitivity to governing input parameters, and determine appropriate values for routine use in source term calculations. Results are summarized below.

Input Variables

Realistic values for the volatile mass fraction of tin in Zircaloy were used, namely 1.45 wt/%. Based on the observations made by R. Gauntt (above), the release rate of tin from unoxided Zr

---

9 Email communication with J. Birchley, Paul Scherer Institute, Switzerland, September 2004.

10 The MELCOR model used in the SOARCA calculations represents an updated description of the Peach Bottom core design, composed of 10x10 fuel assemblies and associated fuel channels. The total Zircaloy mass in this core designs is approximately 20% lower than the value used in the early test calculations.

was assumed to be a factor of ten smaller than the rate from ZrO_2 (i.e., SC7100 = 0.1 for Zr and 1.0 for ZrO_2.) These values were not changed in the sensitivity calculations.

The non-fuel release model is tied to the particular model for fission product release selected for a calculation. Therefore, calculations were performed using CORSOR-M (current MELCOR default) and CORSOR-Booth/ORNL (the model recommended as current 'best-practice'). For each release model, two calculations were performed using different values of the scalar multipliers. A baseline calculation used values of 1.0 to reflect the assumption that the release rate of volatile species from structural components is similar to the release rate from fuel. The second calculations used multipliers developed by J. Birchley of PSI in his analysis of Phebus test FPT-1. Birchley's analysis followed the same basic approach used here; that is, he defined realistic physical properties of the structural materials and adjusted the multipliers on the CORSOR release rate expressions to match the measured total mass of generated aerosol. The result was a scalar multiplier of 200 for tin in Zircaloy. His analysis was based solely on CORSOR-M. For the sake of consistency in the current sensitivity analysis, a value of 200 was applied to the CORSOR-M and CORSOR-Booth release rate expressions in the second set of full-scale BWR calculations [11]. This is equivalent to changing the values of SC7011 to 20 and 200 for Zr and ZrO_2, respectively.

Results of Sensitivity Calculations

The total mass of tin aerosol released from Zircaloy in the core is shown in Figure 1 for each of the four sensitivity calculations. Values range from 195 kg (or 18% of the available mass) to 34,600 kg (or 3200% of the available mass), depending on the release model and scalar multiplier used. Curves for the calculated mass of fission product tin are also shown in Figure 46 as a point of reference.

Conclusions

Reasonable values of the integral release were achieved using unmodified CORSOR release coefficients (i.e., the same as fission product release from fuel). Depending on the particular release expression used, the total quantity of structural tin released range from 18 to 47% of the total available as an alloy agent in Zircaloy fuel cladding. In contrast, non-physical quantities of aerosol were generated when the release rate for tin from Zircaloy was represented by an expression that greatly exceeds the nominal rate for fission product tin from fuel. Reasons why large scalar multipliers on the CORSOR release expression would generate results in good agreement with FPT-1 data, but generate non-physical results for a full-scale reactor calculation are not offered here.

Guidelines for MELCOR Input

Pending further study of non-fuel release option input variables, the following approached is adopted for representing the release of structural aerosol in full-scale reactor source term analysis:

---

[11] It is important to note that a direct extension of the multipliers developed by calibrating the CORSOR-M release model to FPT-1 results is tenuous at best. Birchley expressed considerable caution in applying his results beyond the analysis of this single experiment. However, it is the only independent value available for consideration, and is used here simply to examine modeling sensitivity.

(1) The non-fuel release option is not recommended to account for release of Ag-In-Cd from PWR control rods. Rather, testing and evaluation of the new model installed in the developmental version of the code is recommended.

(2) The non-fuel release option can be used to account for the release of tin from Zircaloy fuel cladding. Pending target values for the release of Manganese from steel, it is not recommended that the option be used to account for aerosol generation from control rod structure(s). Tin aerosols can be assigned as a non-radioactive source to RN class 12. However, this method eliminates (future) flexibility to define different release properties of fission product tin and structural tin. A better approach is to define a unique RN material class for the tin aerosol; in the current analysis, structural tin is assigned to RN Class 17.

(3) The CORSOR-Booth release expression is currently the 'best-practice' option for modeling fission product release from fuel. The input data described below assume this model is used in reactor source term calculations.

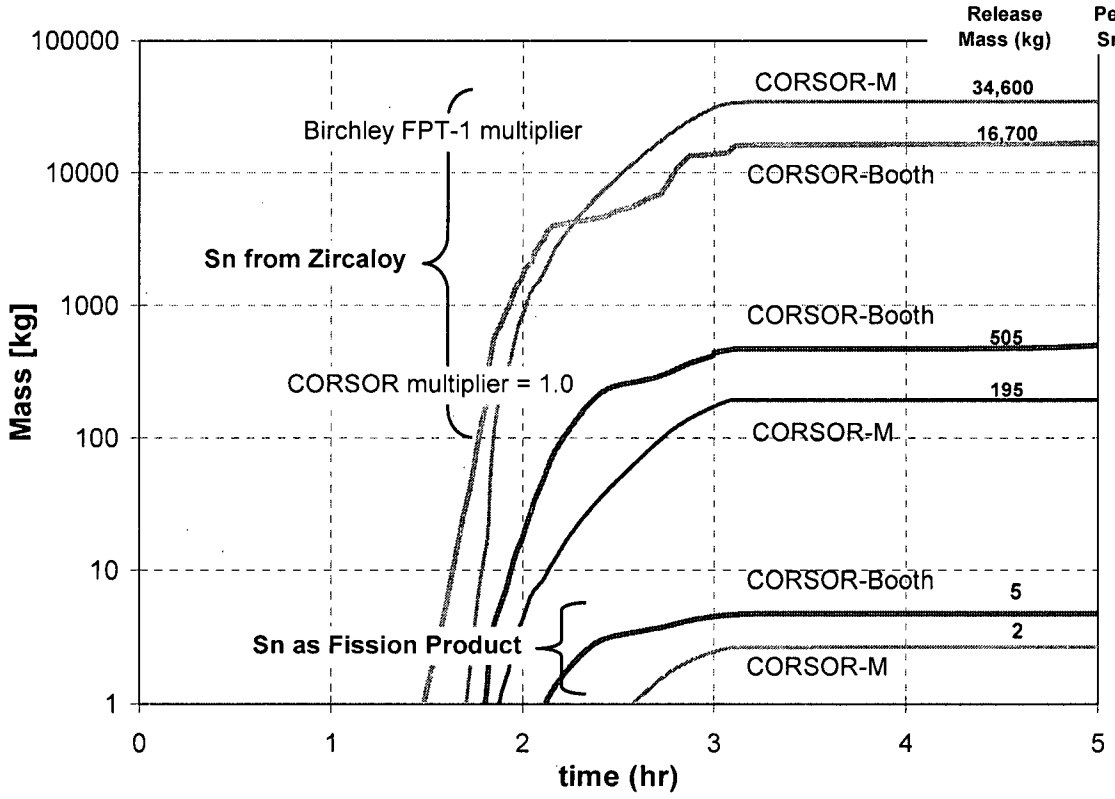

Figure 46 Released Mass of Tin from Zircaloy Cladding during a BWR ST-SBO.

(4) Different multipliers are recommended for metallic Zr versus its oxide to reflect observed differences in Sn found in unoxided versus oxided Zirconium debris from Phebus. To do this, the following input should be provided on card RNCRCLxx:

Unoxidized Zirconium and Oxidized Zirconium in the COR Package should be assigned to RN class 17.

Note: This assignment differs from the default values in MELCOR 1.8.6, which associates Zr with Class 8 (Cerium). This is the class that includes fission product zirconium, which is not a volatile species. The default for this material should be changed to RN class 12 (Sn).

The fraction of material mass associated with these classes was assumed to be 0.0145 for Zirconium. This value is the mass fraction of tin (Sn) in Zirc-2 and Zirc-4 [46]. This is the only volatile constituent in fuel cladding.

(5) The release rates for these core structures are assigned scalar multipliers to represent the difference between diffusion-limited release through UO_2 and structural metals (Zircaloy or steel.) Specific values are proposed as follows:

Unoxidized Zr = 0.1

ZrO_2 = 1.0

The multiplier for fuel should remain at 1.0 (default) and values of 0.0 should be applied to other COR materials.

3.1.4 Independent Peer Review

A review of the proposed approach to modeling severe accident progression for the State-of-the-Art Reactor Consequence Analysis (SOARCA) project was conducted at a public meeting in Albuquerque, New Mexico on August 21-22, 2006 [3]. This review focused primarily on best modeling practices for the application of the severe nuclear reactor accident analysis code MELCOR for realistic evaluation of accident progression, source term, and offsite consequences for each operating commercial nuclear power plant in the United States. It also included consideration of potential enhancements to the MELCOR code as well as consideration of the SOARCA project in general.

The review was conducted by five panelists with demonstrated expertise in the MELCOR code application and analysis of severe accidents at commercial nuclear power plants. The panelists were drawn from private industry, the Department of Energy national laboratory complex, and a company working on behalf of German Ministries. The review was coordinated by SNL and attended by Nuclear Regulatory Commission staff.

3.2 MELCOR Code Enhancements for the SOARCA Project

At the start of the SOARCA projects, three MELCOR code development activities were identified to enhance the code. Each of these activities had previously been included manually in the best practices approach for analysis, through (a) changes to default setting, (b) user-specified control logic, or (c) the addition of user-specified filter models, respectively. The incorporation of these items as defaults or code models simplified their implementation. The changes are summarized below.

Update MELCOR defaults to reflect current best-estimate modeling practices

In support of SOARCA MELCOR calculations using Version 1.8.6 and as the new standard for Version 2.1, some default values were updated based on best-estimate modeling practices. The values are summarized in Appendix A. The new defaults reflect long-term practices to better model severe accident phenomena, improve numerical robustness, or activate newer models. In addition, the standard modeling practices include modeling cesium molybdate using radionuclide package (RN) Class 17. Previously, the Class 17 did not have physical parameters representative of any specific substance. Consequently, all physical properties were added as defaults to facilitate modeling cesium molybdate without additional user input.

The new ORNL-Booth release model and updated modeling parameters described in Section 3.1.1.2 were implemented as new defaults.

Add a simplified thermo-mechanical fuel collapse model

As described in Section 3.1.1.2 under the description of the fuel degradation and relocation treatment, a simple parametric model was developed to simulate thermal-mechanical collapse of fuel rods only supported by highly oxidized Zircaloy shells at high temperatures. Previously, the implementation of the control system logic to perform these calculations required several thousands of lines of input. The new model was coded into the MELCOR code to eliminate the burden of creating a file of user-specified control logic. The model is activated through a simple user directive that identifies the appropriate lifetime failure function table. The lifetime failure function table specifies the time remaining to collapse versus the local oxidized cladding temperature. The logic is only implemented once the unoxidized cladding thickness drops below 0.1 mm.

Fission product vapor scrubbing with aerosol scrubbing

In previous calculations, it was observed that the SPARC fission product scrubbing model in MELCOR would not recognize fission product vapors except elemental iodine. However, the temperature of the carrier gas and fission products flowing to pool spargers could have a significant vapor pressure, thereby containing a mixture of vapors and aerosols. The SPARC model automatically scrubs all aerosols but only elemental iodine vapor. Consequently, all fission product vapors except elemental iodine would flow through the pool without any retention. The model was updated to calculate scrubbing based on the same parameters used for

elemental iodine. This problem was particularly significant for cesium-iodine vapor, which can have a relatively high vapor pressure when discharged into a BWR sparger deep within the wetwell pool. The SPARC vapor scrubbing model accounts for the non-condensable fraction, the bubble size, the discharge gas temperature, the pool subcooling, and the pool depth.

4. RATIONALE FOR NEGLECTING ACCIDENT PHENOMENA PREVIOUSLY CONSIDERED IMPORTANT TO RISK

The next two subsections describe the modeling approach taken in the SOARCA project to address three important phenomenological issues, (1) alpha-mode containment failure, (2) direct containment heating leading to containment failure, and (3) BWR Mark I drywell liner melt-through in the presence of water. These phenomena have been noted in several past studies of severe accident behavior to be leading causes of early failure of the containment pressure boundary, and thereby important contributors to early and potentially large radiological releases to the environment. This fact alone motivated the NRC and the nuclear industry to invest considerable time and resources in several experimental and analytical studies of the phenomena governing these postulated containment failure mechanisms. The outcome of this work (in summary) is a finding that although the phenomena are conceivable, the conditions required for them to occur are so remote that they are now considered 'physically unreasonable.'

WASH-740 [5] was perhaps the first study to attempt to identify potential means by which radioactivity in a power reactor could be released by some non-specified catastrophic event, be transported through the environment and produce public health consequences and land contamination. Relatively little physical evidence was available to support an assessment of the probability of such events and order-of-magnitude analysis estimates of their possibility were made using conservative assumptions about the conditions under which they might occur. The WASH-1400 report [6] also known as the Reactor Safety Study (RSS) or the Rasmussen Report, made use of probabilistic methods to attempt to quantify likelihood of serious reactor accidents and their consequences. However, estimation of the source terms from hypothesized severe events was hampered by poor understanding of the phenomena operative in severe accident situations and the lack of appropriate analysis tools for their estimation.

Due to their importance in an early, large release of fission products, all three of these containment failure modes were the subject of considerable research. After considerable experimental, analytical, and probabilistic work, the requisite phenomena have been determined to have a sufficiently low probability to allow their exclusion from the present analysis. Section 4.1 describes the resolution of alpha-mode containment failure as a low likelihood event. Similarly, Section 4.2 discusses the low likelihood of direct containment heating due a prior creep rupture of RCS piping as well as a low likelihood of containment failure with direct containment heating. Finally, Section 4.3 discusses the low likelihood of drywell liner melt-through in a BWR Mark I containment if there is water on the drywell floor.

4.1 Alpha-Mode Containment Failure

One such hypothesized severe accident posed in the WASH-1400 study is the so-called alpha mode failure event. The alpha-mode event is characterized by the supposition that an in-vessel steam explosion might be initiated during core meltdown by molten core material falling into the water-filled lower plenum of the reactor vessel. The concern was that the resulting steam explosion could impart sufficient energy to separate the upper vessel head from the vessel itself and form a missile with sufficient energy to penetrate the reactor containment. This of course

would produce an early failure of the containment building at a time when the largest mass of fission products is released from the reactor fuel. The WASH-1400 study ~~boldly~~ estimated the likelihood of an alpha-mode event, conditional on the assumption that a core-melt accident had occurred, was on the order of 0.01, acknowledging that this estimate carried with it a large uncertainty band. This hypothesized scenario subsequently served as the basis for the so-called SST-1 source term that was used in the 1982 Siting Study [7]. Such a pessimistic source term, when combined with particularly ~~unfortunate~~ (and unlikely) weather conditions would lead to significant health consequences.

In following years, significant research was focused on characterizing and quantifying this hypothesized accident in order to attempt to reduce the significant uncertainties involved. As early as 1981, [8] scientific investigations of the physical melt-water interaction processes, such as melt fragmentation and explosion triggering, and the behavior of prototypic reactor materials were calling into question the alpha-mode likelihood posed in WASH-1400, owing to lowered estimates of energy conversion efficiency for prototypic fuel melts and less effective energy transfer to the vessel head estimated by more detailed structural analysis of the reactor vessel. In this early study Corradini concluded that in-vessel steam explosions, if triggered, would have a very low likelihood of forming a sufficiently energetic missile to fail the containment.

Theofanous and Yuen produced a number of studies, culminating in a conclusion paper in 1995 [9] that made use of the Risk Oriented Accident Analysis Methodology for quantifying the density function for the containment failure frequency from in-vessel steam explosions. This study determined that in-vessel steam explosions are not likely to fail the reactor vessel, much less the containment by a missile generated during vessel failure, and described the likelihood of either as "physically unreasonable."

At almost the same time, a similar study of alpha-mode potential for the Sizewell B Pressurized Water Reactor (PWR) was completed by Turland and Fletcher [10]. This analysis developed event trees with input data defined by twelve probability distributions for parameters such as the amount of participating melt, likelihood of triggering, and the kinetic energy of the slug impacting the upper head using the best available knowledge regarding the operative processes. By sampling these distributions using the Monte Carlo method Turland and Fletcher obtained conclusions similar to the Theofanous study, namely that the likelihood of containment failure by missile generation is very small, on the order of 10^{-5}, given a core melt event has occurred. New knowledge concerning the behavior of realistic reactor materials and the difficulty ~~to~~ attaining triggering can be reasonably assumed to further reduce this likelihood.

Research into the potential for in-vessel steam explosions continued and various models of the phases of the melt-water interaction process were developed by numerous researchers. Experimental data supporting these developments were initially focused on use of simulant materials such as thermites and Al_2O_3 melts. Notable experimental programs include the FARO and KROTOS programs [11], [12], and [13]. Subsequent to these experiments, a more recent testing program called TROI has been carried out by the Korean Atomic Research Institute [14], [15]. Taken collectively, these experiments generally show that high melt superheats are required to trigger a steam explosion and triggering is not seen with realistic molten mixtures of UO_2/ZrO_2. Some TROI tests making use of eutectic mixtures of urania and zirconia *have* been

observed to trigger a steam explosion. However, these mixtures are quite specific in that they represent a minimum in the melt range and are typically superheated. An unlikely combination to be found in prototypic corium melts.

Finally, a group of leading experts in this field referred to as the Steam Explosion Review Group concluded in a position paper published by the Nuclear Energy Associations Committee on the Safety of Nuclear Installations [16] that the alpha-mode failure issue for Western-style reactor containment buildings can be considered resolved from a risk perspective, posing little or no significance to the overall risk from a nuclear power plant.

4.2 Direct Containment Heating

Similarly, direct containment heating was another important event identified to cause early containment failure. NUREG-1150 was an important risk study that included DCH as an early containment failure phenomenon [17]. Extensive research was performed to characterize DCH. During this effort there were many phenomena identified that can preclude a high-pressure vessel failure (i.e., natural circulation leading to creep rupture of the RCS boundary, see [18]). First, the extensive natural circulation research shows that RCS failure prior to vessel failure due to RCS creep rupture is most likely. In the unlikely event there is a high-pressure vessel failure (i.e., not within SOARCA's screening criteria for consequence evaluations), the resolution of the DCH issue for the Zion nuclear power plant found the early containment failure to be very unlikely [19]. The issue resolution utilized a probabilistic framework that decomposes the DCH problem into three probability density functions that reflect the most uncertain initial conditions (UO_2 mass, zirconium oxidation fraction, and steel mass). Uncertainties in the initial conditions are significant, but reasonable bounds could be identified that are not unnecessarily conservative. The phenomenological models in the probabilistic model were compared with an extensive database including integral simulations at two different physical scales (1:10-scale in the Surtsey facility at Sandia National Laboratories (SNL) and 1:40-scale in the COREXIT facility at Argonne National Laboratory). The loads predicted by these models were significantly lower than those from previous parametric calculations. The containment load distributions do not intersect the containment strength (fragility) curve in any significant way, resulting in containment failure probabilities less than 10^{-3} for all scenarios considered. Sensitivity analyses did not show any areas of large sensitivity. Consequently, current PRAs do not represent DCH as a likely accident progression event and have not been included within SOARCA's best-estimate approach guidelines.

4.3 Drywell Liner Melt-through in the Presence of Water

The issue of Mark I drywell shell (liner) melt-through at Peach Bottom was assessed by the NUREG-1150 molten core-containment interaction panel. The results of expert panel elicitation are reported in Reference [29]. There were two schools of thought on this issue and hence the response was uncertain. Differences between the two schools centered on the lateral mobility of debris on the drywell floor, and the extent to which it would exit the reactor pedestal and traverse the radius of the outer drywell floor with sufficient internal energy to melt and penetrate the steel liner. Since the completion of NUREG-1150, the NRC has sponsored analytical and experimental programs to address and resolve this so-called "Mark I Liner Attack" issue. The

results of an assessment of the probability of Mark I containment failure by melt attack of the liner were published in NUREG/CR-5423 [30] and NUREG/CR-6025 [31]. It was concluded that lateral flow of debris toward the drywell wall is likely to occur if debris is not cooled by an overlying pool of water. This mode of containment failure is, therefore, retained in the calculations of severe accident progression in a Mark I containment described here (the modeling approach to debris spreading on a dry floor is discussed in Section 3.1.3.)

However, in the presence of water on the drywell floor, the leading edge of the expanding molten pool would cool, increasing its viscosity, reducing its temperature, and thereby inhibit the outward expansion of debris toward the drywell liner. Further, these processes would prevent the leading edge from having a sufficiently high temperature to challenge the integrity of the steel liner even if contact were achieved. The probability of early containment failure by melt-attack of the liner in the presence of water was, therefore, judged to be so low as to be considered 'physically unreasonable.'

Again —
Do we need to
add a section
on hydrogen burn / deflagration /
detonation?
- Effects on F.P. aerosolization
time
- DDT effects on timing of
containment failure, thereby
effects on subsequent
F.P. releases

This Page Intentionally Left Blank

5. REFERENCES

[1] Gauntt, R. O., Cash, J.E., Cole, R. K., Erickson, C. M, Humphries, L.L., Rodriguez, S. B., Young, M. F., 2005, "MELCOR Computer Code Manuals, Vol. 1: Primer and User's Guide, Version 1.8.6," NUREG/CR-6119, Vol. 1, Rev. 3, U.S. Nuclear Regulatory Commission, Washington, DC.

[2] Bixler, N., "~~State-of-the-Art Reactor Consequence Analysis (SOARCA) Project Best Modeling Practices for MACCS~~," Sandia National Laboratories, SAND-XXXX, 2008.

[3] Laur, M.N., 2006, "Meeting with Sandia National Laboratories and an Expert Panel on MELCOR/MACCS Codes in Support of the State-of-the-Art Reactor Consequence Analysis Project," Memo to J.T. Yerokun, Agency Document Access and Management System Accession Number ML062500078, U.S. Nuclear Regulatory Agency, Washington, DC, September.

[4] U.S. Nuclear Regulatory Commission, "Technical Bases for Estimating Fission Product Behavior During LWR Accidents," NUREG-0772, 1981.

[5] Downes, K.W., Beck, C.K., Cowan, F.P., Fleck, J.A., Kuper, J.B.H., McLaughlin, J., Singer, I., Smith, M., 1957, "Theoretical Possibilities and Consequences of Major Consequences in Large Nuclear Power Plants," WASH-740, United States Atomic Energy Commission, March.

[6] 1975, "Reactor Safety Study, An Assessment of Accident Risks in U.S. Commercial Nuclear Power Plants," NUREG-75/014, U.S. Nuclear Regulatory Commission, October 1975.

[7] Aldrich, D.C., Sprung, J.L., Alpert, D.J., Diegert, K.V., Ostmeyer, R.M., Ritchie, L.T., Strip, D.R., Johnson, J.D., Hansen, K., Robinson, J., 1982, "Technical Guidance for Siting Criteria Development," NUREG/CR-2239, U.S. Nuclear Regulatory Commission, Washington, DC.

[8] Corradini, M.L. et al, 1981, "An Analysis of Containment Failure by Steam Explosion Following a Postulated Core Meltdown in a Light Water Reactor," Nuclear Engineering and Design, 66:287-298.

[9] Theofanous, T.G., Yuen, W.W., 1995, "The Probability of alpha-mode containment failure," Nuclear Engineering and Design.155:495-473.

[10] Turland, B., Fletcher, D.F., et al., 1995, "Quantification of the probability of containment failure caused by an in-vessel steam explosion for the Sizewell B PWR," Nuclear Engineering and Design 155:445-458.

[11] Annunziato, A., Magallon, D., et al., 1996, "Progress of the FARO/KROTOS programme," Cooperative Severe Accident Research Meeting, U.S. Nuclear Regulatory Commission.

[12] Huhtiniemi, I., Magalon, D., Hohmann, H., 1999, "Results of recent KROTOS FCI tests: alumina versus corium melts," Nuclear Engineering and Design 189:379-389.

[13] Huhtiniemi, I., Magallon, D., 2001, "Insight into steam explosions with corium melts in KROTOS," Nuclear Engineering and Design, 204:391-400.

[14] Song, J.H., et al., 2002, "Experiments on the interactions of molten ZrO2 with water using TROI facility," Nuclear Engineering and Design, 213:97-110.

[15] Song, J.H., Park, I.K., Shin, Y.S., Kim, J.H., Hong, S.W., Min, B.T., Kim, H.D., 2003, "Fuel coolant interaction experiments in TROI using a UO2/ZrO2 mixture," Nuclear Engineering and Design, 222(1):1-15.

[16] NEA/CSNI, 2000, "Technical Opinion Paper on Fuel-Coolant Interaction," NEA/CSNI/R(99)24, American Meteorological Society, 1978, "Accuracy of Dispersion Models," Bulletin of the American Meteorological Society, 59.

[17] Nuclear Regulatory Commission, 1990, "Severe Accident Risks: An Assessment for Five U.S. Nuclear Power Plants," NUREG-1150, U.S. Nuclear Regulatory Agency, Washington, DC.

[18] Bayless, P.D., et al., "Severe Accident Natural Circulation Studies at the INEL," NUREG/CR 6285, INEL 94/0016, February 1995.

[19] Pilch M.M.; H. Y., and Theofanous T.G., "The probability of containment failure by direct containment heating in Zion," Nuclear Engineering and Design, Vol. 164, Number 1, 1 August 1996.

[20] NUREG/CR-5582, "Lower Head Failure Experiments and Analyses," SAND98-2047, Sandia National Laboratories, 1998.

[21] M.T. Farmer, S. Lomperski, and S. Basu, "Results of Reactor Material Experiments Investigating 2-D Core-Concrete Interaction and Debris Coolability," Proc. Proc. Int. Conf. Adv. Power Plants, ICAPP'04, Pittsburgh, Pennsylvania, June 2004.

[22] Stewart, W.A., Pieczynski, A.T., and Srinivar, V., "Natural Circulation Experiments for PWR Degraded Core Accidents," EPRI Report NP 6324 D, 1989.

[23] Stewart, W.A., Pieczynski, A.T., and Srinivar, V., "Natural Circulation Experiments for PWR High Pressure Accidents," EPRI Report TR 102815, 1993.

[24] Boyd, C.F. Hardesty, K., "CFD Analysis of 1/7th Scale Steam Generator Inlet Plenum Mixing During a PWR Severe Accident," NUREG 1781, October 2003.

[25] Boyd, C.F., Helton, D. M., Hardesty, K., "CFD Analysis of Full Scale Steam Generator Inlet Plenum Mixing During a PWR Severe Accident," NUREG 1788, U.S. Nuclear Regulatory Commission, May 2004.

[26] Wagner, K. C., Wagner, KC, "MELCOR 1.8.5 Analysis of Natural Circulation Flow in the Westinghouse High-Pressure SF6 Experiments," Draft SAND Report, Sandia National Laboratories, June 2001.

[27] Fletcher, C. D., and Beaton, R. M., "SCDAP/RELAP5 Base Case Calculation for the Station Blackout Uncertainty Study," Letter report to D. M. Helton, US NRC, August 2006.

[28] Fletcher, C. D., and Beaton, R. M., "Evaluation of Uncertainties in SCDAP/RELAP5 Station Blackout Simulations," Letter report to D. M. Helton, US NRC, August 2006.

[29] Harper, F. T., et al., "Evaluation of Severe Accident Risks: Quantification of Major Input Parameters, Experts' Determination of Containment Loads and Molten Core Containment Interaction Issues," Sandia National Laboratories, NUREG-CR-4551, SAND86-1309, Vol. 2, Rev. 1, Part 2, April 1991.

[30] Theofanous, T.G., et al., "The Probability of Liner Failure in a Mark I Containment," NUREG/CR-5423, 1989.

[31] Theofanous, T.G., et al., "The Probability of Mark I Failure by Melt –Attack of the Liner," NUREG/CR-6025, November 1993.

[32] Ramamurthi, M., and M. R. Kuhlman, "Final Report on Refinement of CORSOR – An Empirical In-Vessel Fission Product Release Model," Battelle Report, October 31, 1990.

[33] S.R. Greene, "MELCOR 1.8.2 assessment: comparison of fuel fission product release models to ORNL VI fission product release experiments," ORNL/NRC/LTR-94/34 (1995).

[34] T. Nakamura and R. A. Lorenz, "A Study of Cesium and Krypton Releases Observed in HI and VI Tests Using a Booth Diffusion Model," Oak Ridge National Laboratory Research Paper (May 1987).

[35] B.J. Lewis, et al., "Modeling the release behavior of cesium during severe fuel degradation," J. Nuc. Mat. (227), pp83-109, (1995).

[36] F.C. Iglesias, et al., "Fission product release mechanisms during reactor accident conditions," J. Nuc. Mat. (270) pp 21-38, (1999).

[37] H. Manenc, P. Mason and M.P. Kissane, "The modeling of fuel volatilization in accident conditions," J. Nuc. Mat. (294) pp 64-68 (2001).

[38] B.V. Dobrov, et al., "Kinetics of UO2 oxidation in steam atmosphere," J. Nuc. Mat. (255) pp 59-66 (1998).

[39] N.E. Bixler, "VICTORIA 2.0: A Mechanistic Model for Radionuclide Behavior in a Nuclear Reactor Coolant System Under Severe Accident Conditions,"NUREG/CR-6131, SAND93-2310 (1998).

[40] V. Strizov, "MELCOR 1.8.5 Validation: Modeling of Fission Product Release," NSI-SARR-149-03, Russian Academy of Sciences, Nuclear Safety Institute, Dec 2002.

[41] B. Clement and T. Haste, "Comparison report on International Standard Problem ISP-46 (Phebus FPT-1)," Note Technique SEMAR 03/021, Draft Final Report, April 2003.

[42] R. A. Lorenz and M. F. Osborne, "A Summary of ORNL Fission Product Release Tests with Recommended Release Rates and Diffusion Coefficients," NUREG/CR-6261, (1995).

[43] G. Ducros, et al., "Fission product release under severe accident conditions: general presentation of the program and synthesis of VERCORS 1-6 results," Nuc. Eng. And Des. (208) pp 191-203 (2001).

[44] Powers, D.A., L.N. Kymetic and R.C. Schmidt, "A Review of the Technical Issues of Air Ingression during Severe Reactor Accidents," NUREG/CR-6218, SAND94-0731 (1994).

[45] K. Natesan and W.K. Soppet, "Air Oxidation Kinetics for Zircaloy-4," Argonne Letter Report, Dec 2002.

[46] Petrie, L.M et al., "Standard Composition Library," NUREG/CR-0200, Rev. 6, Vol. 3, ORNL/NUREG/CSD-2/V3/R6, Oak Ridge National Laboratory, September 1998.

[47] Soffer, L., et al., "Accident Source Terms for Light-Water Nuclear Power Plants," NUREG-1465, U.S. Nuclear Regulatory Commission, 1995.

This Page Intentionally Left Blank

Appendix A MELCOR Updated Default Parameters

Table A-1 MELCOR 1.8.6 Updated Default Parameters

#	Description	Parameter(s)	Field(s)	Value(s) used in SOARCA	Current Default Value(s)
1	COR package candling heat transfer coefficient.	COR00005	HFRZUO HFRZZR HFRZSS HFRZZX HFRZSX HFRZCP	7500 W/m^2-K 7500 W/m^2-K 2500 W/m^2-K 7500 W/m^2-K 2500 W/m^2-K 2500 W/m^2-K	1000 W/m^2-K 1000 W/m^2-K 1000 W/m^2-K 1000 W/m^2-K 1000 W/m^2-K 1000 W/m^2-K
2	COR package radiation heat transfer parameters	COR00003	FCELR FCELA	0.1 0.1	0.25 0.25
3	COR package min. porosity for flow and heat transfer	SC1505	(1) (2)	0.05 0.05	0.001 0.001
4	COR package min. CVH volume fraction	SC4414	(1)	0.01	0.001
5	COR package 1-dim. stress/strain distribution	SC1600	(1)	1.0	0.0
6	COR package min yield stress temperature	SC1603	(2)	1700.0 K	1800.0 K
7	COR package temp. for enhanced debris to lower head conduction	SC1250	(1)	2800.0 K	3200.0 K
8	CVH/FL direct versus iterative solution algorithm	SC4415	(1)	1.0	0.5
9	HS temperature convergence criterion	SC4055	(2)	0.5	5.0e-04
10	CAV package emissivity of oxide, metallic, and surrounding materials	CAVnnak	EMISS.OX EMISS.MET EMISS.SUR	0.9 0.9 0.9	0.6 0.6 0.6
11	Multipliers for surface boiling heat transfer and material (oxide/metallic) conductivity	CAVnnak	BOILING COND.OX COND.MET	10.0 (multiplier) 5.0 5.0	CORCON-Mod3 1.0 1.0
12	DCH package default classes – new default class 17 (Cs_2MoO_4)			* arrays initialized with 17 classes	* arrays initialized with 16 classes
13	RN class 17 physical properties	SC7120 SC7120 SC7170 SC7170 SC7170	(1,17) (2,17) (3,17) (4,17) (9,17)	351.75 kg/kg-mole 425.75 kg/kg-mole 0.67 kg/kg-H_2O 0.67 kg/kg-H_2O 4030.0 kg/m^3	28.97 kg/kg-mole 28.97 kg/kg-mole 0.0 kg/kg-H_2O 0.0 kg/kg-H_2O 1000.0 kg/m^3

Appendix B MELCOR Modeling Best-Practices

Table B-1 Standard MELCOR Modeling Practices, Modeling Parameters, and Sensitivity Coefficients for Analysis of Severe Accidents

Item	Record	Field	Value(s) used in SOARCA	Description
1.	BUR000	IACTV	0 (Active)	Burn package activation
2.	BUR1xx (xx = CV)	IGNTR	86 for CVs where ignition is to be prohibited.	Apply to RCS control volumes to preclude combustion.
3.	BUR1xx (xx = CV)	TFRAC	1.0	Time fraction of burn before propagation to neighboring CV is allowed. Value of 1.0 means a flame must travel the radius of the control volume before propagating to its neighbor.
4.	FLnnn0T	ZBJT0, ZTJT0	ZTJT0 = ZBJT0 + Δz (For axial containment flow paths only)	To insure that MELCOR properly estimates vertical burn propagation in containment, and adjacent buildings, it is necessary to define "vertical" flow path "from" and "to" elevations with a small dZ. If the "from" and "to" elevations are set equal (which has been historical practice to ensure complete vertical pool drainage), the MELCOR burn package uses criteria for horizontal burn propagation.
5.	FLnnnFF	KFLSH	1	Calculate superheated pool flashing for all liquid LOCA connections to initially dry containment regions. KFLSH activates the model. Activate RN1lkkk as needed for impact into specified heat structures.
6.	FLnnn02	IBUBF & IBUBT	-1 +2	Vapor heat transfer in pools for RCS FLs. SPARC scrubbing in pools for spargers, quencher, vents, and BWR downcomers.
7.	RN2FLTXX00	FPVAPOR	Various geometric values	MELCOR SPARC pool scrubbing model was modified to scrub all gaseous RN classes for
8.	COR00001	DRGAP	0.0	Thickness of gas gap between fuel pellets and cladding set 0.0 to account for swelling of operating fuel.
9.	COR00001A	ILHTYP ILHTRN	0 BWR =0, PWR =1	Lower head is a hemisphere Transition is at RCOR (BWR) or RVES (PWR)
10.	COR00009	HDBPN HDBLH MDHMPO MDHMPM TPFAIL CDISPN	100 W/m^2-K 100 W/m^2-K 'MODEL' 'MODEL' 9999 K 1.0	This record activates the internal molten pool to lower head heat transfer models and provides reasonable solid debris to lower head heat transfer coefficient.

Item	Record	Field	Value(s) used in SOARCA	Description
11.	COR00012	HDBH2O VFALL	2000 W/m^2-K 0.01 m/s	HTC in-vessel falling debris to pool (W/m^2-K) Velocity of falling debris (m/s).). Perhaps not correct for shallow pools and not necessary in deep pools since adoption of no 1-D CCFL limitation via the one-dimensional Lipinski model.
12.	CORCR0	IAICON	2	For PWRs only Activate control rod release model, 2 = Model is active, vaporization is allowed from both candling material and conglomerate.
13.	CORZjj01	PORDP	0.4	Porosity of particulate debris
14.	CORijj04	DHYPD	Core - 0.01 m LP - 0.002 m	Particulate debris equivalent diameter (LP values for DHYPD, HDBH2O, VFALL tuned to get appropriate end-of-pour debris temperature. 2mm based on FAERO fragmented debris size). Perhaps not correct for shallow pools.
15.	CORZjjNS	TNSMAX	1520 K 1700 K	Control blades failure temperature (BWR) Core top guide failure temperature (BWR)
16.	CORijjDX	FBYXSS	Calculated.	For BWRs only. Fraction of lower head COR cells normally displaced by control rod guide tubes should be 'excluded' from volume available to particulate debris. Volume recovered when tubes (as supporting structure) fails.
17.	SC-1131(1)	TRDFAI	2800 K	Fuel rod collapse temperature (addressed with CORijjFCL records)
18.	SC-1141 (2)	GAMBRK	0.20 kg/m-s	Molten Zr breakout flowrate parameter to yield 2 mm/s as evidenced in CORA experiments
19.	SC-1701 (1)		0.01	Open volume fraction for subnode blockage criterion. This is the default setting.
20.	SC-4401(3)	XPASMX	15	Maximum number of iterations permitted before solution is repeated with a decreased (subcycle) timestep.
21.	DCHNEMnn00	ELMNAM ELMMAS	Use ORIGEN results for core, if available.	Elemental fission product mass at shutdown for calculation of decay heat.

Item	Record	Field	Value(s) used in SOARCA	Description
22.	DCHNEMnnmm	DCHEAT	Use pre-combined methodology for Cs, I, and Mo	Elemental fission product decay heat per unit mass (based on shutdown RN inventory). • Define specific decay heat for CsI (Class 16) as 0.51155 of value for Class 2 (Cs) plus 0.48845 of value for Class 4 (I). • Define specific decay heat for Cs_2MoO_4 (Class 17) as 0.7348 of value for Class 2 (Cs) plus 0.2652 of value for Class 7 (Mo). If ORIGEN results are not available for the core, perform an input deck with BE burn-up and cycle history. Redistribute RN mass as follows, • Class 2 initial mass represents the NUREG-1465 Cs gap mass not already included in Class 16. • Class 4 initial mass is empty (10^{-6} kg) • Class 7 initial mass is remaining Mo mass not included in Class 17. • Class 16 has all I and an appropriate amount of Cs mass for CsI stoichiometry. • Class 17 has the remaining Cs not included in Classes 2 and 16 plus Mo for Cs_2MoO_4 stochiometry.
23.	DCHCLSnnn0, DCHCLSnnnm	RDCNAM, CLSELM	New RN definitions for Classes 1-12, 16-18	If ORIGEN results are available, synthesize ORIGEN data to define a single representative element for each class with decay heat data that reflects decay heat for all elements within the class (DCHNEMxxxx input.) Redefine each class to include only the representative element.
24.	DCHDEFCLS0	DEFCLS	13, 14, 15	Specifies that MELCOR DCH default classes are to be used.
25.	DCHCLNORM	CLSNRM	'No' when ORIGEN results are available. 'Yes' when MELCOR is used to estimate initial inventories.	New ORIGEN input for elements/classes defines the total core decay heat. Otherwise, let MELCOR normalize the elemental decay heats to the rated power. Do not use RN1DCHNORM. Default behavior normalizes Class 10 (Uranium).
26.	HScccc400 & HScccc600	CPFPL CPFAL	See discussion	Minimum value of CVH pool fraction such that heat transfer is calculated to Pool/Atmosphere. For heat structures within the RPV, use 0.9. For PWR SG Tubes, use 0.1. All other structures modeled use default value of 0.5.

Item	Record	Field	Value(s) used in SOARCA	Description
27.	HScccccc401 HScccccc601	EMISWL RMODL PATHL	0.27 EQUIV-BAND 0.1 m	Mean emissivity of SS type 316 Equivalent band radiation model. Nominal optical distance in steam (m). For SS heat structures within the reactor vessel and those being monitored for creep-rupture failure.
28.	HSDGccccc0	ISRCHS ISDIST GASNAM	HS # 1 SS	Heat structure for application of degas model. Degassing model requires 1 mesh. Name of released gas. For SS boundary structures modeled with the HS package that are coupled to the core.
29.	HSDGccccc1	RHOSRC HTRSRC TEMPL TEMPU	7930 kg/m^3 $2168x10^5$ J/kg 1695 K 1705 K	Gas source density. Gas source heat of reaction. Lower temperature for degassing. Upper temperature for degassing. For SS boundary structures modeled with the HS package that are coupled to the core.
30.	MPMATxxxx	MLT	2800 K 2800 K	Uranium-dioxide Zirconium-oxide Because of the interactions between materials, liquefaction can occur at temperatures significantly below the melt point. The interaction between ZrO_2 and UO_2 results in a mixture that is fluid at above about 2800 K (compared to the melting temperatures of 3113 K and 2990 K, respectively, for the pure materials). Similarly, although pure B4C melts at 2620 K, interaction with steel produces a mixture that is fluid at above about 1700 K.
31.	RN1001	NUMSEC NUMCMP NUMCLS	10 2 20 (PWR) 18 (BWR)	Default Default For BWR & PWR: 16 = CsI, 17 = Cs_2MoO_4 Now Class 17 includes default settings for Cs_2MoO_4.

Item	Record	Field	Value(s) used in SOARCA	Description
32.	BWR structural tin release RN/DCH data for RN Class 18			For BWR: RN Class 18 = SnO_2 (non-radioactive) Define SnO_2 (DCHCLSnnn0) 18 = 'SnO2' SnO_2decay heats (DCHNEMnn00) 0 W/kg (no decay heat) SC(7110) vapor pressures SnO_2: $Log_{10}(P(mm\ Hg)) = 15400/T + 8.15$ SC(7111) diffusion coefficients SnO_2: Sigma = 3.617, E/K = 97 SC(7120) elem./compound molecular weights Sn: MW = 150.7 kg/kg-mole
33.	PWR control rod RN data for RN Classes 18, 19, and 20			For PWR RN Class 18 = Ag, 19 = In, 20 = Cd Define Ag, In, Cd (DCHCLSnnn0) 18 = 'Ag-CR', 19 = 'In-CR', 20 = 'Cd-CR' Ag, In, Cd decay heats (DCHNEMnn00) 0 W/kg (no decay heat) SC(7110) vapor pressures Ag: $Log_{10}(P(mm\ Hg)) = 1000/T + 1.26x10^4 + 7.989$ In: $Log_{10}(P(mm\ Hg)) = 400/T + 1.27x10^5 + 8.284$ Cd: $Log_{10}(P(mm\ Hg)) = 500/T + 5.31x10^3 + 7.99$ SC(7111) diffusion coefficients Ag: Sigma = 3.48, E/K = 1300 In: Sigma = 3.61, E/K = 2160 Cd: Sigma = 3.46, E/K = 1760 SC(7120) elem./compound molecular weights Ag: MW = 107.8 kg/kg-mole In: MW = 114.8 kg/kg-mole Cd: MW = 112.4 kg/kg-mole
34.	RNCA100	ICAON	1 (Active)	Chemisorption model is active (default).
35.	RN1002	IHYGRO	1 (Active)	Hygroscopic model activation. (RNACOND set to default, 0 = condensation of water onto all aerosols.

Item	Record	Field	Value(s) used in SOARCA	Description
36.	RNCRCLxx	ICRMT / ICLSS / FRAC	2 / 18 / 0.0145 3 / 18 / 0.0145	For BWRs, apply the non-fuel release model. Assign aerosol generated from Zr and ZrO_2 to RN Class 18 (SnO_2). The mass will be added as a non-radioactive mass to this class. The fraction of material mass available for release as an aerosol from these materials is 0.0145 (Sn fraction in Zirc-2 and -4.) Note: must also add input for the release rate (SC7103) for RN Class 18. Values should be identical to those used (default) for Class 12 (fission product Sn).
	SC7100			Multipliers for various structural material types
		(2) Zr	0.1	
		(3) ZrO2	1.0	
		(4) steel	0.0	
		(5) steel ox.	0.0	
		(6) B4C	0.0	
37.	RNFPNijjXX	NINP RINP1 RINP2	Use ORIGEN results, if available.	NINP = RN Class, RINP1 = mass, RINP2 = axial peaking factor. Distributes mass based on distribution developed with ORIGEN. If ORIGEN results are unavailable, NINP = 0, RINP1 = axial peaking factor, RINP1 = radial peaking factor. Where, $\Sigma_i\Sigma_j$ RINP1 * RINP2 = 1.
38.	RNGAPijjnn	NINP RINP1 RINP2	1 (Xe) = 0.05 2 (Cs) = 1.00 3 (Ba) = 0.01 5 (Te) = 0.05 16 (CsI) = 0.05	Where, NUREG-1465 recommends the following gap quantities, • Xe = 5% • Cs = 5% • Ba = 1% • Te = 5%
39.	RN2FLTXX00	FPVAPOR	Various geometric values	For all flow paths entering pools via quenchers or spargers, specify the flow path to scrub all gaseous RN classes.